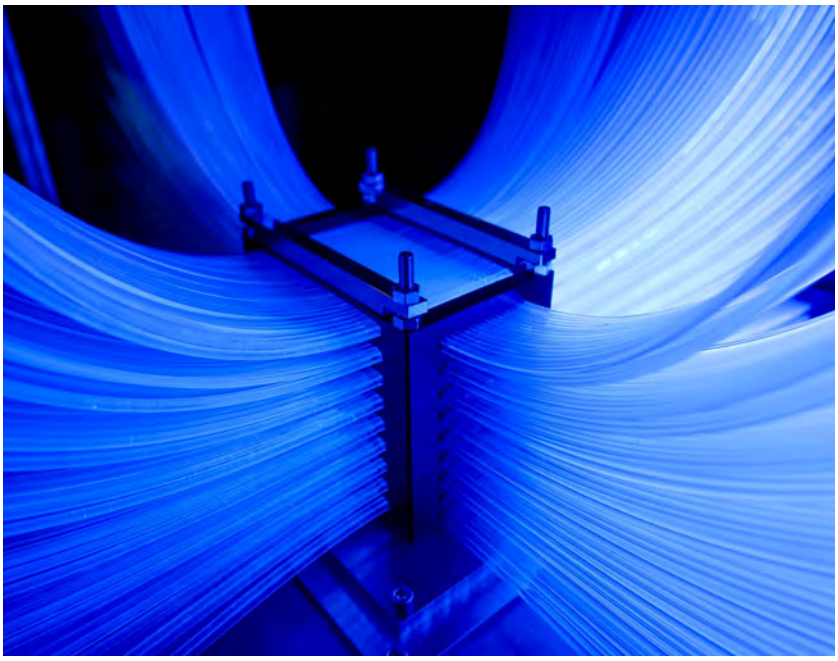

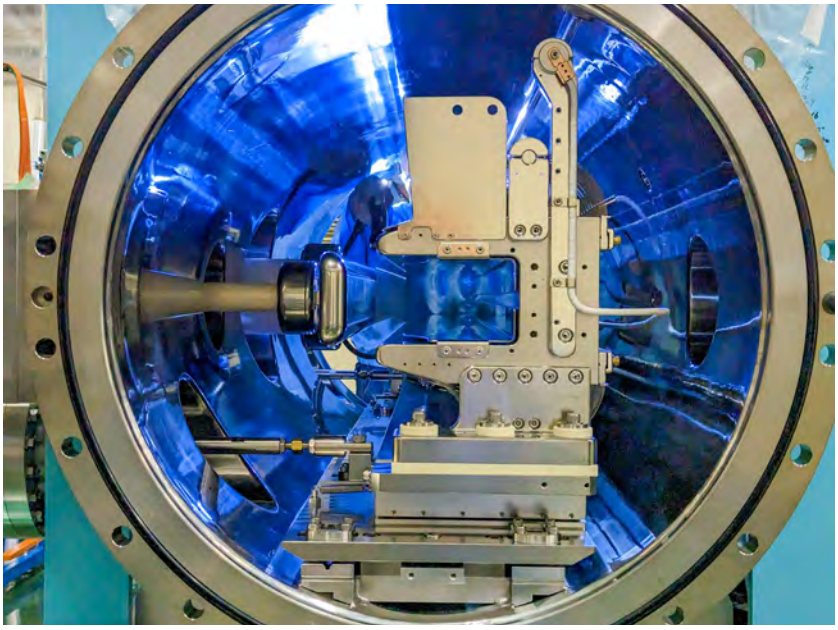

J-PARC

ANNUAL REPORT 2023

Vol.1: Highlight

Editorial Board (April 2024 – March 2025)


Yong LIU *(Accelerator Division)*


Kaoru SAKASAI *(Materials and Life Science Division)*


Tetsuro SEKIGUTI *(Particle and Nuclear Physics Division)*


Masami IIO *(Cryogenics Section)*

No image

Jiro SUZUKI *(Information System Section)*


Bruce YEE-RENDON *(Transmutation Division)*


Fumihiro MASUKAWA *(Safety Division)*


Masatoshi TSUKADA *(Users Office Team)*


Narumi SUGIYAMA *(Public Relations Section)*

Cover photographs


Photograph ① : Active fiber target
Image credit: Takeshi HARADA


Photograph ② : White MLF
Image credit: Yu OISHI


Photograph ③ : Blue landscape inside the electrostatic septum
Image credit: Ryotaro MUTO

J-PARC Annual Report 2023

Contents

Preface

In Japanese fiscal year (JFY) 2023, from April 2023 through March 2024, we made great progress at J-PARC on many fronts and also experienced some failures, a few of which are covered below.

In JFY2023, we had two fire incidents, which resulted in reduction of the user beam time although no personnel were injured. The first one happened on April 25, 2023, and involved fire that started from the transformer used in a newly built MR power supply. The cause was a design error of the transformer's discharge measure. The second one happened on June 22, 2023, starting from a polarity exchanger of a magnet power supply for a magnet in the primary-proton transport line from MR to the

Hadron Experimental Facility. Its cause was the aging of the insulator used in the polarity exchanger. Due to the fires, the user beam time before the summer was reduced to 44.5 days from the original 60 days for the MLF and to 12.6 days from the original 57 days for the MR users. We deeply apologize for the inconvenience suffered by all users.

We succeeded in delivering 830 kW stable beam from RCS to the MLF. For MR, we achieved the 760-kW operation, which exceeded the original design power of 750 kW, which was the goal for more than 20 years counting from the start of construction. Now we have set a new goal of 1.3 MW for the future Hyper-Kamiokande experiment and we are working to further improve the beam power.

For the MLF, the total of 109.5 days of beam time was delivered to users while the planned operation period was 160 days. From 690 submitted proposals, 376 experiments were executed.

One of the highlights in particle and nuclear physics experiments was that new results from the KOTO experiment, searching for CP-violating decay of K_L meson to π^0 and two neutrinos, were obtained. No signature beyond the background was found and a new upper bound on the branching ratio 2.0×10^{-9} was set.

The upgrade work of Neutrino Experimental Facility for higher beam power of 1.3 MW for HyperKamiokande project has been continued.

In this volume, we report on the progress made at J-PARC in JFY2023.

On behalf of the J-PARC staff members,
Director of J-PARC Center
Takashi Kobayashi

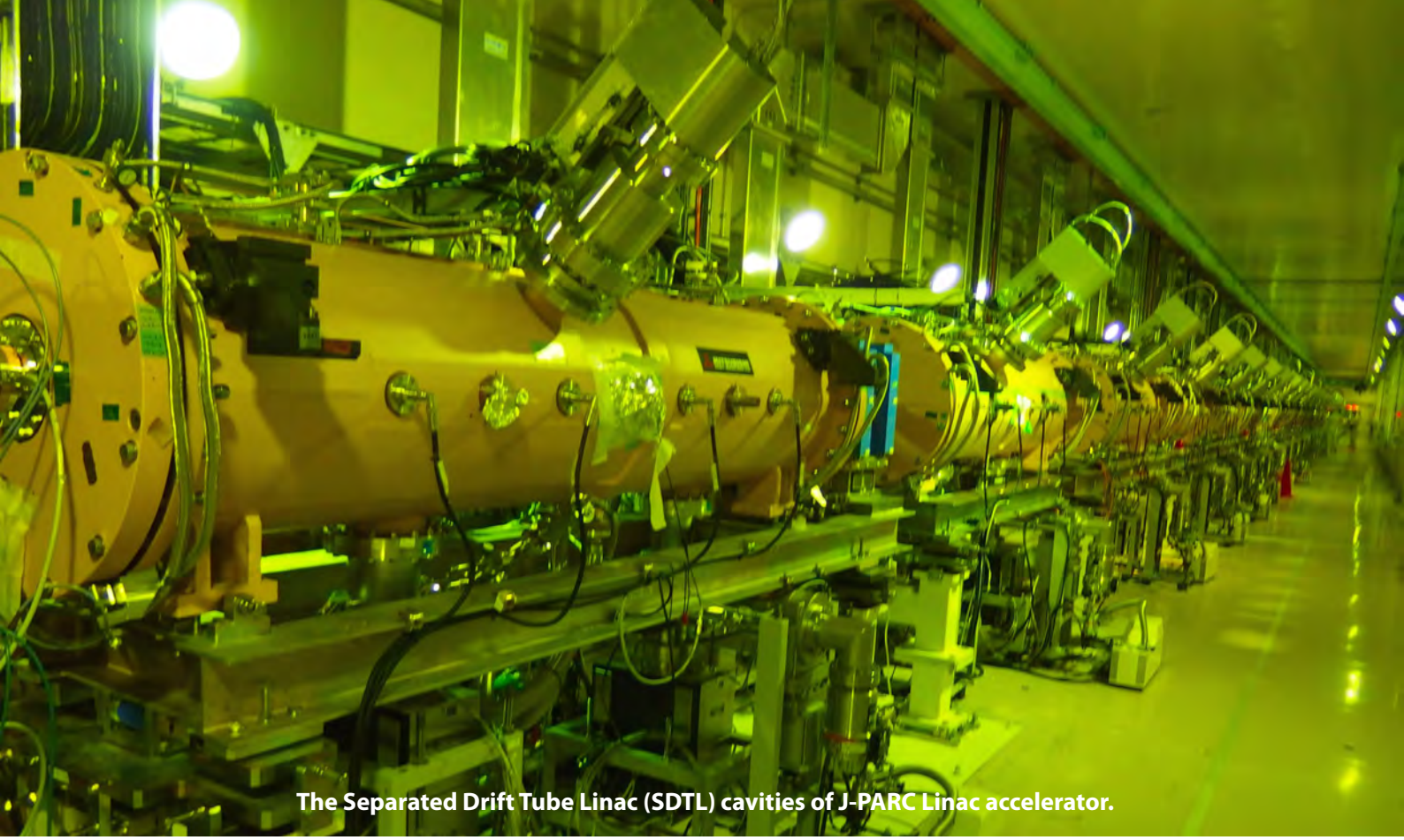

The Separated Drift Tube Linac (SDTL) cavities of J-PARC Linac accelerator.

Accelerators

Overview of the Accelerator

The J-PARC facility consists of three accelerator facilities: Linac, RCS (Rapid Cycling Synchrotron) and MR (Main Ring synchrotron). The proton beams extracted from the RCS are delivered to the Materials and Life Science Experimental Facility (MLF) for neutron and muon experiments as well as injected to the MR. The MR has two beam extraction modes such as the fast extraction (FX) mode to the Neutrino Experimental Facility (NU) and the slow extraction (SX) one to the Hadron Experimental Facility (HD).

The operation status of the accelerator in Japanese fiscal year (JFY) 2023 is shown in Fig. 1. On April 25, power supply fire occurred in the MR, and the MLF and MR operations were suspended until mid-May and mid-June, respectively. On June 22, another power supply fire occurred in the HD power supply building, and all beam

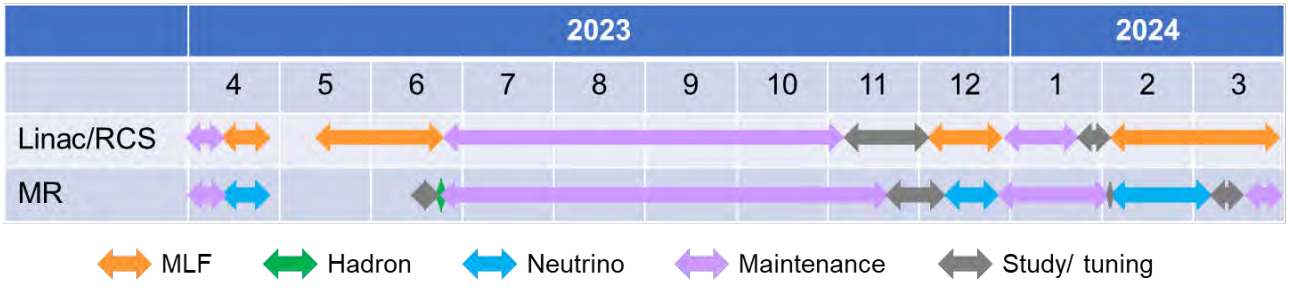

Fig. 1. Operation status of the accelerator in JFY2023.

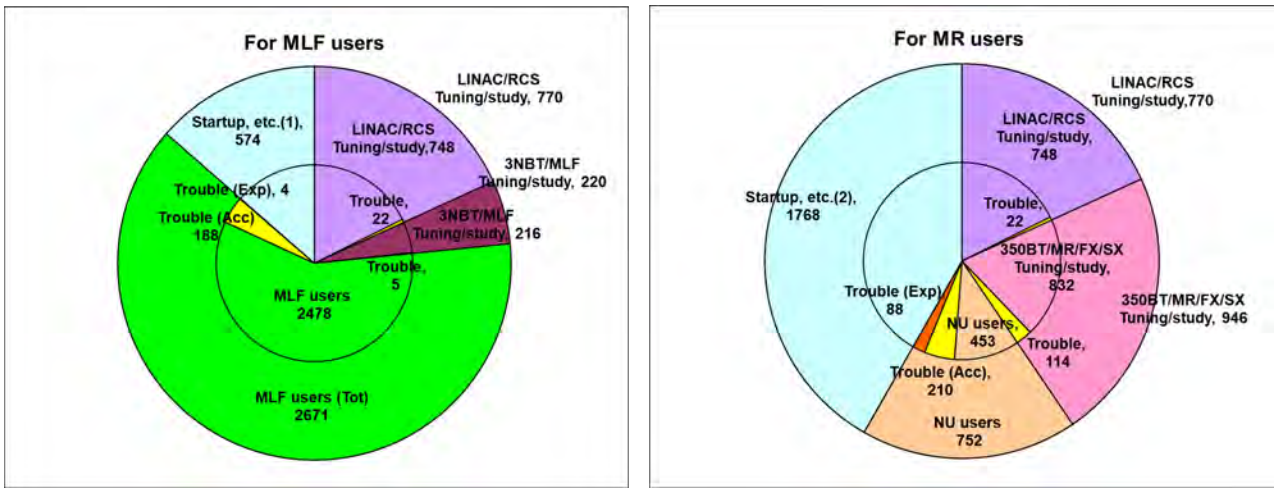

Fig. 2. Operation statistics for JFY2023.

operations scheduled until the end of June before the summer maintenance were cancelled.

(1) Operation for the MLF

The MLF operation for JFY2023 started on April 16 with a beam power of 840 kW. Due to the insufficient cooling capacity of the RCS cooling water system caused by rising outside temperature and humidity, the beam power was reduced to 800 kW on June 2 and to 700 kW from June 8 to 22. After the summer maintenance, beam operation was resumed at 660 kW due to the availability of the MLF target, but the beam power was later increased to 880 kW as of March.

The net user operation hours and the beam availability rate for the MLF facility in JFY2023 were 2,478 hours and 93%, respectively (Fig. 2).

(2) Operation for the NU and HD

As for MR, in order to shorten the cycle repetition period from 2.48 s to 1.36 s, a major modification of MR was carried out for about one year from JFY2021, including an upgrade of the main magnet power supply, the acceleration cavity, the injection/excitation system, the collimator system and so on. Some failures of the renewed equipment occurred at the beginning of the operation after the major modification, however, the 760 kW eq and 30 GeV beam acceleration was conducted successfully on April 16, which marked the achievement of an important milestone. Moreover, the NU user operation started on December 25 with a beam power of 760 kW.

The net user operation hours and the beam availability rate for the NU facility in JFY2023 were 453 hours and 60%, respectively (Fig. 2).

No user operation for the HD facility was conducted in JFY2023, but the user operation is scheduled to resume in early 2024 with the aim of achieving a beam power of more than 65 kW, the maximum value achieved to date.

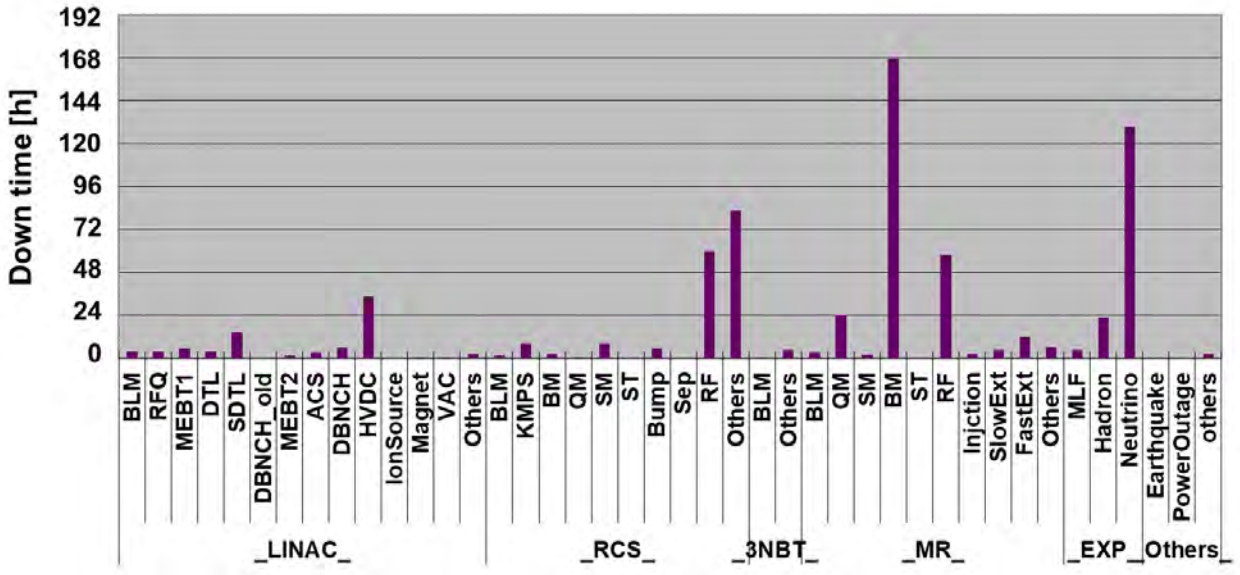

Fig. 3. Downtime for each accelerator components in JFY2023.

(3) Downtime for each accelerator component.

The downtime for each accelerator component in JFY2023 is shown in Fig. 3.

The longest downtime in JFY2023 was 167 hours due to a bending magnet power supply failure in MR. This was caused by the power supply failures of bending magnet 1 in June and bending magnet 3 in December, both of which were IGBT unit troubles. In both cases, the restoration took about four days due to the investigation of the cause of the failure and the replacement with a spare IGBT.

The next longest downtime of the accelerator components was due to a failure of the cooling water system in the RCS (indicated as "Others" in Fig. 2). In this case, there was a failure of a pump in the secondary cooling water system (the primary system directly cools the accelerator components, while the secondary system cools the water in the primary system). The restoration work took about five days because it was necessary to arrange for a crane and other large equipment to replace the pump with a spare one.

The third longest downtime was due to failures of the RF-related equipment in the RCS (marked "RF" in Fig. 2). This failure occurred several times, which took various times to restore. The failure that took the longest time to fix was the damage to the capacitor in the RF cavity amplifier. This was caused by a discharge on the capacitor surface due to water drop on the surface, which came from a leak at a joint in the cooling water piping in the amplifier. It took about 18 hours to resume beam operation due to the replacement of the capacitor and repair of the cooling water piping.

Although not as long as the above three failures, the beam operation was terminated for 34 hours due to a failure of the klystron high-voltage power supply ("HVDC" in Fig. 2) in the linac. This also occurred several times, involving both long and short time to restore. The most time-consuming failure for restoration was a malfunction of the klystron for the ACS08 (ACS: Annular-ring Coupled Structure) linac. The klystron was replaced in mid-March 2024 due to a sudden increase in the trip rate. The trip was caused by a discharge between the electron gun body and the anode.

Linac

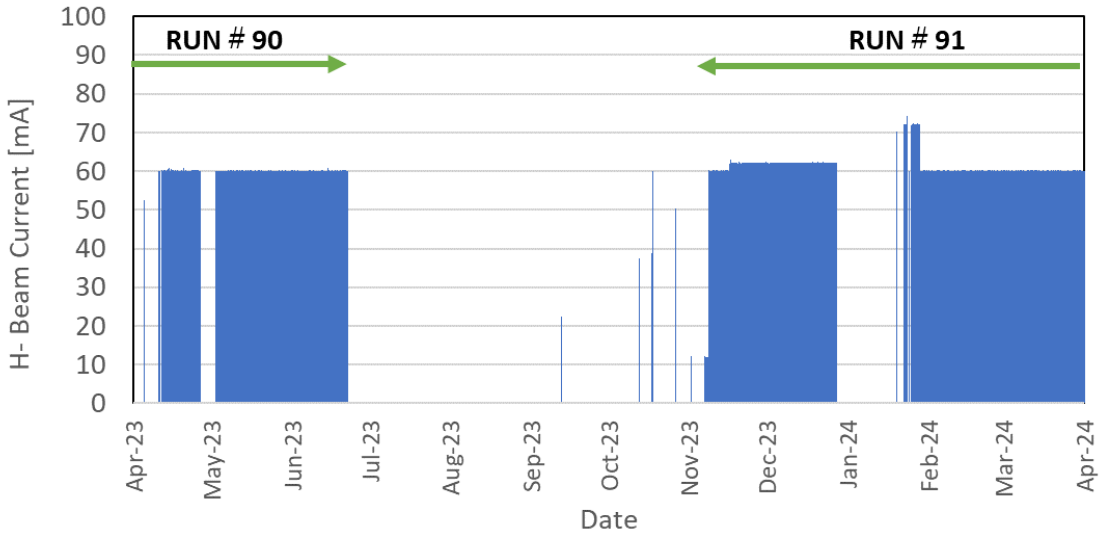

Fig. 4. Operation history of the ion source in FY2023.

Overview

The J-PARC linac has been operated with a nominal peak beam current of 50 mA. High availability of more than 90% (to the MLF) was also maintained during FY2023 at the linac. The beam studies have been conducted to resolve some issues, such as the beam loss mitigation, confirmation of feasibility for further high-intensity operation due to the demand of the downstream facilities.

Accelerator components status

The operation history of the ion source in FY 2023 is shown in Fig. 4. Presently, the ion source is being operated with an H^- beam with a beam current of 60

mA for the user operation. After the winter shutdown, the ion source extracted more than 72 mA beams for high-intensity beam study. Figure 5 shows the history of the continuous operation time and the beam current increase of the RF ion source (from 2014). The replacement cycle has been gradually extended with an increased operational experience. In RUN#90 (November 2022 – June 2023), the continuous operation time of the ion source has been extended to 4,412 hours (6.1 months), and the ion source was not replaced during RUN#90. Almost all components of the J-PARC RF-driven H^- ion source can be manufactured by domestic companies. However, only the RF internal antenna coil still has been purchased from a foreign company. Therefore, we have been conducting the J-PARC-made antenna as an internal antenna. We investigated the outgassing characteristics during the production of a high-density plasma by using the J-PARC-made antenna at the ion source test bench. The residual gas and spectroscopic analyses have confirmed that no noticeable impurities were emitted from the antenna. The horizontal and vertical emittances of the H^- beam extracted by using the J-PARC-made antenna coil were similar to those in the case of the antenna coil currently in use. An endurance test of the RF input energy to the antenna coil was also carried out more than approximately equivalent to 5,500 hours of the ion source operation.

The RFQ trip rate at the 25 Hz beam operation to the MLF in FY2023 was approximately 12 times per day. This situation is almost the same as before. An auto-restart system for the RFQ trip has been running for four years. The system resumes the beam at the next macro-pulse after the RFQ trip. Also, the beam stop associated with the RFQ trips (e.g., MPS by the beam loss downstream) occurs approximately twice every 3 days.

RF trips due to the discharge frequently occurred in

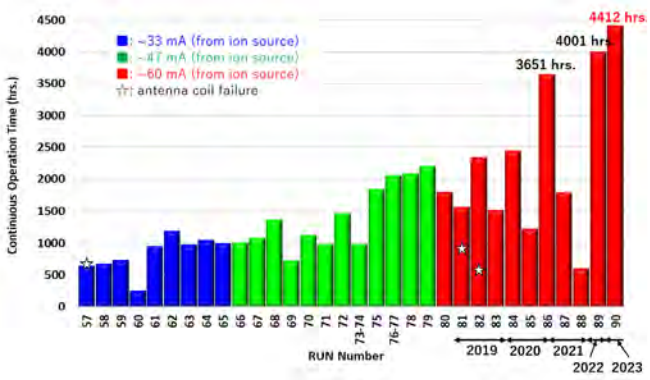

Fig. 5. History of the continuous operation time of the RF ion source.

Table 1. Cavity Cleaning History

	S04A	S04B	S05A	S05B	S06A	S06B
2015				Acetone Disappeared		
2016			Acetone Remained → Expand	No recurrence	Acetone Disappeared	Acetone Disappeared
2017	Acetone Remained	Acetone Remained	Acetone Remained → Expand (fast)		No recurrence	No recurrence
2018						
2019			Acetone Remained → Expand (fast)			
2020			DSA Remained → Expand (slow)			
2021			DSA Disappeared			
2022	DHA Disappeared	DHA Disappeared	No recurrence			
2023	No recurrence	No recurrence				

DTL3 since the summer maintenance in 2022. Therefore, the ceramic window of DTL3 was replaced with a new one during the spring maintenance period at the end of March 2023. After the replacement, the DTL3 trips due to the discharge were significantly reduced. The average trip rates for each cavity of DTLs and SDTLs in FY2023 were approximately 0.2 trips per day.

After the Great East Japan Earthquake in 2011, we could not operate with the design rf power in some SDTL cavities due to the multipactor effect. Since we had the unstable power region near the operating power at SDTL 4, 5, and 6, the inner surfaces of these cavities were cleaned using organic solvent and acid solution. The history of the cavity cleaning is summarized in Table 1.

The acid cleaning of S04A and S04B was performed during the 2022 summer maintenance. However, based on previous experience with cavity cleaning, there is a possibility that the unstable region will appear again after a few years. Therefore, the RF measurements of SDTL cavities were continued for more than one year after cleaning, and it was confirmed that unstable regions had not appeared. Currently all SDTL cavities are operating stably at the design operation power.

The operation of the ACS cavities was more stable than the other accelerator sections. The number of trips of all the ACS cavities was less than once per day.

RF system status

We use 20 klystrons for the 324-MHz system, and 25 klystrons for the 972-MHz system. The operation time of the six oldest klystrons reached more than 92,000 hours for the 324MHz system, which corresponds to the entire period since the start of the linac operation. In 2023, no 324-MHz klystron was replaced. The operation time

of the most klystrons for the 972MHz system reached more than 61,000 hours. The operation time of the klystrons as of the end of March 2024 is shown in Fig. 6. Two klystrons were replaced in FY2023. In October 2023, one 972 MHz klystron was replaced due to water leak at the pipe connection. The leak will be repaired, and this klystron will be stored as a spare. And one klystron was replaced due to decrease in electric breakdown voltage in March 2024.

Beam monitor status

With the increase in beam power in the J-PARC accelerator, the fluctuation of beam output at the linac has recently become a problem. In particular, beam output fluctuations during user operation are directly linked to the beam utilization efficiency, so there is an increasing need to monitor them with higher precision than ever before.

Therefore, the linac beam monitor group developed and constructed a new beam current measurement system, which will be put into practical use in the spring of 2024. The new measurement system integrates and outputs the beam current signal of the macrobunch beam. By adopting this method, the new system eliminates the effects of RF noise caused by the acceleration cavity, making it possible to measure beam current with higher accuracy.

Furthermore, by installing this new beam current measurement system in a distributed manner from upstream to downstream of the linac, it has become possible to pinpoint more precisely than before the location where current reduction due to beam loss occurs.

This new beam current measurement system has made it possible to detect beam current fluctuations of less than 0.1 percent, which was previously difficult, and greatly contributes to the stability of the beam output to the downstream facilities.

Beam study

In JFY2023, we continued efforts to achieve higher stability and quality of the linac output beam for the high-power operation of J-PARC, up to 880kW at MLF and 760kW at NU.

RCS longitudinal painting scheme is significant for beam loss mitigation, which is dependent on reliable longitudinal manipulation and stability of the linac output beam centroid and spread. As shown in Fig. 7, we developed a scheme and successfully realized a wide range of linac output centroid momentum for the RCS beam study while keeping the design functions of two debunchers for RF jitter suppression and momentum spread control.

This scheme is the cornerstone of the RCS stable low-loss operation with longitudinal painting with off momentum of -0.15%.

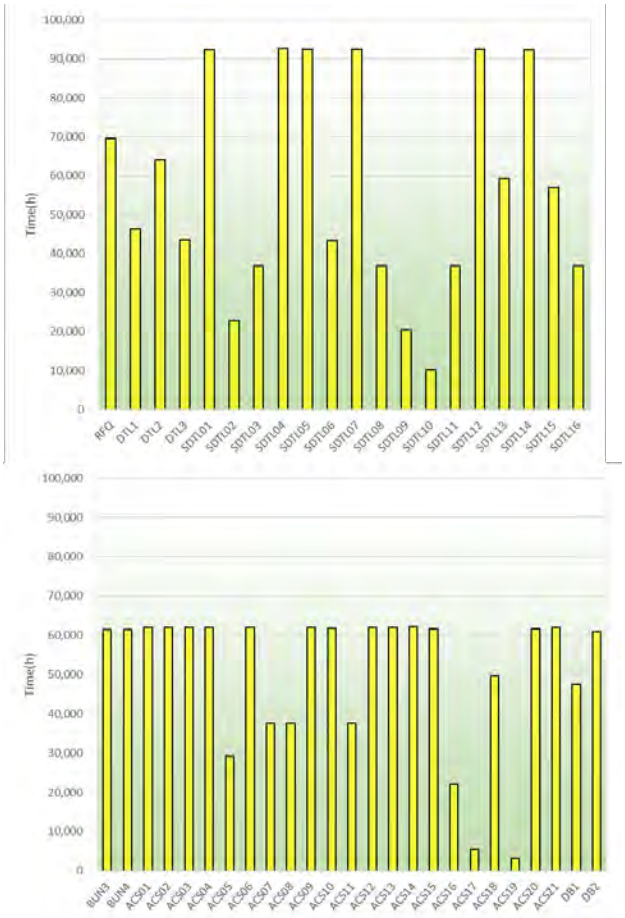

Fig. 6. The operation time of the 324-MHz klystron (top) and the 972-MHz klystron (bottom) as of the end of March 2024.

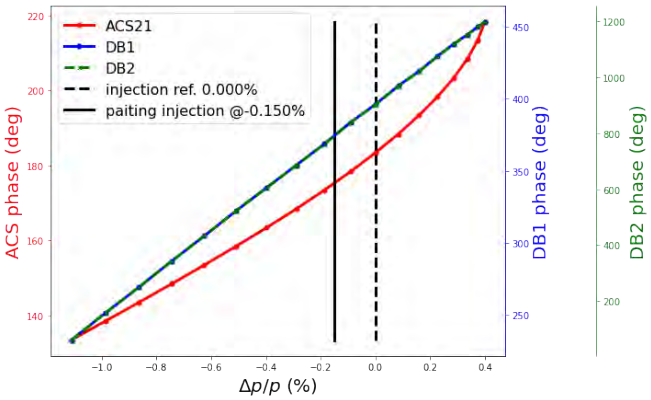

Fig. 7. Tested setting datasets of last three RF cavities in J-PARC linac for wide linac output centroid momentum in January 2024. Range -0.20 to +0.10% was used in the RCS studies.

On the other hand, we continued the preparation steps for linac moment global compensation. Fig. 8 shows the important progress for the calibration between measurement and simulation to match the model to the real accelerator with beam-cavity responses.

For a more reliable user operation and higher beam intensity, beam commissioning with higher peak currents has been conducted several times. It has revealed that further reduction of beam loss is required to achieve these goals. One of the most serious types of beam loss is the leakage beam by the chopper, commonly referred to as "extinction". To improve the extinction, we conducted joint measurements with the RCS, as these beams are lost in the RCS. We developed a method to measure the extinction in the linac and successfully realized the measurement scheme with a good correlation to the RCS loss, as shown in Fig. 9. Thanks to this method, we can evaluate chop leakage more efficiently before the RCS tuning.

Using this method, the extinction is measured as a function of the voltage in the buncher cavity installed upstream of the chopper, as shown in Fig. 10. It demonstrates that a higher buncher level can decrease extinction. However, a higher level sufficient to reduce the extinction results in the deformation of the nominal beam, necessitating a more refined beam tuning scheme, which is currently being developed.

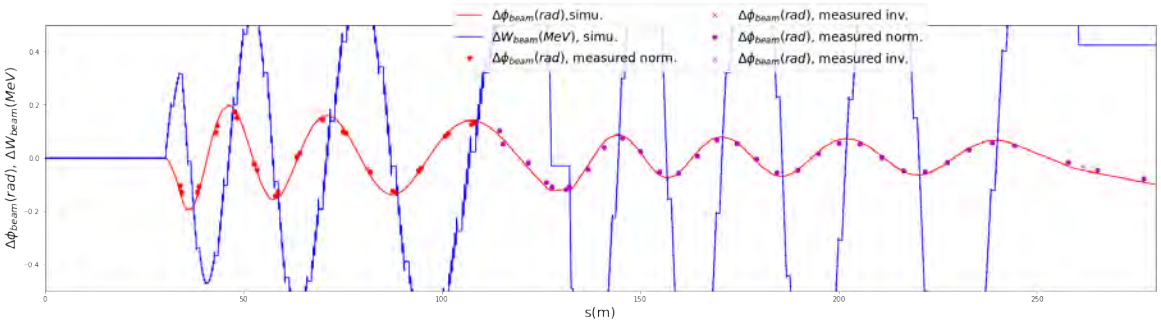

Fig. 8. Calibration data for the beam-cavity response measurement and simulation.

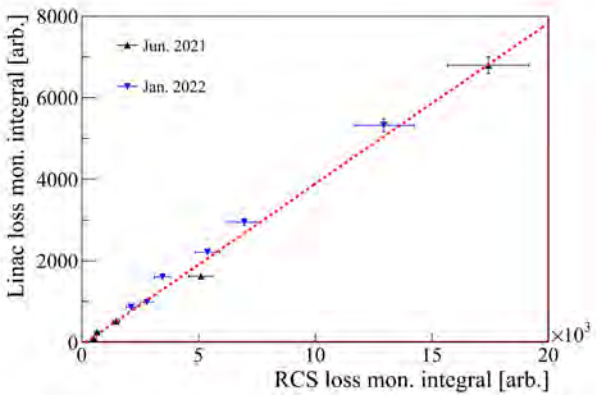

Fig. 9. Beam loss at the linac and the loss at the RCS (extinction), measured by the new method.

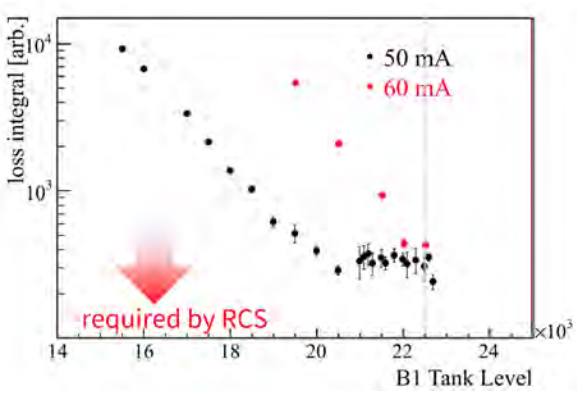

Fig. 10. Extinction as a function of the buncher voltage.

RCS

Operational status

In fiscal year 2023, the output power from the RCS was limited for several reasons. The first cause was the failure of the RF system in the RCS. Just before the summer shutdown period of 2022, one of the transformer-rectifier assemblies of the RF system failed. Subsequently, only 11 RF cavities have been operated and up to 800 kW beams are achievable under this condition. As a result, the maximum output beam power has been limited due to this failure. We prepared a spare assembly, but it did not work well, thus we made a new assembly in JFY2023. Finally, it was restored at the end of JFY2023.

After mid-June in 2023, we needed further reduction of the output beam power due to insufficient cooling water performance in summer conditions. We had to reduce the beam power to approximately 700 kW for the MLF.

The restart of the user operation after the summer shutdown was postponed by 12 days due to the delay of the maintenance work of the neutron target. Furthermore, a poor performance of the bubbler system in the mercury target, which moderates the shock of the incident proton beam, caused beam power reduction. The performance of the bubbler system slightly improved, and the beam power was also gradually increased. Figure 11 shows the changes in the RCS output power with respect to time.

The limitation of the beam power was not the only problem, there were also some cases of beam suspension due to the trouble in JFY2023. J-PARC had two fire accidents in the power supply system (PS). The first one occurred in the PS of the main ring magnet, and the other occurred in the PS of the beam transport magnet for the Hadron experimental hall. Although these accidents did not directly affect the RCS itself, it was necessary to check for the possibility of similar fire in the RCS and the accelerator operation was suspended during this process.

In addition to these two fire accidents, two major incidents occurred at the RCS: a capacitor break in the RF amplifire and a pump failure in the secondary cooling water system. We spent approximately 14 hours and 5 days for recovery, respectively. Figure 12 shows the inside of the broken pump.

The availability of the RCS is summarized in Table 2. The operation time for the MLF over the year was approximately 2783 h, excluding the commissioning time, and downtime due to the RCS was approximately 154 h. The availability for the MLF was evaluated by these values and it was 94.5%. For the Neutrino users, the availability of the RCS was 86%. There was no user time for the Hadron experiments because the fire accident in Hadron occurred during the commissioning phase in the Hadron experiment.

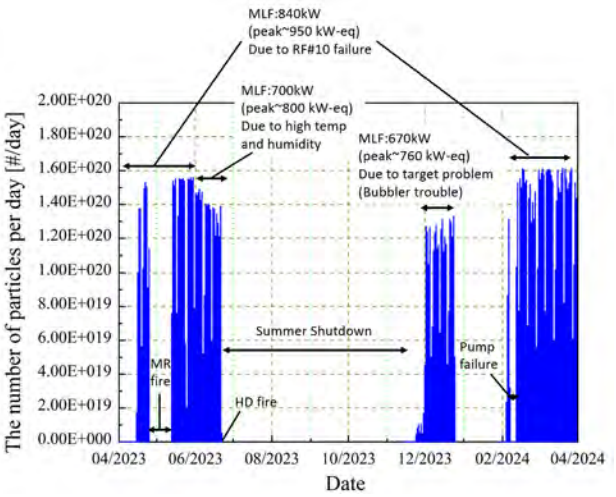

Fig. 11. Changes in the RCS output particles over time.

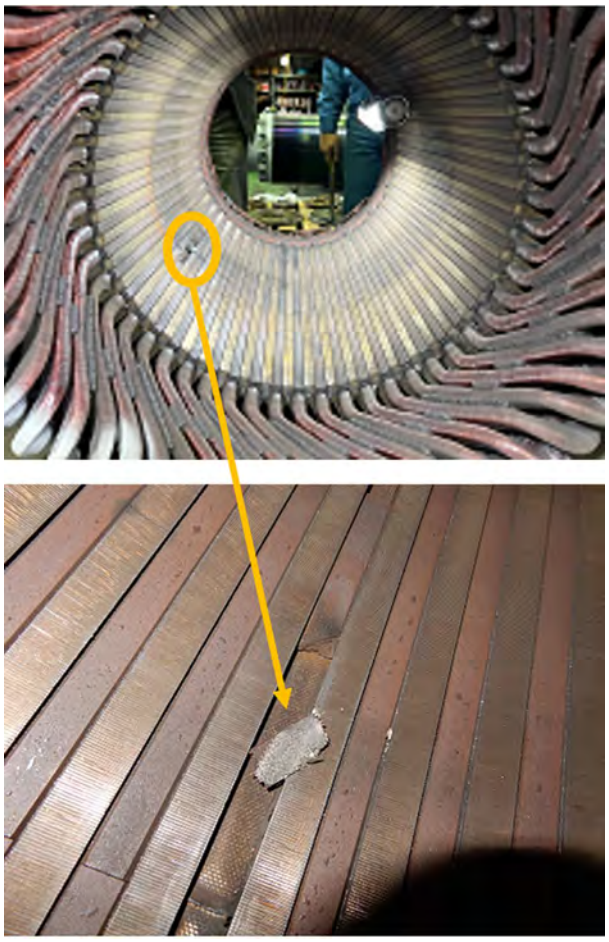

Fig. 12. Inside of the broken pump. A coil support was broken.

Table 2. Summary of availability

Facility	User time (h:m)	Trouble in RCS (h)	Availability of RCS (%)
MLF	2783:16	154:16	94.5
Neutrino	564:25	120:36	86.0

Note that these values include only the incident in the RCS and do not include the effect of the fires. The actual availabilities to the users were less than these values.

The operation status of the RCS was stable enough in JFY 2022. The availability of the RCS is summarized in Table 1. In JFY2022, the operation time for the MLF was ~3301 h, excluding the commissioning time, and the downtime due to the RCS was ~52 h. The availability to the MLF was evaluated using these values and found to be 98.4%. In JFY2022, the RCS delivered beams only to the MLF due to the MR upgrade activity, and thus there was no operation time for Neutrino and Hadron users.

Hardware improvement

● New RF cavity

We developed a new cavity that can reduce the required anode current for a higher current acceleration of over 1 MW. This new cavity can not only accelerate a beam with power of over 1 MW, but is also able to reduce the power consumption in the user operation with 1 MW.

We had one new cavity and installed two new cavities during summer shutdown period of 2023. After installation of two new cavities, the power consumption was reduced from 719 kW to 427 kW at 760-kW beam acceleration per cavity. We could reduce approximately 900 kW in total. We will complete the replacement of the new cavity by 2028.

● Foil development

In J-PARC RCS, The Hybrid type Boron-doped Carbon (HBC) foil produced in KEK had been used for charge exchange injection. Recently we developed the pure carbon foil as a candidate injection foil. Figure 13 shows the comparison of the HBC foil and pure carbon foil under beam irradiation. A large deformation occurred in the HBC foil. In contrast, in the pure carbon foil case, the edge was slightly deformed but retained its original shape. The pure carbon foil is considered to be less deformed than the HBC foil. We will continue the study of the lifetime of both foils.

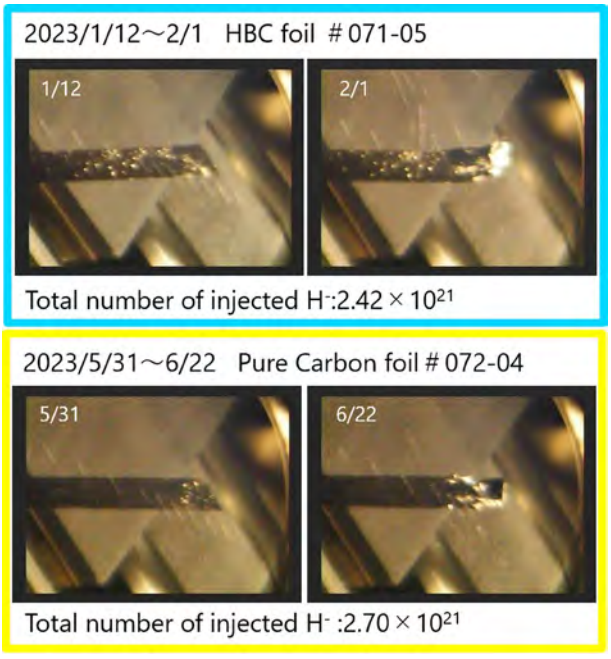

Fig. 13. Comparison of the HBC foil and the pure carbon foil under beam irradiation.

Beam study results

In the 1-MW beam operation, beam instability occurred with some operation parameters. The beam instability restricted the allowable operation parameter for the 1-MW operation. In the RCS, the primary source of instability is the transverse impedance of the extraction kicker magnets. A new damping system was developed to suppress the instability. In the previous year, one module had been implemented and we confirmed its performance. We installed one additional damping module in the summer shutdown period in 2023 and evaluated its function. To confirm the effect of the dumping module, we created a favorable condition for occurring beam instability and corrected the chromaticity during the whole acceleration period. Figure 14 shows the instability appearance as a function of the betatron tunes. The line indicated the center orbit of the beam, and it was distorted when instability occurred. We have selected the tunes that are likely to cause instability in

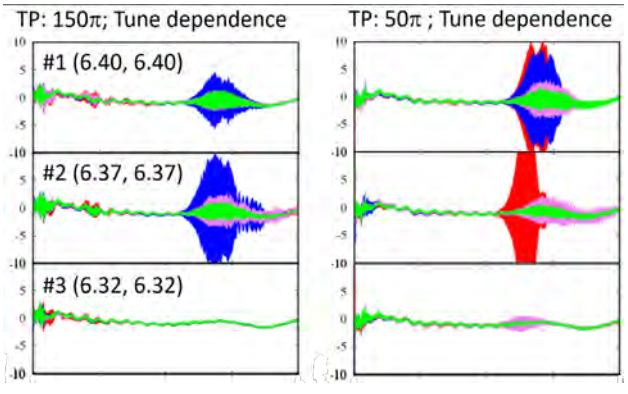

Fig. 14. Instability appearance as a function of the betatron tunes.

the above two cases. If we adopt two dumping modules, the orbit distortion will be minimal. Now, tune dependence and detail characteristics of beam instability have been well understood in both theory and simulations. For further tunability, we produced two more diode units in 2023 which will be installed in 2024.

Summary

In JFY 20023, the RCS had some troubles, and the availability was worse than in previous years. Due to the failure of the transformer-rectifier assembly of the RF system, the beam power was restricted to approximately 800 kW for the MLF. This value was also reduced due to the poor performance of the cooling water system. Concerning the transformer-rectifier assembly failure, we replaced it just before the end of JFY 2023 and the situation was rectified.

We installed two new RF cavities, which worked well and reduced the power consumption. We developed the pure carbon foil as another candidate of injection foil, and it showed satisfactory performance at present.

We continued the beam test with the new damping system in the kicker magnet power supply. The beam instability has been further reduced and tunability improved by inserting one more module. We plan to install the remaining two modules in JFY2024, and this change is immensely promising for further beam loss reduction.

MR

Overview

The J-PARC Main Ring (MR) provides 30-GeV proton beams to the neutrino experimental facility (NU) by fast extraction (FX) and to the hadron experimental facility (HD) by slow extraction (SX).

In MR, a project is currently underway to upgrade the beam power to NU from 515 kW (as of 2021) to 1.3 MW with faster repetition rates and higher beam intensities. For this purpose, MR has upgraded the main magnet power supplies, injection and FX devices, RF systems and collimators with a beam shutdown period of about one year from July 2021. With the hardware upgrades, the MR operation cycle in the FX mode has been shortened from 2.48 s to 1.36 s. MR started beam commissioning in the FX mode at the end of June 2022 and resumed the continuous beam operation for the NU users from the beginning of FY2023.

The SX mode operation at 30 GeV for the HD users was also conducted in FY2023 for the first time after the hardware upgrades. Beam delivery with the same operation cycle of 5.20 s as before the hardware upgrades was achieved. In addition, a beam study with a shorter operation cycle of 4.24 s was conducted toward further beam power ramp-up from 65 kW (as of 2021) to 80-100 kW.

Two magnet power supply fires occurred in MR and HD significantly reduced the beam operation time, but MR conducted both FX and SX operations in the limited time available and reached several important milestones after the high repetition rate upgrade.

Magnet power supply fire at MR

MR started beam operation in the FX mode on April 15 for FY2023. Beam tuning and operation proceeded smoothly, but on April 25, a fire incident occurred in a newly manufactured main quadrupole magnet power supply (QDN), and the beam operation was interrupted.

The QDN power supply had an initial charging circuit to supply energy to a capacitor during startup, and a transformer in the circuit developed an insulation failure and caught fire (Fig. 15). Because the initial charging circuit was connected to the main chopper circuit, a high-frequency noise coming from IGBT switching in the chopper circuit was constantly applied to the secondary coil of the transformer. The effects of corona discharges caused by high-frequency noise had not been taken into consideration during the design stage of the transformer. As a result, insulation deterioration due to corona discharges progressed gradually,

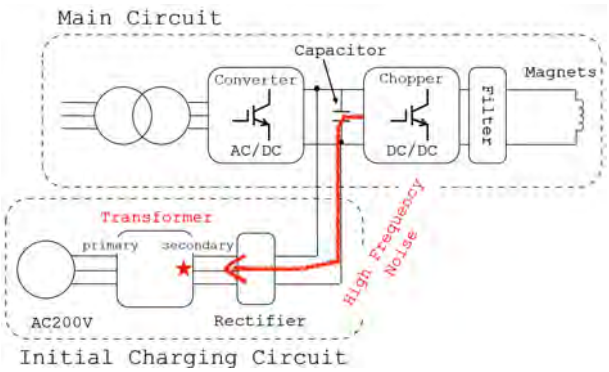

Fig. 15. Schematic of the circuit diagram of the QDN power supply.

eventually resulting in spark discharges and fire one year after the start of use.

After the accident, the initial charging method was changed to another way, which did not use a transformer. The original initial charging circuit was removed, and a bypass circuit was added parallel to the main circuit for initial charging. Similar measure was taken for another power supply of the same type. Fortunately, only the transformer ignited, and no other components were affected, but the MR operation was suspended for 48 days by this accident.

MR restarted the beam operation on June 13 in the SX mode. However, a fire incident occurred again on June 22 in a magnet power supply at HD, and the operation of the J-PARC facility for the first half of FY2023 was terminated at that point; the summer maintenance began 8 days ahead of schedule.

Major works during the summer shutdown period

Following the two fire incidents at MR and HD, a general inspection of the electrical equipment in the entire J-PARC facility was conducted along with the regular maintenance during the summer maintenance period.

In addition, MR developed further RF upgrade to realize more stable and reliable high-intensity beam acceleration (Fig. 16). The available fundamental RF voltage was increased from 480 kV (eight 4-gap cavities) to 495 kV (three 3-gap and six 4-gap cavities). In addition, the anode power supplies for the fundamental RF cavities were also upgraded to accommodate higher beam loading; the number of inverter output units in each anode power supply was increased from 15 to 16 for 4-gap cavity (12 for 3-gap cavity).

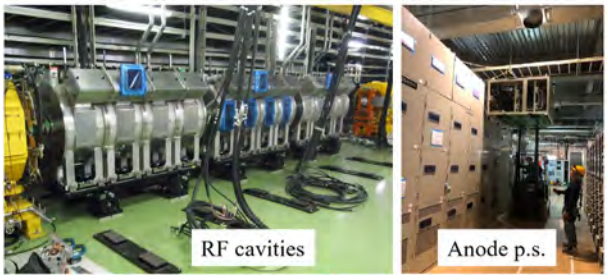

Fig. 16. Upgrade of the RF systems.

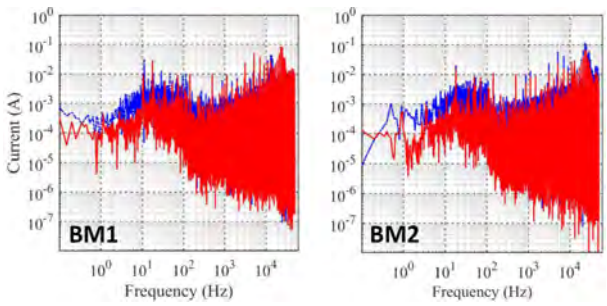

Fig. 17. FFT spectra of the output currents of the bending magnet power supplies before (blue) and after (red) bypassing the ground line.

In addition, the operation test of the main magnet power supplies was vigorously conducted. Two of the six bending magnet power supplies had large output current ripples, which significantly affected the beam through a distortion of the super-periodicity. Thus, the operation test of the two power supplies was performed for the current ripple reduction as the top priority issue. In the operation test, it was found that significant noise affected the DCCT signal used for feedback control, and that the ground line near the DCCT was the source of the noise. By routing the ground line away from the DCCT, the noise on the DCCT was reduced, successfully resulting in significant reduction in the output current ripple (Fig. 17).

The maintenance and upgrade works were completed as planned in the summer shutdown period.

FX beam tuning and operation

MR operated in the FX mode in April 2023, November-December 2023 and February 2024. After beam tuning and operation in April 2023, and via summer maintenance, the NU user operation with the operation cycle of 1.36 s began in earnest on November 20.

During the summer maintenance period, several works involving vacuum break were performed, such as reassembling and installing the RF cavities. Since significant beam loss due to vacuum deterioration was initially observed at those locations, the beam operation, including beam scrubbing for beam pipes, was performed from a low beam power of 260 kW. The beam power was increased step by step while monitoring the pressure and beam loss levels in the ring. The

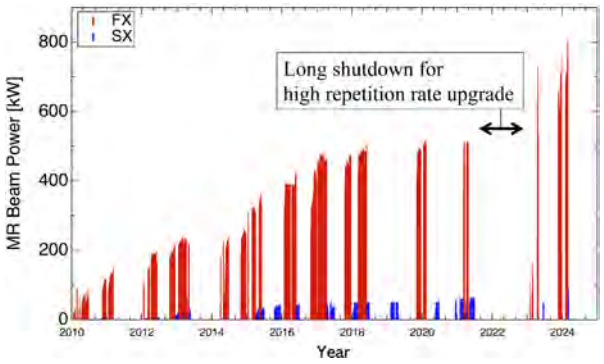

Fig. 18. History of the MR beam power in the FX (red) and SX (blue) operations.

beam scrubbing progressed smoothly, and the beam power reached 610 kW on November 27, and then 710 kW on December 14 (Fig. 18).

In addition, a new method of optics correction was successfully demonstrated in between the NU user operation. Quadrupole field errors, including fluctuations of focusing properties due to eddy currents, were accurately derived from a response of the closed orbit to a single kick, and the three-fold symmetry of the optical system was successfully established with high accuracy by correcting those errors (Fig. 19). Such a continuous effort steadily reduced the beam loss, and MR finally reached a major milestone on December 25, achieving a beam power of 760 kW exceeding the original design value (750 kW); the beam loss was estimated to be 1.1% and most of it was well localized at the collimator section (Fig. 20).

Significant progress was also made during the FX beam operation period in February 2024. Detailed adjustments for the beam optics system including dynamical tune manipulation at the early stage of acceleration to avoid a 3rd order resonance, the collimator gaps, etc. succeeded in further reducing and localizing beam loss. Thereby, continuous beam operation at 800 kW is now in sight. We aim to achieve a beam power of 800 kW in the first half of FY2024, while continuing our efforts to further reduce the beam loss.

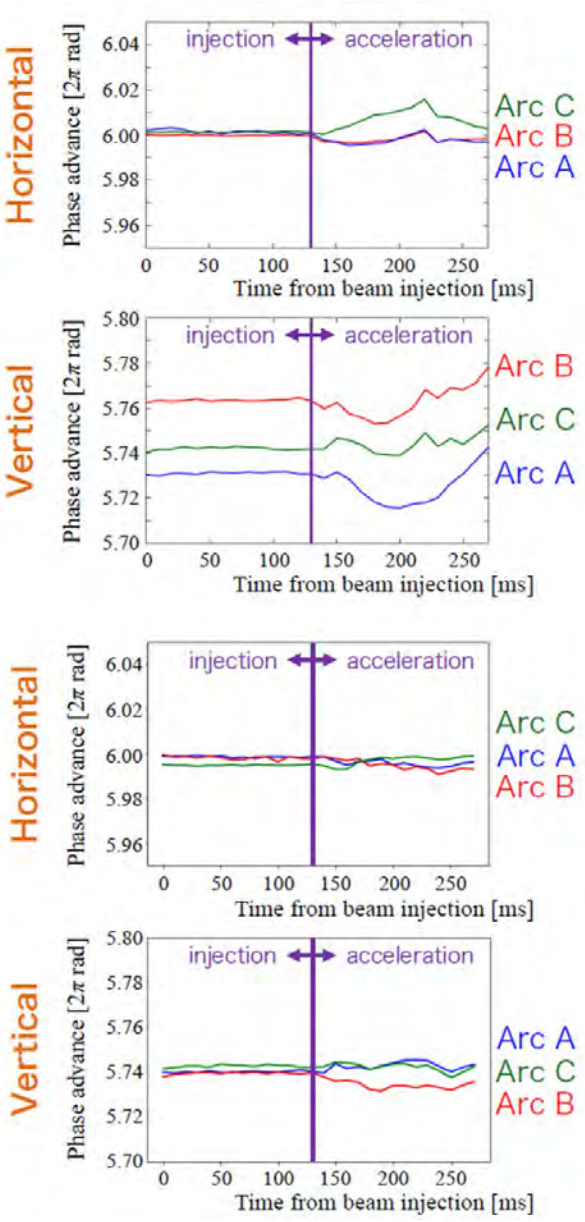

Fig. 19. Phase advance for each arc section, A, B and C measured as a function of time before (upper) and after (lower) the correction.

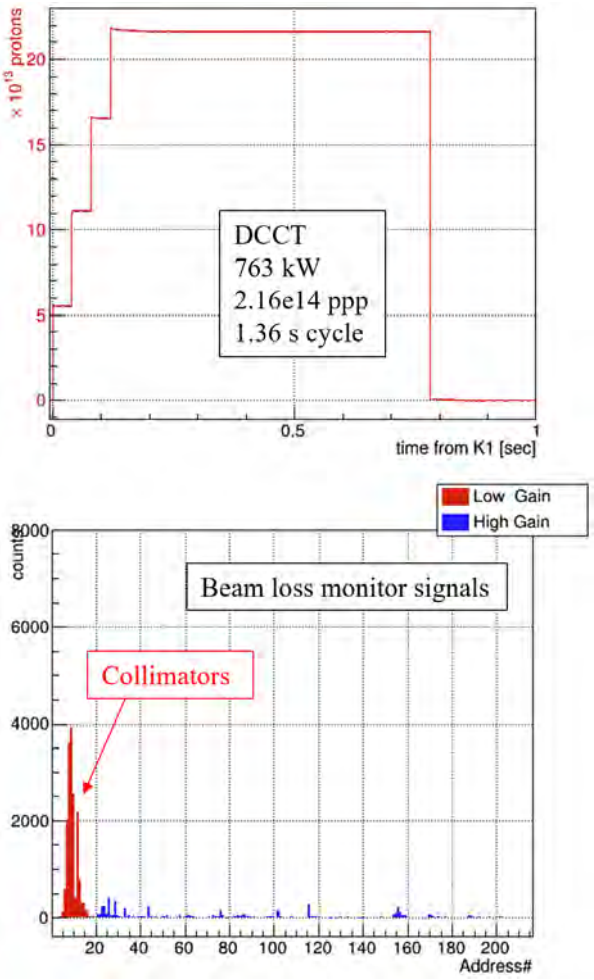

Fig. 20. DCCT and beam loss monitor signals during the 760-kW FX beam operation.

SX beam tuning and operation

In June 2023, MR conducted SX beam tuning and operation at 30 GeV for the first time after the high repetition rate upgrade and achieved a beam power of 50 kW (Fig. 18) with 99.5% extraction efficiency and 48% spill duty factor (Fig. 21) at the operation cycle of 5.20 s which was the same cycle as before the accelerator upgrade.

Beam test at a shorter operation cycle of 4.24 s was also conducted in March 2024. Optics tuning, beam instability study, etc. were successfully carried out. Beam instability in the de-bunching process at the flattop is one of the critical issues to be solved for realizing further beam power ramp-up in the SX mode. The beam test showed that dynamic manipulation of the longitudinal distribution by RF was very effective to suppress the beam instability. We aim to achieve a beam power of 80 kW at the operation cycle of 4.24 s early in FY2024.

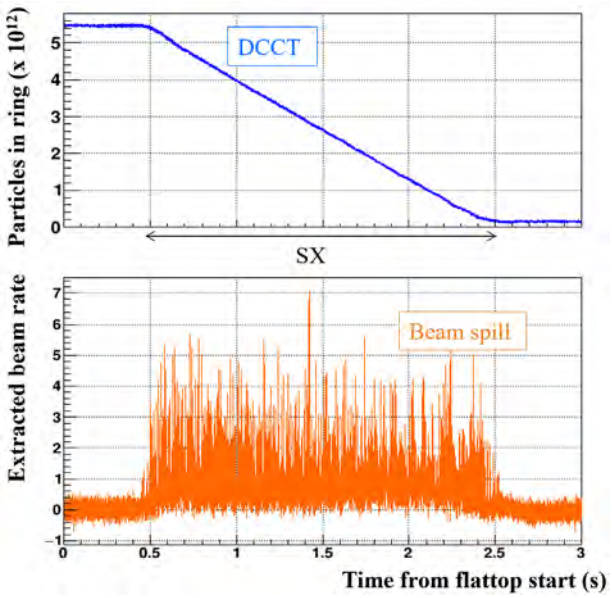

Fig. 21. DCCT and beam spill structure during the 50-kW SX beam operation.

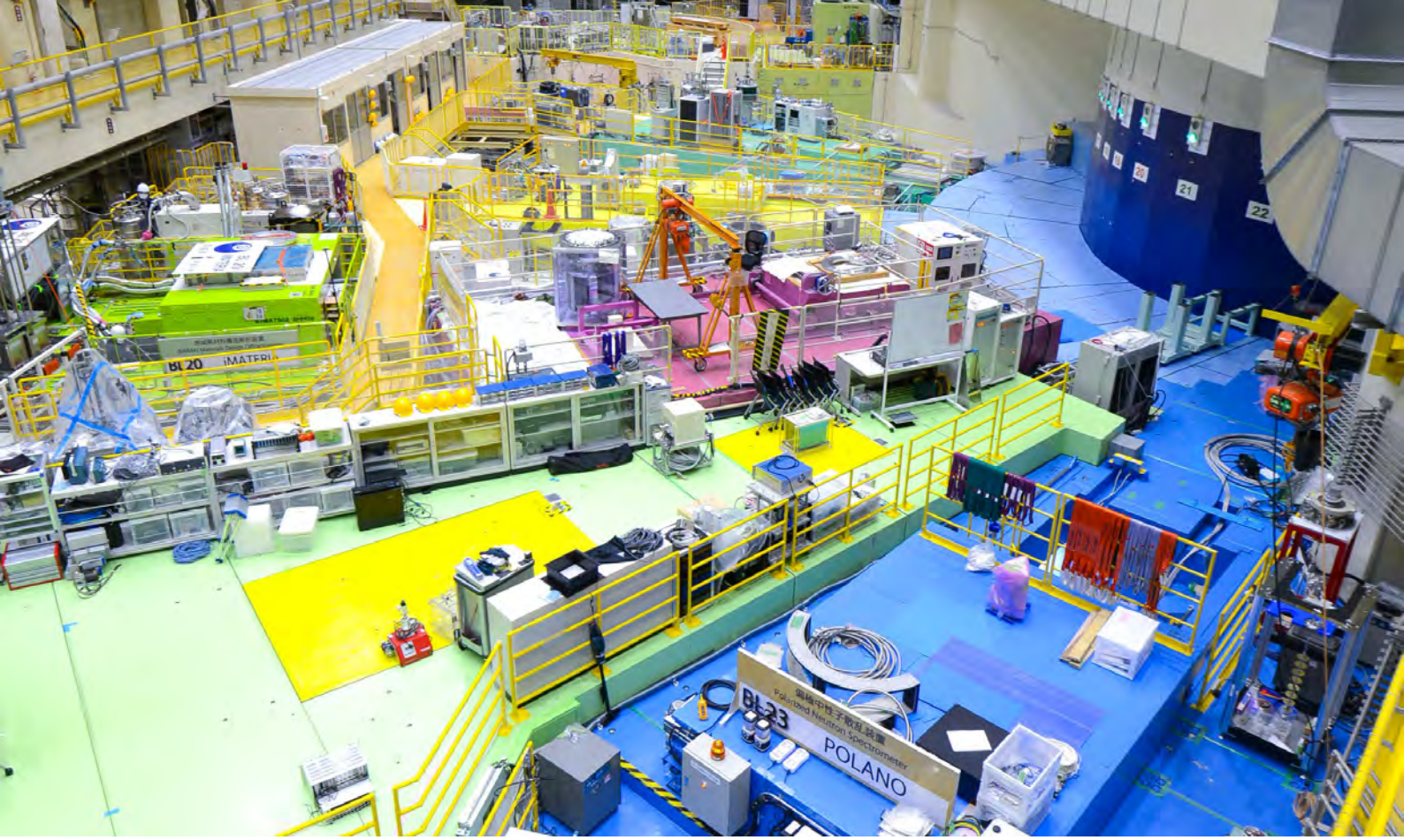

Materials and Life Science Experimental Facility

Overview

The FY 2023 user programme started in April with a beam power of 930 kW at the outlet of the 3GeV rapid cycling synchrotron (RCS) (820 kW at the MLF), and the beam power was varied from 740 kW to 950 kW at the outlet of the RCS, corresponding to 660 kW to 840 kW at the MLF, between April 2023 and February 2024 to maintain stable operation. Accidents and malfunctions reduced the beam time of the user program: 1) two fire accidents in the Hadron facility and the Main ring occurred in the 2023A period, 2) malfunctions of the cryogenic hydrogen system occurred shortly before the launch of 2023B. The availabilities of the beam operation for user program in FY2023 were 64.6% in 2023A and 77.1% in 2023B. 21 neutron beamlines and 7 muon areas were in operation. The muon H2 area was constructed in April 2023, and its commissioning has begun. H2 is the part of the ultra-slow muon production and re-acceleration up to 4 MeV for g-2/EDM and TμM in the future.

From FY2023, a new center of CROSS, Neutron Industrial Application Promotion Center, was commissioned by Ibaraki Prefecture to operate two Ibaraki BLs, BL03 and BL20. In addition to the existing Neutron Science and Technology Center of CROSS, which is in charge of 7 public BLs, these two centers of CROSS will work together to promote and support users for 9 out of 21 BLs in MLF.

More than 250 papers were published in 2023, with results ranging from fundamental physics to industrial applications. To promote research on the integration of art and science, one Muon Facility Project has been newly initiated to receive and objectively evaluate proposals from archaeologists and scholars specializing in the broad field of cultural heritage, collaborating with researchers from the National Museum of Japanese History, National Museum of Nature, etc. A budget

for this project has been allocated by the Ministry of Education, Culture, Sports, Science and Technology (MEXT) until fiscal year 2027.

The development of a large-area (768 x 512 mm) detector system for BL18, SENJU, was completed and its installation started in 2023. A high energy resolution X-ray spectroscopy by newly developed superconducting transition edge sensor (TES) detector with an energy resolution 10 times higher than that of conventional semiconductor detectors was realized for muon experiments. On-beam commissioning of polarized neutrons on BL23 POLANO has started with the combination of the SEOP as polarizer, the magnetic systems for the guide field, the Helmholtz coils and the subsequent bending mirror as analyzer. A compact on-beam SEOP setup has been developed to allow easy realization of polarized neutron experiments.

A deuteration laboratory (D-lab) was established and registered as a P1 facility. Besides deuteration of chemical samples, genetic recombination experiments for the synthesis of deuterated bio samples were started from May 2023. D-lab operates in collaboration with Gifu Pharmaceutical University, Kyoto University, ANSTO-NDF, and other institutions.

Two annual meetings were held. The Neutron & Muon School was held on December 18-22 as KEK-IINAS (Inter-Institution Network for Accelerator Science) School at J-PARC & JRR-3 campus. 105 of the participants attended on-line lecture, 17 of the participants attended the face-to-face lecture and the hands-on training. The annual meeting of the neutron industrial application was held in Akihabara with 339 participants consisting of 225 in person and 119 online. This annual meeting was held to merge the results of the MLF and the Japan Research Reactor - 3 (JRR-3) of JAEA. The MLF also hosted two international events. The 4th International Training School on Sample Environment at Scattering Facilities ISSE School was held on October 22-27 at the J-PARC campus. 18 “students” (17 from overseas) such as early career SE staff, graduate students and postdoctoral researchers and 20 “teachers” and staff (3 from overseas) participated. This school is a series of sample environment schools following the 11th International Workshop on Sample Environment at Scattering Facilities (ISSE) held at Nasu in 2022. Another one was the 11th Workshop on Neutron Wavelength-Dependent Imaging (NEUWAVE-11), which was held at the National Museum of Emerging Science and Innovation (Miraikan) in Tokyo on October 22-26 and was attended by 90 people (50 from abroad).

Neutron Source Section

1. Beam operation

The beam operation for the user program in fiscal year 2023 started on April 16 with beam power of 930 kW at the outlet of the 3GeV rapid cycling synchrotron (RCS) (820 kW at MLF). The beam power was raised up to 950kW at the outlet of RCS (840 kW at MLF) on April 20. However, the beam operation was suspended by the first fire accident at the 30 GeV main ring (MR), which occurred on April 26, and resumed on May 14. The beam power dropped to 800 kW at MLF on June 2 and to 750 kW at MLF on June 8 due to external temperature rise. The second fire accident at MR occurred on June 22, which ended the beam operation and a long maintenance work started.

As cryogenics loop system had trouble, the beam operation for the user program after the maintenance work was delayed and resumed on December 3 with beam power of 660 kW at MLF with certain pressure loss of cooling water flow and mercury flow in the new target. The beam operation stopped on December 25 for the holiday season and resumed on February 5 after replacement of the cooling system of the air conditioner at the MLF building. As the sufficient bubbling effect in the target could be confirmed, the beam power was increased back to 810 kW at MLF from February 12.

The availabilities of the beam operation for user program in FY2023 were 64.6% before the long outage and 77.1% after it.

2. Maintenance work

Some important remote-handling operations in the hot cell were performed. One was the replacement of the used proton beam window at the shielding plug with a new one by remote-handling operation. The proton beam window is mounted on the shielding plug and integrated into one unit. The unit of the proton beam window was replaced in the previous year. The assumed life of the proton beam window is about 10,000 MWh. The operation was successfully completed.

Another notable operation was the remote

han-dling test of the moderator and reflector assembly carried out using a spare assembly as in the previous year. An assembly consists of three moderators, a reflector, and a shielding plug, and only the used moderators and reflector are replaced while the shielding plug is reused just like the proton beam window. Because the operating lifetime of a moderator and reflector assembly is comparatively long, 30,000 MWh corresponding to 8 years at 1 MW, the last remote handling operation was done during the commissioning period before the beam operation of MLF started more than 10 years ago, so the inheritance of skills and experiences is very important. As the remote handling procedures were checked carefully, several failures to be solved could be found. The failures will be fixed and re-examination will be done with full-remote-handling to handle the actual radioactive assembly in the near future.

On September 4, specimens were cut out from the forefront wall of the used target vessel, which was operated with 2,273 MWh and 950 kW/pulse at maximum. The damage on the specimen of the inner wall of the mercury vessel, which was protected against the pitting damage by micro-bubble injection into mercury flow, was small (0.44 mm in the maximum). In addition, the damage on the specimen of the outer wall, the mercury boundary wall, was negligibly small, which was a promising result for the stable beam operation of 1 MW at MLF. On September 13, the used mercury target vessel was replaced with a new one with an improved bubble generator.

3. International workshop

Five researchers from the Neutron Source Section visited the Oak Ridge National Laboratory in the USA for the first time in 6 years and an international collaboration workshop was held from March 19 to 21, 2024, with the Spallation Neutron Source (SNS) of ORNL to discuss the neutron source system issues. Useful discussions for target vessel development, PIE tests, and so on, could be performed and the continuous collaboration was confirmed.

Neutron Science Section

1. User program

Despite the world-wide abrupt increase of the cost of fuel and electricity, the operation of the neutron user program at the MLF was quite stable except for the stops due to unexpected events. Initially, 60 days of operation were planned for 2023A and 80 days for 2023B, but the number of actual operating days was reduced to 44.5 days for 2023A due to fire incidents, and to 65 days for 2023B due to two issues, the cryogenic hydrogen system of the neutron target and the cooling water pump of the Rapid-Cycle Synchrotron.

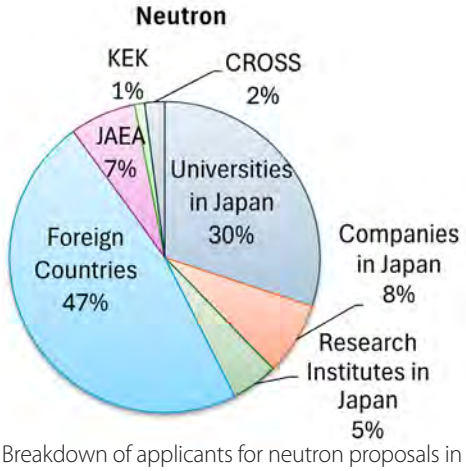

Fig. 1. Breakdown of applicants for neutron proposals in 2023B.

We had 277 and 289 neutron general proposals for the period of 2023A and 2023B, respectively. Almost half of the proposal applications came from foreign counties, and the other half came from domestic users. Figure 1 shows the breakdown of applicant's affiliation in case of the neutron proposal round 2023B. Also, we had about 1000 users (unique number of users for both neutron and muon), back to the level before the COVID.

We have recently instituted a new system requiring the submission of a Beamtime Utilization Report in addition to the MLF Experimental Report. This report must be submitted as the basis for beamtime usage for each of all proposals.

2. Highlights

There are 23 neutron beamline capacity in MLF, and 21 beamlines are now under operation. POLANO is the most recent generation of spectrometers in the MLF suite, J-PARC. It was designed for the purpose of wide momentum (Q) and energy (E) range inelastic measurements with the capability for polarization analysis. The main purpose of the POLANO is to accomplish polarized neutron scattering with higher neutron energy transfer by the time-of-flight (TOF) technique. By 2019, almost

all the beamline components had been set up except for the polarization devices, and at the time, the user program commenced in unpolarized mode. Recently, the polarization set up installation was completed, and neutron polarization commissioning just started. The newly developed spin exchange optical pumping (SEOP) polarizer system is shown in Fig. 2. In the world today, very few TOF spectrometers are currently available for polarization inelastic measurement. Particularly, *in situ* SEOP system can be utilized in a limited way. Our SEOP realizes over 80% of the 3He spin polarization, which is comparable to the world's highest polarization standards. Since the adiabatic fast passage (AFP) NMR is also equipped on this system, spin flipping can be easily controlled even remotely. We utilize a bending super mirror with 5.5 Qc iron-silicon mirror, which enables us to detect the spin polarization with energy up to 43 meV. This is rather higher energy to handle compared to the existing polarization instruments.

As shown in Fig. 3, the first data were observed using set up of the SEOP for a polarizer and the bending super mirror for an analyzer. The left panel of Fig. 3 shows a two-dimensional map of neutron intensities of the so-called non-spin flip (NSF) process. Striped structure caused by mirror blades is also observed. On the other hand, almost no signals were observed at the same area for spin flip (SF) process (right panel). Thus, a large difference between NSF and SF processes can be clearly observed, and we continue further commissioning toward high-energy polarization inelastic scattering.

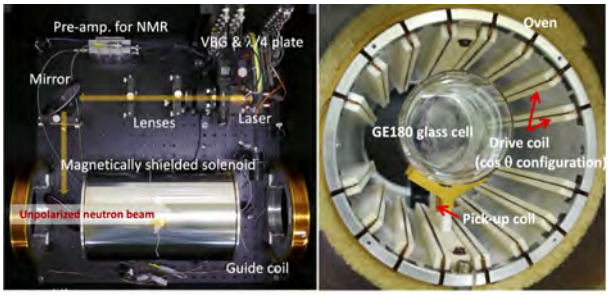

Fig. 2. Newly developed *in situ* SEOP polarizer system. Left: the SEOP system installed in the POLANO beamline. Right: NMR coils and a glass cell.

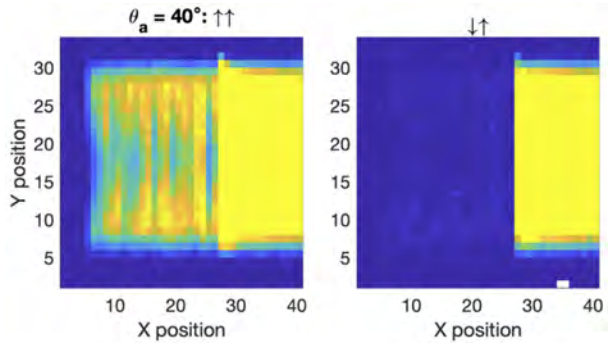

Fig. 3. Observed large difference of scattered neutron intensity between non-spin flip (left) and spin flip (right) processes at a scattering angle of 40 degrees.

3. Other activities

The Neutron Science Section (NSS) is constantly committed to activities that benefit the society, like organizing workshops and delivering lectures, as well as exchange of researchers and providing education for the younger generations. 1) We have a contract for a neutron collaboration program between the European Spallation Source (ESS) and the MLF, called SAKURA Mobility Programme. Workshops sharing ideas and knowledge about wide areas of the neutron science and instrumentation have been held. This year, a visiting program on discussion of neutron data analysis has been carried out, and a member of SENJU (BL18) joined the workshop. 2) NSS hosted two large meetings, one was NEUWAVE-11, the workshop for neutron imaging and the other was the 4th International Training School on Sample Environment at Scattering Facilities (ISSE school 2023), where the world-wide engineers of neutron facility try to practical training for their further skills. 3) Also, the NSS actively supports the following events: the 15th MLF Symposium in Quantum Beam Science Festa and the 7th Neutron and Muon School, which is a series of neutron and muon experimental training courses for younger scientists held every year at J-PARC and JRR-3.

For the other outcome from neutron beamlines at MLF, 256 scientific articles have been published in the year of 2023. 23 press releases have been also done.

4. Awards

A. Sano-Furukawa was awarded the Nishida Prize for Promotion of Geo- and Planetary Science for the research on hydrogen in the Earth's materials at high pressure and temperature based on synchrotron X-ray and Neutron beams.

The Best Poster Award of the Japan Institute of Metals and Materials 2023 Fall Meeting was granted to W. Mao and a member of TAKUMI (BL19) for the work of excellent combination of strength and ductility of an ultrafine-grained stainless steel at cryogenic temperatures studied by *in situ* neutron diffraction.

Also, the Best Poster Award of the 24th International Collaboration of Advanced Neutron Sources (ICANS XXIV) for the performance assessment of the cold-neutron disk-chopper spectrometer at J-PARC was received by M. Nirei.

Neutron Instrumentation Section

The neutron instrumentation section has been developing position-sensitive neutron detectors for upgrading of the neutron scattering instruments in the MLF. Our gas-based two-dimensional (2D) neutron detector system has been used in the BL17, one of the neutron reflectometers in MLF, since 2012 [1]. The readily available data acquisition system has been very useful to develop the detector system because of its multi-functionality and versatility. However, the multi-functionality of this DAQ system limits the count rate capability in the case of less than a few hundred kilo counts per second due to heavy loads on the processor. It also adds some complexities to the parameter setting of the detector system. Therefore, we have developed a new DAQ/monitoring module that can acquire the time-resolved neutron position data with increased count rates and simple functionality [2].

Figure 4 shows a photograph of the developed DAQ/monitoring module. This module can record 2D position data with time-of-flight information. The functions and operations of the module have been simplified as much as possible for robustness, long-term stability, and user-friendly interface. The module is designed in accordance with the VME standards, and it has a one-unit size. The module is equipped with a 68-pin and ERA00 connectors on the front panel for incident position data from the 2D neutron detector and T0 signal, respectively. The board also has universal serial bus (USB) and high-definition multimedia interface (HDMI) connectors for data storage and display devices, respectively.

Two operation modes are provided for users, which are standard mode and simple-display mode. The standard mode stores and displays the experimental data, and the simple-display mode only displays the experimental results on the monitor. The simple-display mode is useful for operation tests of the neutron detector and adjustments of neutron beams at an irradiation facility. Users can select either mode depending on their requirements.

To analyze the temporal responses in standard and simple-display modes, test signals of double pulses with varying time intervals were supplied. The counting loss was zero when the time interval was more than 1 μs and 0.6 μs in standard and simple-display modes, respectively. The count loss increased with a decrease in the interval time. Counting rate capability was evaluated with continuous test pulses. Figure 5 shows the counting losses in the developed module as a function of the incidental repetition frequency. The new DAQ/monitoring module can measure signals with no counting loss up to 1 MHz and 1.6 MHz in standard and simple-display modes, respectively. These results demonstrated the ability of the module to improve the counting rates and ensured the feasibility of the new DAQ/monitoring system.

References

[1] K. Toh *et al*., Nucl. Instrum. Meth. A, vol. 726, pp.169-174, Oct. 2013.

[2] K. Toh, *et al*., 2022 IEEE NSS/MIC Conference Records. DOI: 10.1109/NSS/MIC44845.2022.10399243

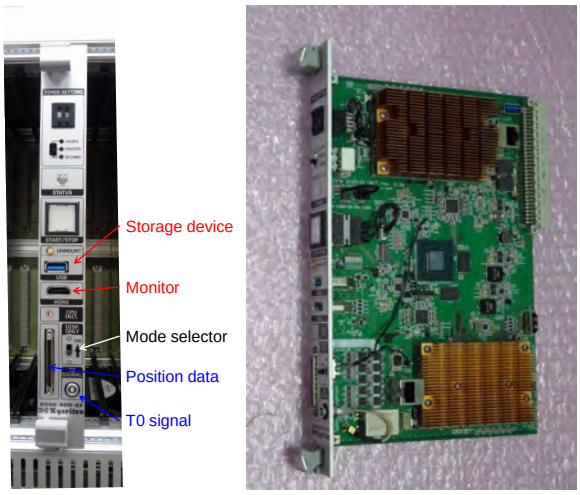

Fig. 4. Photograph of the front panel (left) and the entire view (right) of the new DAQ/monitoring module.

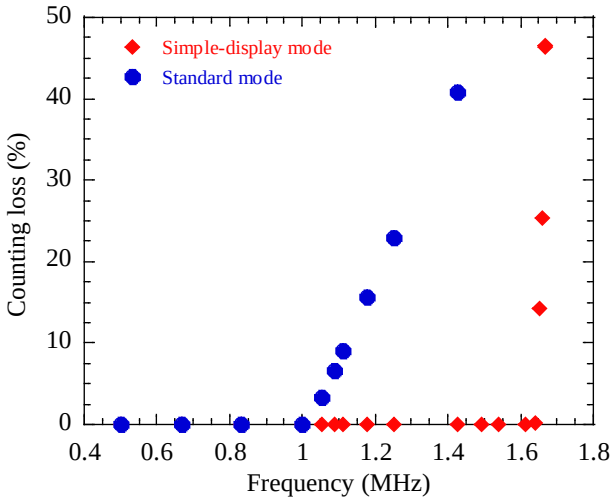

Fig. 5. Signal counting loss with new DAQ/monitoring module evaluated with continuous test pulses.

Muon Section

1. Overview

The fire incidents in other facilities in J-PARC stopped the MLF operation. Review and modification were conducted on all devices in the Muon Facility to prevent trouble due to similar origins. In addition, the MLF has been operating since the first beam in 2008, and measures to handle the deterioration had to be considered. The MLF continues to improve its robustness to ensure the stable and safe operation of the high-power beams. This article focuses on these measures.

2. Muon target monitor

The monitor system of the rotating target is under development for detecting abnormalities and obtaining the signs of long-term wearing in the rotating target. The torque of the rotating motor driver was analyzed to derive the intrinsic frequencies of the target wheel (0.25 Hz) and the bearing (0.1 and 0.15 Hz) in the rotational parts, as shown in Fig. 6. It is required to detect a change in the frequency data, eliminate the trivial effect like the temperature dependence, and to classify its characteristics. For this purpose, the spectral centroid method was adopted, in which the gravity center of the FFT spectrum was calculated to detect a change in the data easily. This method was confirmed to detect the abnormal vibrations (1.5-2.5 Hz) due to the force applied externally in the off-beam test. The off-beam data indicate a typical pattern and its slow changes. This could correlate with the wear of the bearings and could be applied to predict their remaining life.

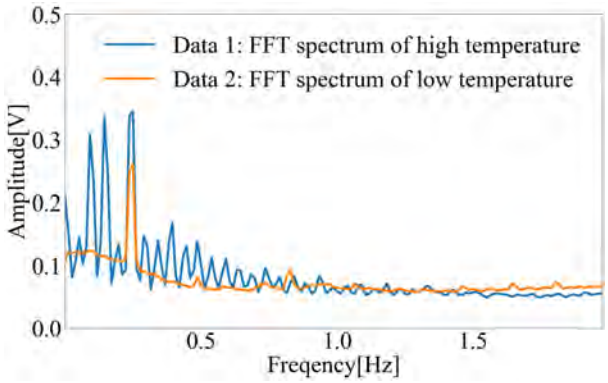

Fig. 6. PTypical FFT spectra.

3. Magnet power-supply monitor

The measures applied to prevent the fire incidents were determined as follows: (1) hardware inspection with a suitable periodicity (annual) and (2) installing a new monitoring system to detect signs of the power supply (PS) anomalies by monitoring current and voltage deviations. MUSE has 82 PSs for beamline magnets: 71 for constant-current ones, 9 for superconducting ones, and 2 for kicker magnets. Each of them has different interlocks. Figure 7 shows a scheme for controlling the PS by the EPICS program. When a user or staff inputs a PS operation command or current setting value on EPICS, the information is transmitted to the PS. The read-back information including the output current, voltage value, and interlock status is returned to the program. In the modified monitoring system, the EPICS issues a command to turn off the power supply when a current deviation error is detected in the PS and create an alert on the program. The new monitoring system was tested on 4 representative PSs in the 2024A period. The test was successful, and thus the system will be implemented in the remaining constant-current PSs in the next maintenance period. The monitoring systems of the PS for super-conducting magnets and kicker magnets are being developed.

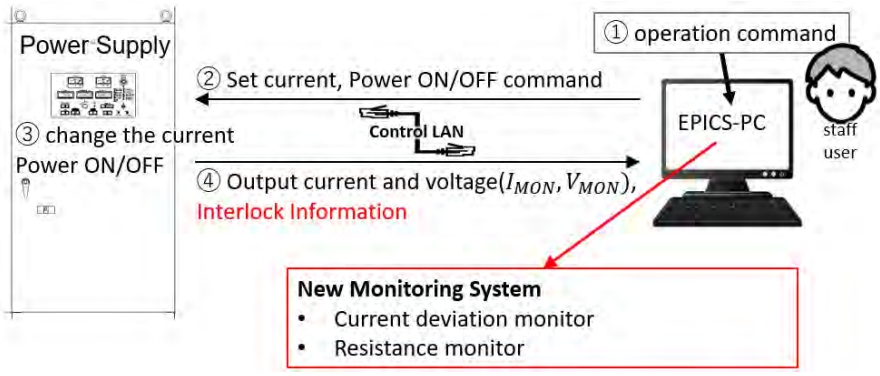

Fig. 7. Schematic of the power supply and the control program.

4. Transparent material for the Lyman-α laser

Materials that exhibit high transmittance in the UV wavelength region are generally those composed of light elements. Fluoride is used as optical windows for the VUV region because oxides show strong optical absorption. Especially LiF, MgF_2, and CaF_2 are widely used as UV windows, since CaF_2 has very low transmittance at Lyman-α wavelength. MgF_2 and LiF are candidates for our application. MgF_2 has been used because it is a birefringent material and the information about its refractive index at Lyman-α wavelength is insufficient which made its use questionable. With the increase in Lyman-α light intensity due to the upgrade of the U-line laser system, the disadvantages of the observed degradation in the LiF window became serious, and the MgF_2 window was decided to be used. The MgF_2 window showed higher transmittance than LiF over the entire 120-300 nm range and 1.5 times higher transmittance at the Lyman-α wavelength, as shown in Fig. 8. Based on these results, the LiF window was replaced by an MgF_2 one, and the intensity of the available Lyman-α light for ultra-slow muon generation was measured. The Lyman-α light intensity was enhanced from 5 μJ to 8 μJ. The MgF_2 does not form a color center even when irradiated with strong Lyman-α light, so the transmittance shows no degradation and can be used for a long period.

5. Present status of the S line

In 2022, the gate valve SGV1, located upstream of the S line, had a problem with Kapton foil, which separates the vacuum between the primary and secondary beamlines, getting stuck in it. The gate valve was replaced in 2022, but some parts of the Kapton fragments remained in the beamline. The work was carried out in July 2023 to recover this debris and to check whether any other Kapton debris remained. The mechanical strength of the recovered Kapton fragments will be checked. On the other hand, to prevent problems with the installed Kapton foil, a viewport and mirror were mounted downstream where the foil could be watched. This enables observation and checking during the beam operation using a web camera.

The kicker, the most important device for the simultaneous operation of the S1 and S2 areas, began to fail frequently around the start of full-time operation of the S2 area in the 2022B term. The failures were caused by the breaking of the Si MOS-FETs used in the Marx high voltage circuit, and aging degradation of the device is suspected. Each time a failure occurs, the Si MOS-FET is transplanted from a spare board and repaired. However, the device itself has already been discontinued, and thus we decided to employ SiC MOS-FETs. In April 2023, a Marx power supply unit replaced by a SiC MOS-FET was checked in the MLF. Comparing the generated voltage waveforms with the old Marx power supply unit, it was confirmed that there were no problems with the rise time and flat top time width, as shown in Fig. 9. Though the SiC MOS-FETs shows a slightly faster turn-off time, no problems occurred when the old and new Marx power supply units were operated together. The new Marx power supply will be replaced with the old one in April 2024, and a long-term operation test is planned.

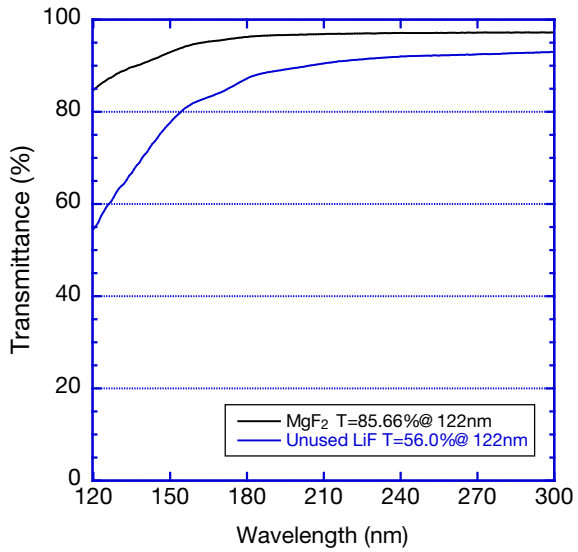

Fig. 8. Transmission spectra of the LiF and MgF_2 window in VUV to UV region. The blue line is the non-irradiated LiF window, and the black line is the MgF_2 window.

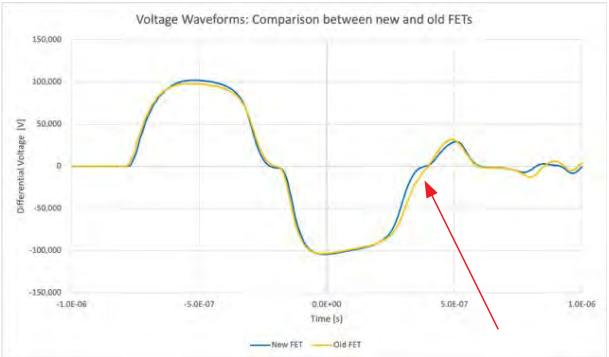

Fig. 9. Comparison of high voltage waveforms between the new and old Marx circuits. The blue curve shows the waveform on the new SiC MOS-FET, and the yellow one is the old Si MOS-FET. The arrow indicates a slight difference around the turn-off time.

Technology Development Section

The MLF deuteration laboratory provides support for the preparation of deuterated samples for neutron users in chemistry and structural biology. In structural biology, using neutron crystallography and small-angle neutron scattering, deuteration of protein samples has advantages. In neutron crystallography, the deuterium atoms in the deuterated protein can be observed more unambiguously than light hydrogen atoms in hydrogen proteins. This facilitates the understanding of enzymatic reactions. The neutron crystallography requires large protein crystals, which take significant efforts to prepare. On the other hand, deuterated proteins can be analyzed using smaller crystals. This is another advantage. When analyzing protein complexes consisting of multiple subunits using small-angle neutron scattering, structural information from specific subunits can be selectively observed by using samples in which only specific subunits are deuterated. This is an advantage that small-angle X-ray scattering does not have. Target protein is produced in *E. coli* by introducing a gene encoding the protein into the cell (This is called recombinant DNA experiments). Culturing *E. coli* in a medium containing deuterated nutrients and heavy water, results in production of deuterated proteins. Thus, recombinant DNA experiments are necessary for preparation of deuterated protein.

In FY2023, we have been allowed to conduct recombinant DNA experiments at the MLF deuteration laboratory. The MLF deuteration laboratory is equipped with a P1 level room to prevent the leakage of recombinant organisms. In FY2023, with the start of recombinant DNA experiments, we began operating experimental equipment such as an autoclave used to sterilize culture media and sterilize used recombinant *E. coli* (Fig. 10 a), a clean bench for performing aseptic operations (Fig. 10 b),microbial culture machines (Fig. 10 c, d, e, f). In many cases, the produced amounts of deuterated proteins are smaller than that of light hydrogen proteins. Therefore, to produce them efficiently, it is necessary to examine the culture conditions of *E. coli*. For this purpose, we started examining the culture conditions on a small scale using a small-scale culture machine (Fig. 10 c). The large-scale culture machine allows scaled-up culture under optimized culture conditions. Large flasks are used in large culture machines (Fig. 10 e), however, in that case, the oxygen in the medium necessary for *E. coli* growth may be insufficient. Using a jar fermenter allows air (or oxygen) to be forced into the culture medium, leading to good growth of *E. coli* and highly efficient protein production. In FY2023, we started producing deuterated proteins for neutron experiments using large culture machines and jar fermenters (Fig. 10 d, e, f).

The heavy water used in the culture medium is very expensive. If heavy water can be recovered from used culture media and reused, the costs for production of deuterated protein can be reduced. Therefore, we also started the operation of a rotary evaporator for distilling heavy water from used culture medium (Fig. 10 g). With the start of genetic recombinant DNA experiments and the operation of the above-mentioned equipment, it is expected that efficient production of deuterated proteins will become possible.

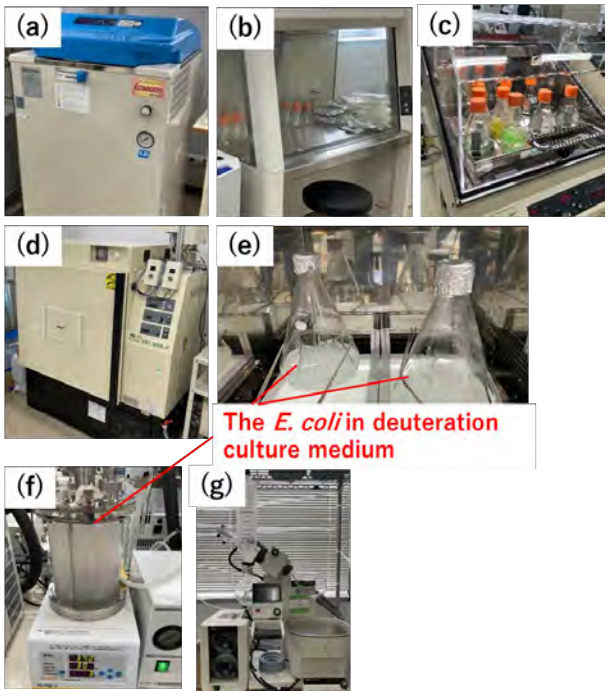

Fig. 10. The equipment for recombinant DNA experiments. (a) An autoclave, (b) A clean bench, (c) A small-scale culture machine, (d,e) A large-scale culture machine and large flasks inside it, (f) A jar fermenter, (g) A rotary evaporator.

Particle and Nuclear Physics

Neutrino Experimental Facility

The neutrino program at IPNS is a cornerstone of Japan's particle physics. In FY2023, the Neutrino Experimental Facility saw major progress after upgrades during the 2021-2022 shutdown. Beam operations restarted on April 17, stabilizing at 540 kW by April 24. However, fires at the MR and Hadron Hall in April and June, respectively, delayed activities until autumn.

Upgrades at the near detector site included installing new High-Angle TPCs and Time-Of-Flight panels, and commissioning the new Super Fine-Grained Detector (SuperFGD), which is a tracking detector, making the site operational by the autumn.

At the far detector site, Super-Kamiokande experienced geomagnetic coil failures in late October and November, requiring temporary repairs to minimize downtime and manage detection efficiency losses.

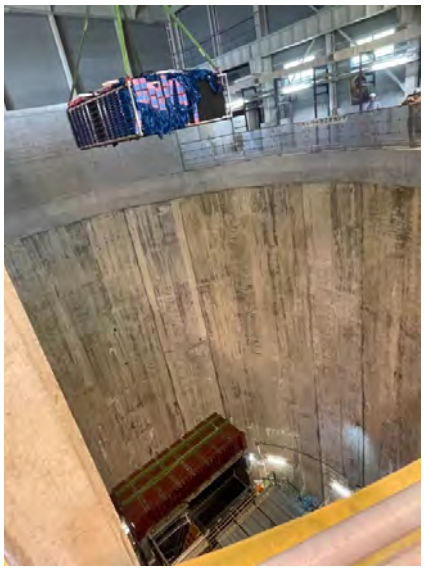

Fig. 1. Installation of SuperFGD into the near detector.

The beam operations resumed on November 21, reaching 600 kW, which resulted in permission for 1.3 MW operations being granted. A significant milestone was achieved in detecting the first neutrino interaction at SuperFGD in December, with power briefly hitting 760 kW.

Following a February maintenance break, operations restarted but were halted on February 23 due to a cooling system failure, canceling activities until March. The year ended with 3.23×10^{20} protons on target.

Meanwhile, the Hyper-Kamiokande project advanced with excavation and quality checks for installing 20,000 photomultiplier tubes by FY2026.

Hadron Experimental Facility (HEF)

IPNS Hadron group is operating the J-PARC Hadron Experimental Facility (HEF) and conducting particle and nuclear physics experiments at HEF as well as R&D for the high-intensity beam.

The J-PARC Hadron Experimental Facility Operation

HEF utilizes the high-intensity proton beam slowly extracted from the Main Ring (MR) synchrotron through the A-line to produce secondary beams for particle and nuclear physics experiments. Some of the 30-GeV primary protons are split off the A-line and used directly by the user experiments at the B-line. A new beamline (C-line), which delivers the 8-GeV primary protons for COMET (search for charged lepton flavor violation), started its beam operation in FY2022.

The first 30-GeV beam operation after the long shutdown for the upgrade of the MR power supplies was performed in June 2023. The beam time was interrupted by a fire incident in the Hadron power supply building. The new beam optics was applied to the primary beamline to eliminate the vertical dispersion at the beam-branching magnet, which resulted in the reduction of the spill microstructure in the B-line. During the short beam operation period, beam and detector commissioning was carried out at K1.8, KL secondary beamlines, and the B-line. At the K1.8BR beamline, measurement of anti-deuteron yield was carried out by the T98 group.

COMET Experiment

COMET aims to identify muon-to-electron conversion with a sensitivity higher than 10^{-14}. The COMET group undertook the construction of the Capture Solenoid (CS) magnet, with preparations underway for the final testing. Simultaneously, preparations for the physics detectors are being carried out in the HEF (Fig.2).

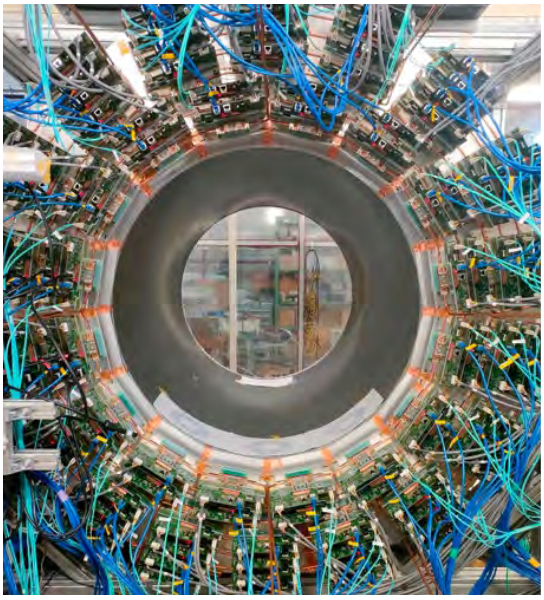

Fig. 2. Cylindrical drift chamber for COMET in the test at the Hadron Assembly Building.

Strangeness / Hadron Physics Experiments

Maintenance of the S-2S detectors and installation of the full set of Ge detector array were carried out at K1.8 beamline after beam commissioning. Reaction spectroscopy of the double-strangeness Ξ hypernucleus, ${}^{12}_{\Xi}$Be, (E70) and X-ray spectroscopy of Ξ^--C atom (E96) are planned to be conducted using S-2S.

Maintenance and reinforcement of detector modules are also in progress at the B-line for the E16 experiment which aims to study in-medium mass modification of vector mesons and the generation mechanism of hadron mass.

The E73 group at the K1.8BR beamline reported a ${}^{4}_{\Lambda}$H hyper- nucleus lifetime of 206±8(stat.)±12(syst.) ps, which has a smaller error than the previous data of 194^{+24}_{-26} ps. The lifetime was measured directly from the time difference between the production via the ^{4}He(K^-,π^0) reaction tagged by the beam K^- with high-energy γ emitted in the forward direction and the

π^- emission from weak decay. The results were obtained from the data taken in 2020 to check the feasibility of the ${}^{3}_{\Lambda}$H lifetime measurement. A production run of E73 will be conducted in 2024.

KOTO Experiment

The KOTO experiment studies the decay of a long-lived neutral kaon into a neutral pion and a pair of neutrinos. The process breaks the CP symmetry directly, and its branching fraction is well predicted in the Standard Model as 3.0×10^{-11}.

KOTO had been carefully analyzing data taken in 2021 and finalized its analysis in the summer of 2023. The expected number of background events was successfully reduced to 0.255. With the single event sensitivity of 8.7×10^{-10}, no signal candidate events were observed in the signal region, and the new upper limit for the branching ratio was set to be 2.0×10^{-9} at the 90% confidence level (preliminary), which is the world-best limit of this search.

KOTO is waiting for the next beam time, starting from April 2024, for further search with a higher beam power.

Future Plans of HEF

The 4th international workshop on the HEF extension project (HEF-ex 2024) was held at Tokai in a hybrid style from February 19 to 21. Sixty-three talks were presented, discussing the extension project of HEF and the latest state of physics research, including both experimental and theoretical aspects. Of the 172 registered participants, 35 were from foreign institutions, about 100 were present in person, and 12 came from overseas. After closing the session, a tour to visit HEF was also organized (Fig.3).

Fig. 3. Participant photo of HEF-ex 2024.

Particle and Nuclear Physics Experiments at MLF

At the MLF, the JSNS2 experiment to search for sterile neutrinos had its third and currently is having its fourth long-term data taking period. From April 2024, it ran with 950 kW beam power. Data corresponding to 4.33×10^{22} POT have been accumulated thus far. Also, for the second phase of the experiment, a new detector, the JSNS2-II, located at 48 m from the target, outside of the MLF experimental hall, is under construction, as shown in Fig. 4. The acrylic tank was installed, and it is in the final phase of the construction.

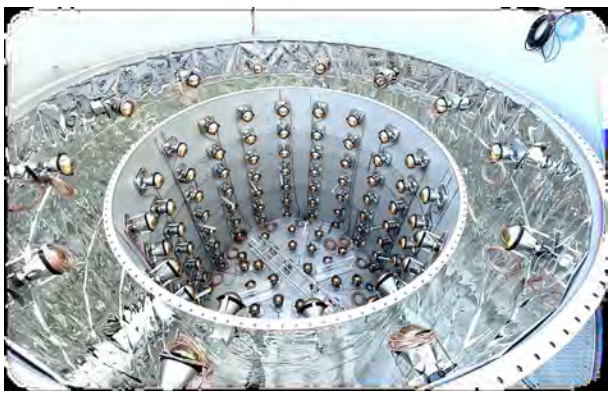

Fig. 4. Acrylic tank installation for the new JSNS2-II detector.

The J-PARC muon g-2/EDM collaboration is set to measure the anomalous magnetic moment and electric dipole moment of muons, indicators of physics beyond the standard model. This experiment, leveraging novel muon cooling, acceleration, and storage technologies, will be conducted at the MLF muon H line's newly developed H2 area. By March 2024, key infrastructure, like the laser room, was completed, with the beamline extension due in FY2024.

In FY2023, new data from muon cooling tests were collected at the S2 area, involving room-temperature muons generated via laser resonant ionization. This involved ionizing muonium with a 244 nm pulsed laser developed at Okayama University and measuring the muons' emittance.

Advancements in muon acceleration include testing the cavity of the Interdigital-H-mode Drift Tube Linac and enhancing the assembly of the Disk-and-Washer type acceleration cavity, which improves the acceleration field's uniformity. A transport line for the Disk-loaded-Structure type accelerator, crucial for the final acceleration stage, was also designed.

At Tsukuba, a demonstration using a low-energy

electron beam is nearing completion. Significant modifications have been made to the muon storage magnet and a new probe system developed to measure magnetic fields. Furthermore, advancements in data readout technologies have been validated, including a system with two FPGAs.

A critical progress evaluation by the IPNS committee in March 2024 provided essential feedback on the experiment's design and readiness.

Theory Group

KEK Theory Center has the J-PARC branch whose mission is to investigate hadron and nuclear physics which are experimentally studied at J-PARC, in collaboration with the experimental groups at IPNS and J-PARC. At the same time, the J-PARC branch serves as a hub gathering theorists and experimentalists in these fields. Actually, in FY2023 it held an international workshop "J-PARC Hadron 2023" which covered all nuclear and hadron physics investigated at J-PARC. Many theorists and experimentalists from the Asian region attended this workshop and had lively discussions on J-PARC hadron physics. It is noted that this workshop was the first international workshop, which was held on site by the J-PARC branch, after the COVID19 pandemic. This workshop contributed to restoring the relations among the Asian researchers in this field. In addition, several meetings were regularly held to discuss deeply specific fields in the J-PARC hadron physics: "Tokai Meeting" for strangeness nuclear physics and related hadron physics, and "A J-PARC-HI Evening" for a future physics program with heavy-ion beams at J-PARC. These meetings were mainly organized by the guest professors of the theory center.

ITDC-Esys-Tokai

The electronics system sub-group in Instrumentation and Technology Development Center (ITDC) constructs electronics systems for IPNS/J-PARC and collaborates with other institutes through a framework called "Open-It".

In the readout system for the muon beam monitor using SiC sensors for the COMET experiment, the circuit board for relaying digital signals requires high radiation tolerance of $O(10)$ n/cm^2. The readout function operated without problems even after the relay board was irradiated with 2.1×10^{11} n/cm^2 neutrons.

We have made improvements to the "ASIC board", a board for mounting the readout ASIC for the g-2/EDM experiment's silicon detector, and have developed a version 3 board that is expected to be mass-produced.

This is a high-density circuit board using the build-up method, and 8 ASICs are mounted on a substrate measuring approximately 100 mm x 40 mm, and one unit can read 1024 channels of silicon strips.

— Research Highlight —
T2K experiment enters a new phase of world-leading neutrino oscillation research

The Tokai-to-Kamioka (T2K) experiment is a long-baseline neutrino oscillation experiment, sending high-intensity neutrino beams from the Japan Proton Accelerator Research Complex (J-PARC) to the Super-Kamiokande detector about 300 km away. The T2K experiment started taking data in FY2010 and got the first-ever observation of the electron neutrino appearance in 2013. The discovery of the not-small oscillation opened the door to verifying the CP violation by measuring neutrino and anti-neutrino oscillations. In 2020, the T2K Collaboration showed the strongest constraint yet on the parameter, called CP violating phase, which governs the breaking of the symmetry between matter and antimatter in neutrino oscillations [1]. However, the significance was not enough to exclude the CP conservation and it was necessary to produce more neutrinos and to obtain a deeper understanding of the neutrino-nucleus interactions for better sensitivity.

The T2K Collaboration has started data-taking in 2023 with an upgraded neutrino beam and new detectors after the long shutdown to upgrade the main ring accelerator. The KEK/J-PARC Center upgraded the main magnet's power supply to increase the proton beam's repetition rate from 2.48 seconds to 1.36 seconds, which supplies more protons to the neutrino production target. Beam commissioning started in November 2023. The stable production of neutrino beam with about 710 kW has been successfully achieved, which is a record beam power with an increase of about 40% compared to before the upgrade. Furthermore, the continuous operation of the neutrino beam was successfully achieved at 760 kW in December, which is greater than the original design beam power (Fig. 5).

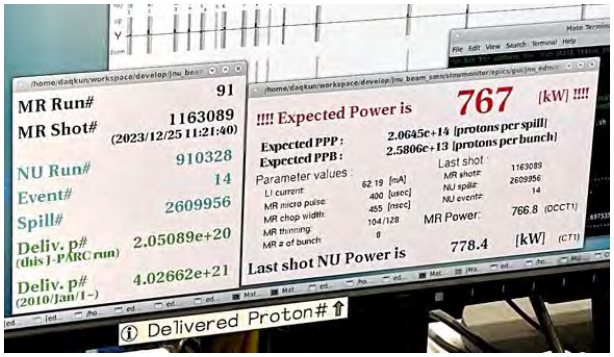

Fig. 5. Record beam power on December 25, 2023, greater than the original design power of 750 kW.

T2K Collaboration upgraded, modified, and exchanged instruments in the neutrino beam facility, such as neutrino production targets, electromagnetic horns, and beam monitors in 2021 – 2023 to accept higher beam power. The heart of the neutrino generation devices are the electromagnetic horns (Fig. 6). The power supply and other components for the horns were upgraded to increase the current of the horns from 250 kA to 320 kA. It improves the focusing efficiency of parent particles of neutrinos, such as charged pions, and the quality of the neutrino beam. The number of neutrinos delivered to the Super-Kamiokande detector was increased by about another 10% by the upgrade.

Furthermore, the T2K Collaboration has started the operation of the new neutrino detectors (Fig. 7) at the Neutrino Monitor Building located 280 m downstream

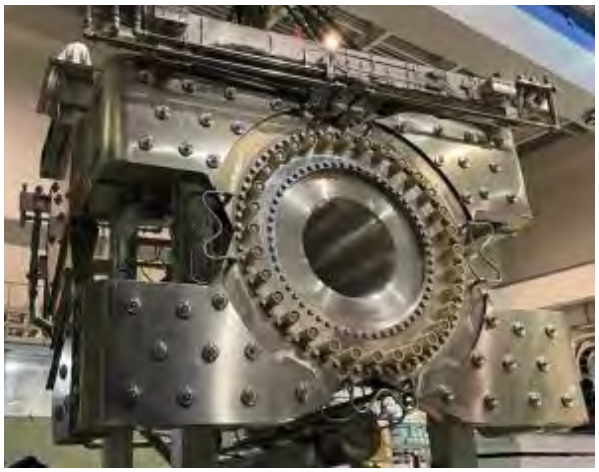

Fig. 6. A photo of the upgraded second horn with improved cooling capacity.

Fig. 7. A photo of the upgraded near detectors: SuperFGD, bottom HATPC, and 4 ToFs.

of the neutrino production target. There are three types of newly installed detectors, called Super Fine-Grained Detector (SuperFGD), High Angle Time Projection Chambers (HATPC), and Time-of-Flight (ToF) detectors.

The SuperFGD has a target mass of about 2 tons and is located at the center of the upgraded detectors. It has a novel structure consisting of roughly 2 million 1 cm^3 plastic scintillator cubes with three holes. About 56,000 optical fibers penetrate the cubes from three directions and are optically coupled with photodetectors at the ends of the fibers. It enables us to measure charged particles with high resolution from three projections. The HATPC is a gaseous detector composed of two field cages that produce a uniform electric field and read-out system of resistive Micromegas modules. It allows for an excellent reconstruction of the track trajectory emitted by neutrino interactions in the SuperFGD. The ToF detectors surrounding the SuperFGD and HATPC are used to determine the direction of particles and particle identification. These detectors were installed sequentially from July to October. We succeeded in observing neutrino event candidates from the newly acquired data (Fig. 8).

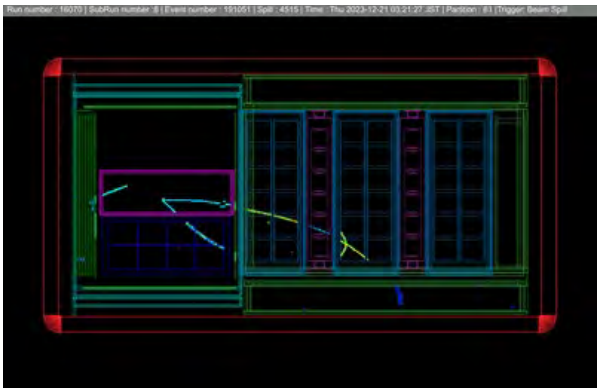

Fig. 8. An event display of a neutrino interaction candidate in the SuperFGD with one track entering the bottom HATPC and another entering the original downstream detectors.

With these improvements, the T2K experiment entered a new phase with an enhanced neutrino beam and novel new detectors. While supplying the beam, a further increase of the beam power is undergoing toward 1.3 MW. Observing about three times as many neutrino interactions (per unit time) will be possible. The T2K will continue the measurement with significantly improved sensitivity to verify the CP violation. These improvements will also play a key role in the next generation of neutrino research with the Hyper-Kamiokande detector, currently under construction. With the combination of the enhanced J-PARC neutrino beam, observing about 20 times as many neutrino inter- actions (per unit time) as before will be possible. The new phase of the T2K experiment is also an important step for the next generation of experiments, and T2K is expected to continue to lead the world in neutrino research, unraveling the mystery of the missing anti- matter from our universe.

Reference

[1] K. Abe *et al*., The T2K Collaboration, Nature **580**, 339 (2020).

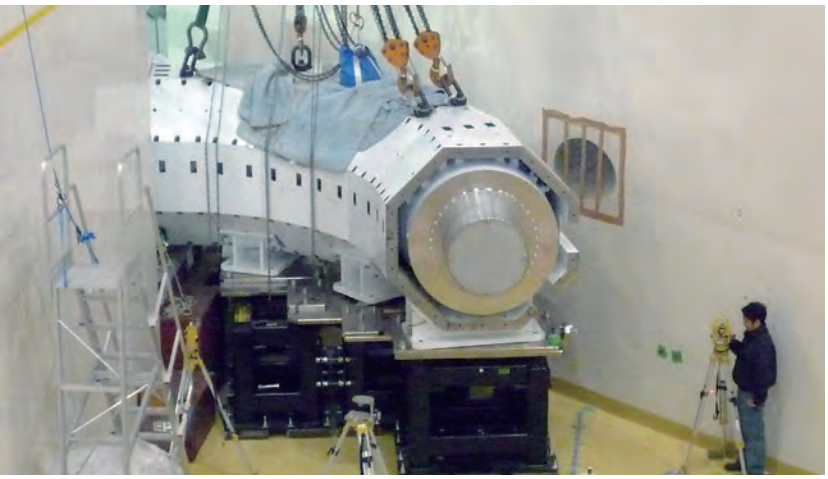

Cryogenics Section

Overview

The Cryogenics Section supports scientific activities in applied superconductivity and cryogenic engineering, carried out at J-PARC. It also supplies cryogen of liquid helium and liquid nitrogen. The support work includes maintainance and operation of the superconducting magnet systems for the T2K neutrino beamline and the muon beamlines at the Materials and Life Science Experimental Facility (MLF) and construction of the magnet systems at the Hadron Experimental Facility (HEF). It also actively conducts R&D works for future projects at J-PARC.

Cryogen Supply and Technical Support

The Cryogenics Section provides liquid helium cryogen for physics experiments at J-PARC. The used helium is recycled by the helium gas recovery facility at the Cryogenics Section. Fig. 1 summarizes the liquid helium supply in FY2023.

Liquid nitrogen was also supplied to the users for their convenience. Its amount in FY2023 is summarized in Fig. 2. Additionally, the LINA experiment using superconducting magnet was carried out in the MLF, therefore the total amount of LHe supply was increased by 5000 L compared with the last year.

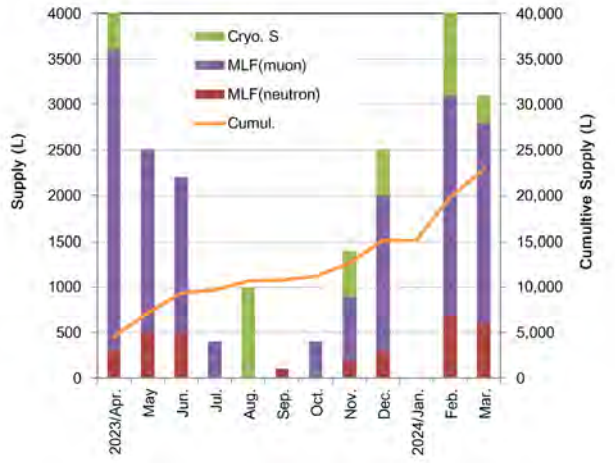

Fig. 1. Liquid helium supply at J-PARC from April 2023 to March 2024.

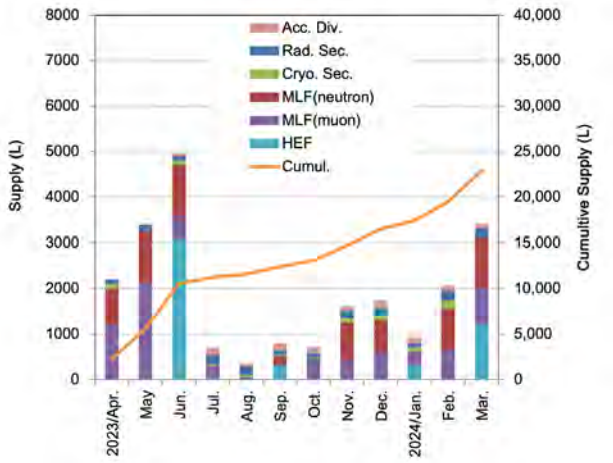

Fig. 2. Liquid nitrogen supply at J-PARC from April 2023 to March 2024.

Superconducting Magnet System for T2K

Table 1. Operation history of the T2K superconducting magnet system.

	2023									2024			
	April	May	June	July	Aug.	Sept.	Oct.	Nov.	Dec.	Jan.	Feb.	Mar	April
Operation	⟷ 4/9-4/27		⟷ 6/11-6/22					⟷ 11/11-12/27			⟷ 1/28-2/27		
Maintenance							⟷						

The superconducting magnet system for the T2K experiment operated during the periods shown in Table 1. The system worked well without disturbing the beam time. The total operation time was 130 days and regular maintenance works were carried out in the autumn. Fig. 3 summarizes the incidents in the refrigeration system from FY2009, which shows that recently the magnet system has been quite stable.

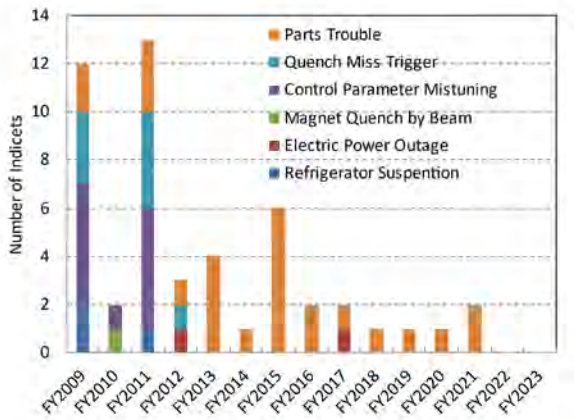

Fig. 3. Annual number of incidents in the SC Magnet system during operation.

Superconducting Magnet Systems at the MLF

The Cryogenic Section contributes to the operation and maintenance of the superconducting magnet systems at the Muon Science Facility (MUSE) in the MLF. The superconducting solenoid in the Decay Muon Line (D-line) was operated from January 11 to July 4. 2022. Annual maintenance, involving the cooling water system, the safety valve and other devices, was performed from July to the end of October.

The section also contributes to the operation of the MRI magnet for the MuSEUM experiment. It was moved from NU1 to H1 area in MUSE in November 2022 and ramped up to 1.7 T for the experiment.

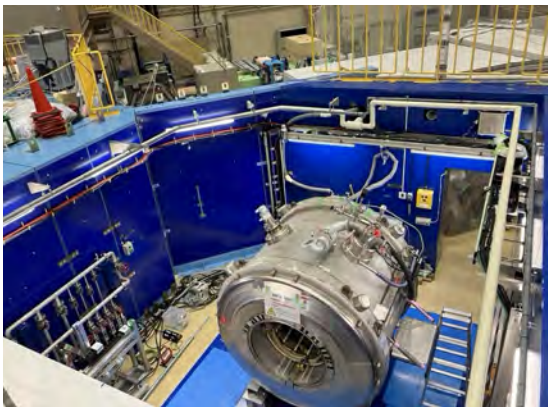

Fig. 4. The MRI magnet in H1 area of MUSE.

Superconducting Magnet Systems at the HEF

The COMET experiment is under construction in the Hadron South Experimental Hall (HDS) of the Hadron Experimental Facility (HEF). The Cryogenics Section was involved in the construction of the superconducting magnets and cryogenic system. The magnet system consists of a pion capture solenoid (PCS), a muon transport solenoid (MTS), a bridge solenoid (BS), and a detector solenoid (DS). The MTS and BS magnets have already been delivered to J-PARC. The PCS magnet is under construction at the factory. The insulation problem in the PCS coil was fixed and the assembly of the cryostat was almost completed in FY2023. The construction of the DS magnet has been finished and the magnet was successfully cooled down for the upcoming magnetic field measurement in the factory.

In FY2022, the J-PARC accelerator provided a beam for the COMET experiment with a simple secondary beamline configuration using only MTS called Phase-α. The MTS was operated at half current rating of 105 A for solenoid corresponding to a magnetic field of 1.5 T. In FY2023, the commissioning of MTS aimed at generating a 3 T solenoid field was performed after the beam time. We succeeded in the combined current transport for Phase-I experiments of 210 A for solenoid (3 T), ±175 A for dipole (±0.07 T). We confirmed that the magnet protection system worked properly at the nominal current by performing current shut-off test. A coil temperature rised up to 53 K in the test and the magnet was recovered to operating temperature in 24 hours by automatic operation of the Helium refrigerator with optimized sequence, as shown in Fig. 5.

During the MTS commissioning we observed several fake quench triggers due to instability of the power supply, whereas only two events of real coil quench was observed at 187 A and 200 A. The control circuit in the power supply was investigated in the magnet operation. It was found that the capacitance of noise filter for the current transformer which makes a control loop of the output current was too large for our magnet system.

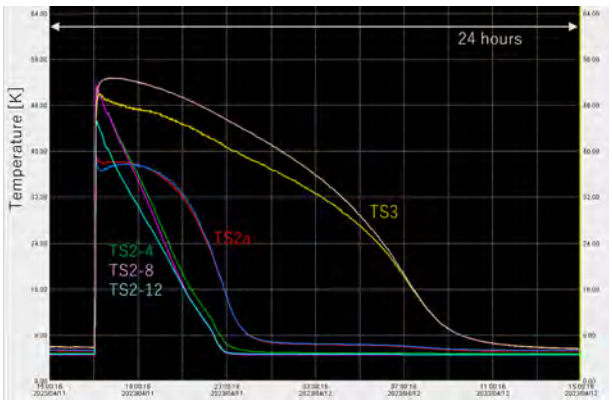

Fig. 5. Trend of the MTS coil temperature after the shut-off test at nominal solenoid current of 210 A.

R&D for the Future Projects at J-PARC

The g-2/EDM project aims for the precise measurement of the anomalous magnetic moment and the electric dipole moment of muons. This experiment was proposed at the MUSE H-Line. A superconducting solenoid with a high field homogeneity, better than 1 ppm locally, plays a very important role as a muon storage ring. The main superconducting coils are cooled by liquid helium, which almost evaporates once magnet quench occurs. The helium gas needs to be recovered and reused to reduce the operation cost. The helium gas bag system to collect the evaporated helium gas is now being designed. It will be built on the roof of the new experimental hall for the project as shown in Fig. 6.

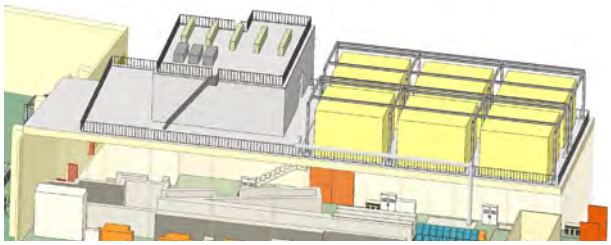

Fig. 6. Schematic design of the helium gas bag system (yellow objects) for the g-2/EDM project

Applied research based on REBCO (rare-earth barium copper oxide) exhibiting high temperature superconductivity is underway to realize a solenoid system for the future muon source at the muon beamline of the MLF second target station. The solenoid will be required to operate in high radiation environments where the absorbed dose reaches 100 MGy. In such an environment, conventional organic insulating methods, such as epoxy resin, will not be applicable. Therefore, we have been developing mineral-insulated HTS coils to which ceramic coating and ceramic bonding technology are applied. As a result of research and development so far, we succeeded in molding a ceramic insulating layer of about 20 μm thickness on both sides of a tape-shaped conductor with a thickness of 0.1 mm and a width of 4 mm over a length of 40 m using a continuous spray and drying method. The about 20 μm thick-insulating layer composed of a one-to-one ratio of aluminum oxide and silicon dioxide has been confirmed to have a withstand voltage of 2 kV. Using these ceramic-coated REBCO tapes, three double pancake type racetrack coils for cooling and excitation testing as part of a U.S.-Japan Science and Technology Cooperation Program in High Energy Physics were fabricated by the so-called wet winding method using ceramic adhesive. Figure 7 shows a picture of the coil during assembly. The coil with a straight section length of 300 mm and a width of 20 mm is optimized for a test equipment Brookhaven National Laboratory (BNL) in the United States. The performance evaluation tests in a liquid helium immersion-cooled test stand with a backup field of approximately 9 T were performed at BNL in the winter of FY2023. Figure 8 shows the test situation at BNL. Although the test coil was damaged due to a quench during the test, it successfully transported a current of 1243 A in an external magnetic field of 6 T at maximum load. This result is estimated to be about 52% of the performance of the conductor itself. The cause of the deterioration may be structural problems with the coil, which has a bending radius of 5.5 mm, and damage during the winding and assembly process. However, it provides valuable knowledge toward the realization of mineral-insulated HTS coils.

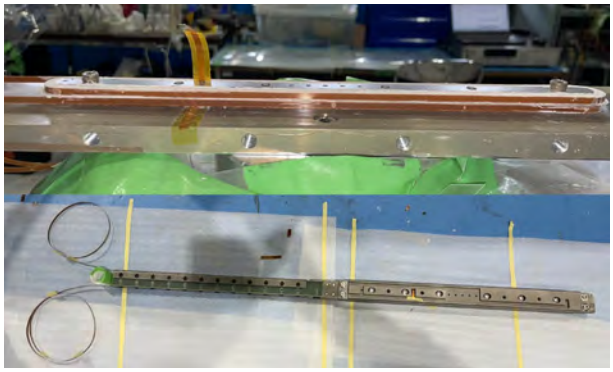

Fig. 7. Photographs of the assembled mineral-insulated racetrack coil based on REBCO coated conductor.

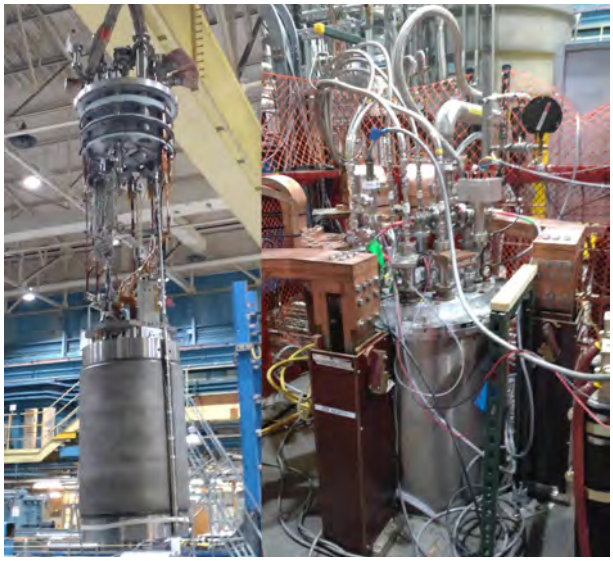

Fig. 8. Photographs of the performance verification test at BNL.

Information System

Overview

The Information System Section plans, designs, manages and operates the network infrastructure of J-PARC and also provides support to ensure its information security. In terms of computing, until now, J-PARC has owed its major computer resource for analyzing and storing data from neutrinos, nuclear physics and MLF experiments to the KEK central computer system, KEKCC. The section connects the J-PARC network to the KEKCC directory and helps the users to utilize the system effectively.

Status of Networking

Since 2002, the J-PARC network infrastructure, called JLAN, has been operated independently from KEK LAN and JAEA LAN in terms of logical structure and operational policy. In 2023, the total number of hosts on JLAN was 5,513, and it decreased by 291 hosts this year. The growth curve of edge switches, wireless LAN access points and hosts (servers and PCs) connected to JLAN are shown in Fig. 1.

In April 2022, the National Institute of Informatics (NII) upgraded SINET (Japan Science Information Network https://www.sinet.ad.jp) from version 5 to 6. SINET is not only a gateway from JLAN to the internet

but also an important connection between the Tokai and the KEK Tsukuba sites in J-PARC.

Figures 2 and 3 show the network utilization of the internet from/to JLAN. Since the bandwidth capacity for the internet through the SINET is 10 Gbps (giga-bits per second), it is clear that there is enough space for additional activity. Figures 4 and 5 show the statistics of data transfer between the Tokai and Tsukuba sites. KEKCC is maintained at the KEK-Tsukuba campus, and most of the transferred data are archived and analyzed on KEKCC. Figure 6 shows the peak network traffic rate between the sites in each year. The network bandwidth capacity between the two sites is 20 Gbps. This shows that the usage level has been approaching a half of it, especially during the period when the Hadron and g-2 facilities were running.

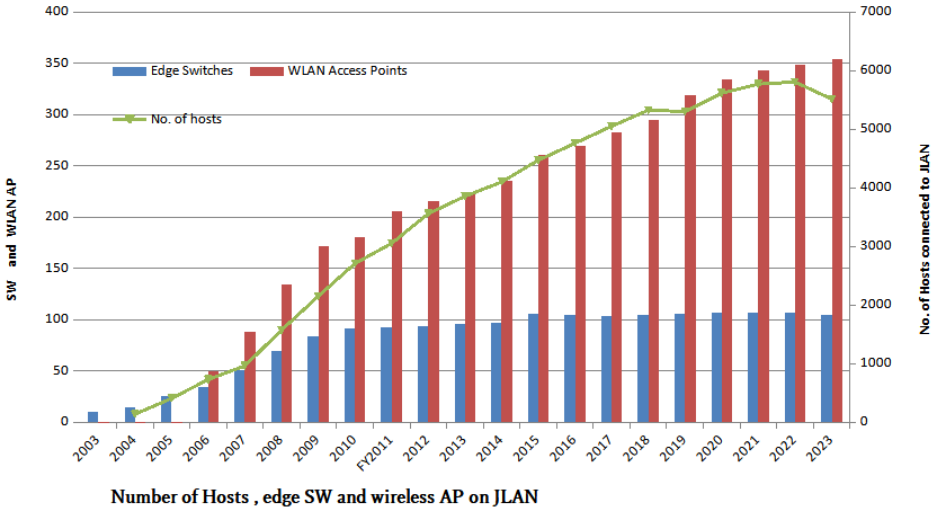

Fig. 1. Number of hosts, edge SW and wireless AP on JLAN.

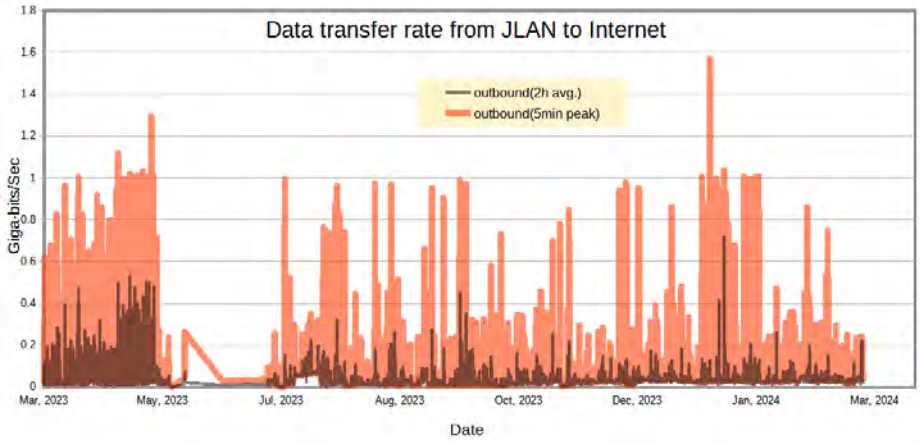

Fig. 2. Network traffic from JLAN to the internet.
(1 hour average and 5 minutes peak value)

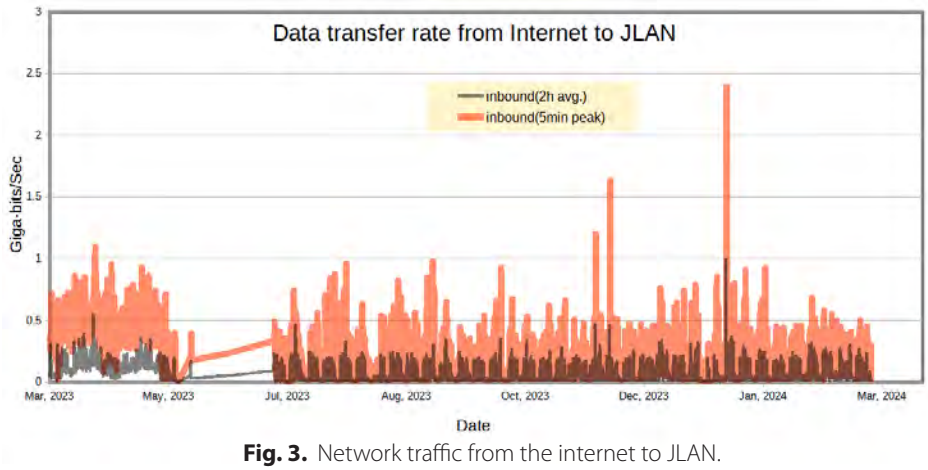

Fig. 3. Network traffic from the internet to JLAN.
(1 hour average and 5 minutes peak value)

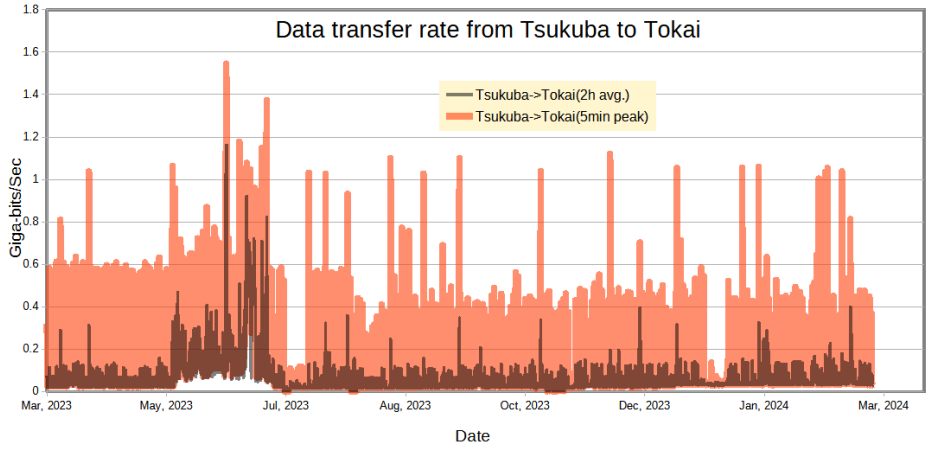

Fig. 4. Network traffic from Tsukuba to the Tokai sites.

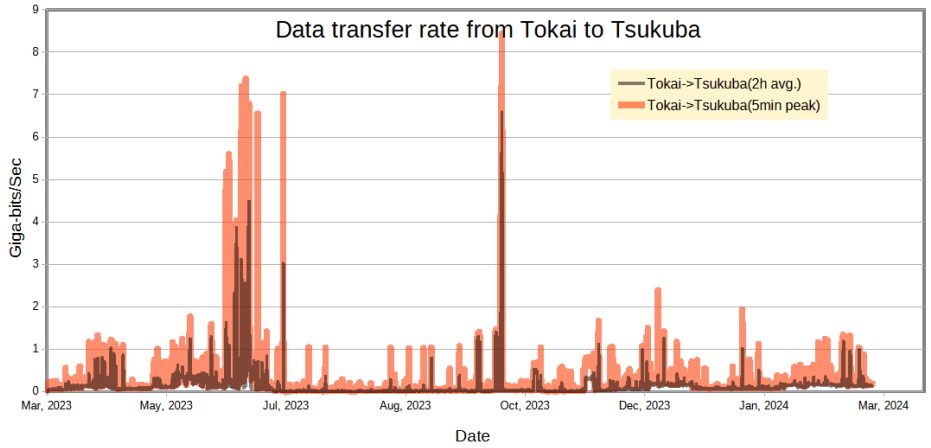

Fig. 5. Network traffic from Tokai to the Tsukuba sites.

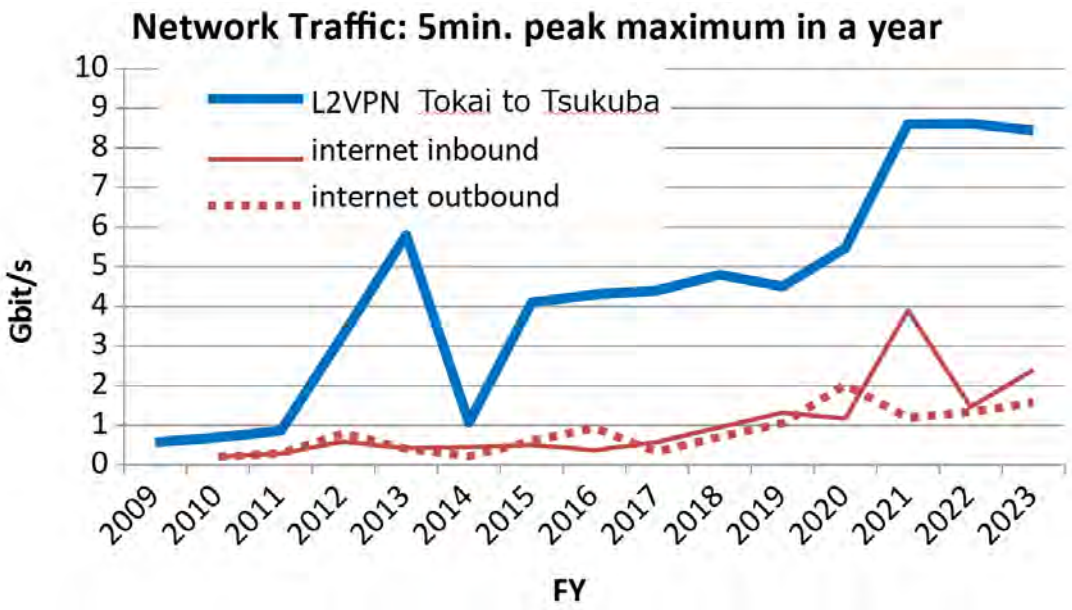

Fig. 6. Peak network traffic between Tokai and the Tsukuba sites for the recent years.

Internet Connection Services for Visitors and Public Users of J-PARC

Since 2009, J-PARC had offered a Guest network (GWLAN) service, which is a wireless internet connection service for short-term visitors, available in almost all J-PARC buildings. In the end of 2014, additional network service called User LAN had started. To use the GWLAN, users are required to receive a password at the J-PARC Users Office beforehand, while in the User LAN, they are authenticated by the same ID and password for the User Support System, which is also used for dormitory reservation and so on. From March 2016, a new service called "eduroam" had been started. The eduroam (https://www.eduroam.org/) is a secure roaming access service developed for the international research and education community and shared among a huge number of research institutes, universities, and other institutions around the world. The eduroam service will be a convenient third option of internet connection service for J-PARC visitors. Figure 7 shows this fiscal year's usage statistics of GWLAN, User LAN and eduroam services.

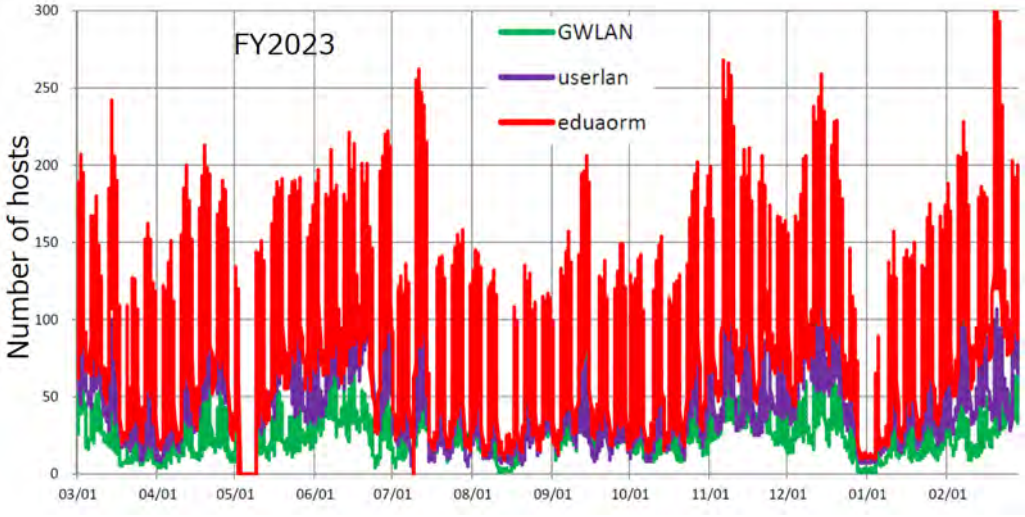

Fig. 7. Usage trends of GWLAN, User LAN and eduroam.

Status of Computing

Table 1. Computing resources in the KEKCC.

CPU (Intel Xeon Gold 6230)	15000 cores
RAID Disk (GPFS)	25.5 Peta Bytes
Tape Library (HSM)	100 Peta Bytes

Since J-PARC does not have computing resources for physics analysis, starting from 2009, the KEK central computing system (KEKCC) at the KEK Tsukuba campus has been mainly used for that purpose. KEKCC is shared by most of the research groups of KEK, including J-PARC. At the Neutrino (T2K), Hadron and Neutron (MLF) experiments, the data taken in J-PARC are temporarily saved at their facilities and then promptly transferred, stored, and analyzed at the system in Tsukuba. The storage of the system is also utilized as a permanent data archive for their data. The third upgrade of the system was completed in 2020, and the computing resources are shown in Table 1. The fourth upgrade will be done in the summer of 2024. Figures 8-10 show the utilization statistics of the computing resources in FY2023. The main users who used the CPU and storage constantly were from the Hadron and Neutrino experiment groups. The MLF group also started to store data on tapes on the system.

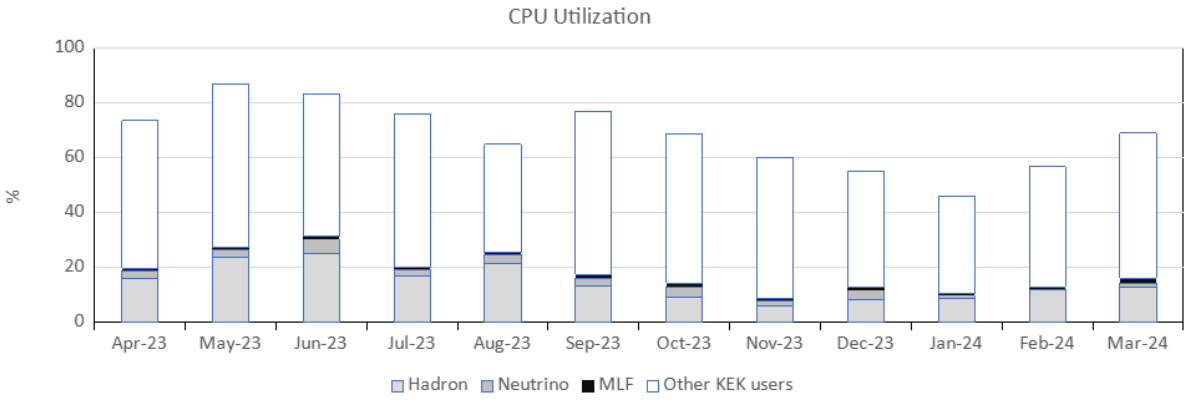

Fig. 8. CPU usage statistics of KEKCC in FY2023.

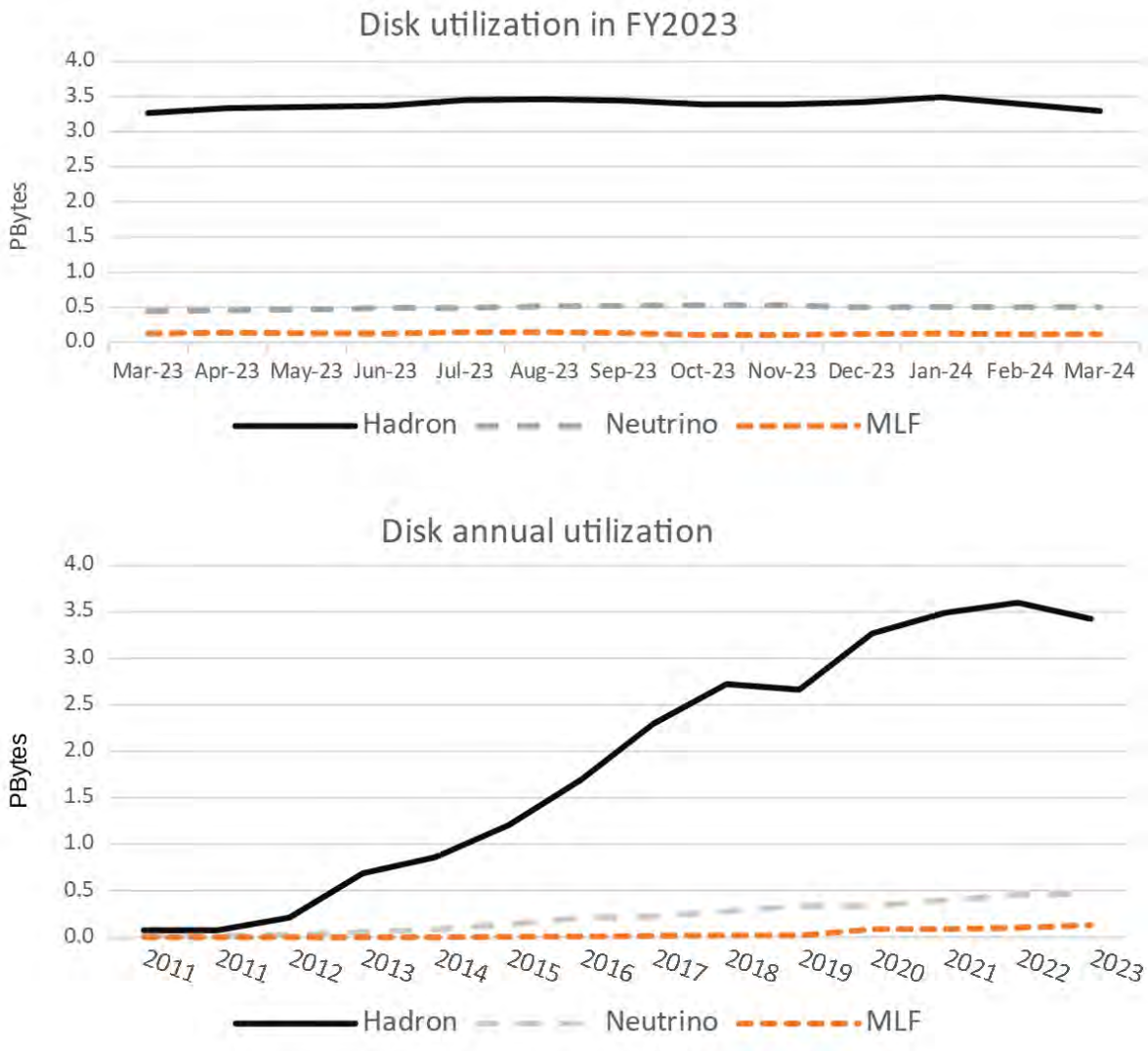

Fig. 9. Disk usage statistics (top: trend of FY2023; bottom: annual trend)

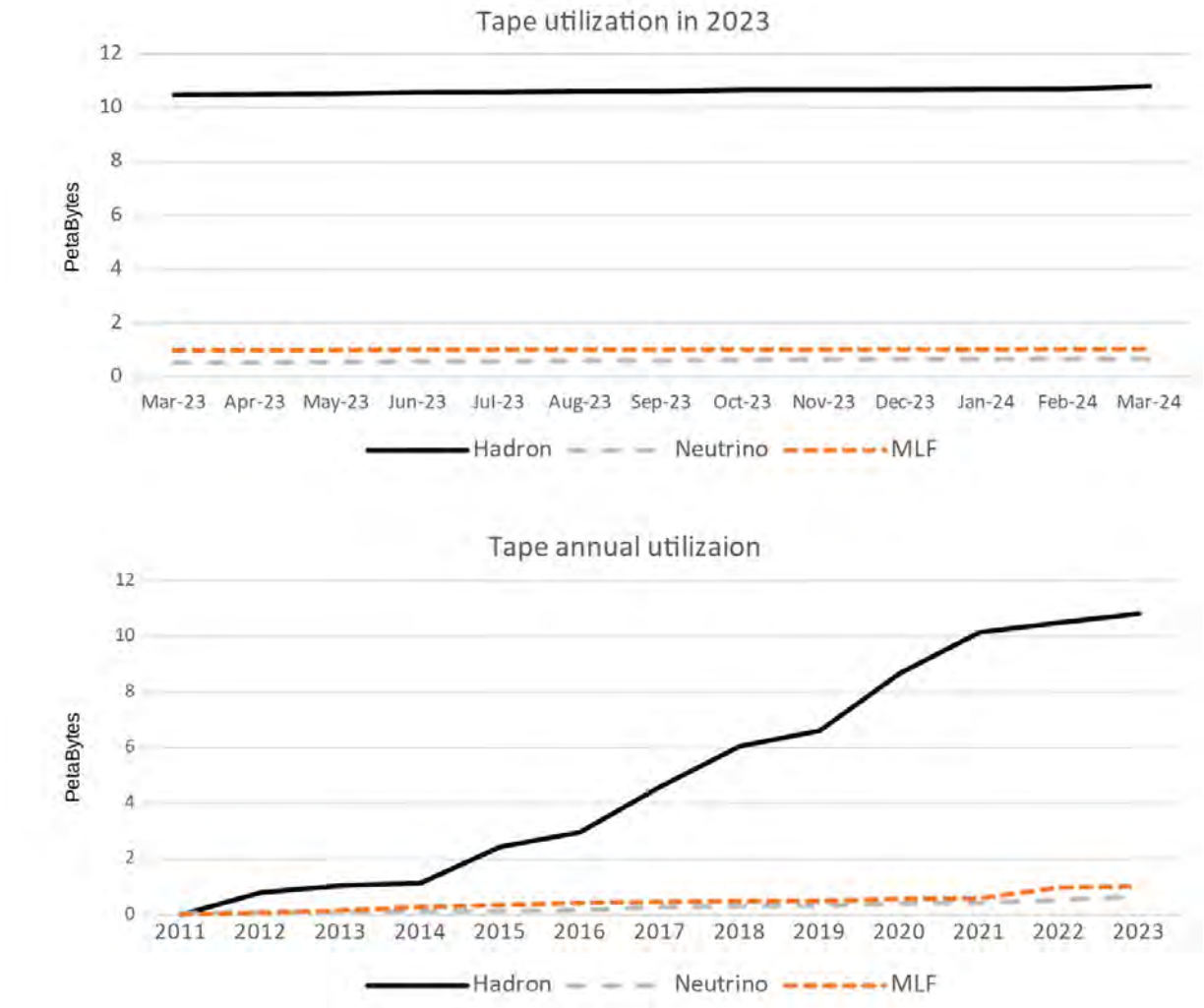

Fig. 10. Tape library usage statistics (top: trend for FY2023, bottom: annual trend)

Transmutation Studies

Overview

We are developing nuclear transmutation technology with accelerator-driven systems (ADS) using the J-PARC's research resources and expertise in high-power accelerator and target technologies. The ADS is an effective nuclear system for volume reduction and mitigation of the degree of harmfulness of high-level radioactive waste produced in nuclear power reactors. We believe that the ADS is one of the most beneficial applications of high-power accelerators for contributing to human society, such as the carbon neutrality and SDGs.

We have developed the basic design of the Transmutation Experimental Facility (TEF). As for the ADS Target Test Facility (TEF-T) for irradiation of beam window materials in a flowing high-temperature lead-bismuth eutectic (LBE) alloy target, the design has been published in the report JAEA-Technology 2017-003. After that, the future direction of the TEF program was discussed. The result was stated in the JAEA's mid-to long-term plan (MLTP) for FY 2022-2029 as follows; "Regarding the J-PARC TEF program, JAEA reframes the facility plan based on the results of related R&D and versatile needs to the facility in addition to nuclear transmutation research."

Now we are building up the concept of the proton irradiation facility, which is the advanced concept of TEF-T, to comply with the MLTP. Figure 1 shows the latest concept of the proton irradiation facility with four important areas of applications. Next to the facility, the installation of a hot laboratory for post-irradiation examination is under planning. A conceptual study of the hot laboratory, including items to be tested, testing flow, testing equipment, and a proposed layout, has been summarized in the report JAEA-Technology 2023-025.

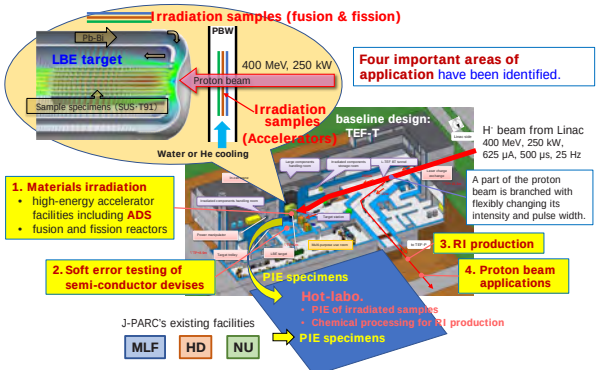

Fig. 1. The concept of the proton irradiation facility.

On July 27, a workshop on the "J-PARC Proton Beam Irradiation Facility" was held. There were 94 participants, with 32 in-person and 62 online. Expectations and needs of the facility were presented for four potential research areas, i.e., material irradiation damage, semiconductor soft error testing, medical RI production, and proton beam applications. The status of the facility design considering the users' needs was presented. In the end, the needs urged stated by the user community and the road map for the construction of the facility were discussed.

As for the R&D activities on the lead-bismuth target technology, progress has been made in materials corrosion tests under oxygen concentration controlled high-temperature lead-bismuth flowing using the OLLOCHI loop. The Initial initial results showed that pre-oxidation of steel specimens was effective in inhibiting corrosion caused by LBE.

As for the design of a super-conducting linac for ADS to provide a 30-MW proton beam to a subcritical reactor, the power consumption by the proposed linac was evaluated. It was found that the targeted acceleration efficiency of 30 % was feasible. Assembling of a superconducting spoke cavity for the linac by electron beam welding has progressed. It was confirmed that the resonance frequency of the cavity was well within the tunable range.

On January 29 and 30, 2024, the tenth TEF Technical Advisory Committee (T-TAC) was held at J-PARC, the first on-site meeting in four years (Fig. 2). J-PARC staff reported the progress in the facility planning and their R&D activities on the ADS development. The main conclusion for the facility planning was as follows: *"T-TAC acknowledges the intent to reframe the facility plan towards applications in addition to ADS. A clear scope (re)definition of TEF and an associated implementation strategy with a realistic planning should be worked out."*

Fig. 2. Group photo of 10th T-TAC.

Research and development

Lead-bismuth target technology development

Management of the Lead-bismuth eutectic (LBE) is one of the key issues of the ADS. At J-PARC, various research activities, such as the operation of a corrosion test loop "OLLOCHI", the operation of a spallation target mockup loop "IMMORTAL", and the development of various sensors for LBE are underway.

1. OLLOCHI

The third campaign of long-term corrosion test in OLLOCHI (Oxygen-controlled LBE LOop Corrosion tests in HIgh-temperature) [1] for 2,000 hours, interrupted by heater trouble along the way, started in March 2023 and completed in April 2024. Test conditions of the third campaign were as follows: the maximum temperature and the temperature difference were 500˚C and 100˚C, respectively. The flow rate was about 1 m/s at the specimens' position. The oxygen concentration (OC) was kept at 1×10^{-6} wt%. The tested specimens were taken out from the specimen holders and are being observed.

Observation and analysis for specimens of the second campaign have progressed. Test conditions of the second campaign were as follows: the flow rate and the OC were the same as the third campaign. The maximum temperature and the temperature difference were 450˚C and 100˚C, respectively. The test duration was 2,000 hours. The T91 (Mod.9Cr-1Mo steel) and SS316L specimens were pre-oxidized prior to testing. There were two pre-oxidation conditions: the first was steam oxidation; the specimens were exposed

to Ar-3%H_2O-0.1%H_2 gas at 400°C for 20 hours. This resulted in the formation of an oxide film of about 0.2 μm on the surface of the T91 specimen. The second was oxidation in LBE, in which the steel specimens were kept in LBE near oxygen saturation at 450°C for 165 hours. An oxide film of about 2 μm was formed on the surface of the T91 specimen. The weight change after corrosion testing was compared for specimens under four different conditions: no pre-oxidation, steam oxidation only, oxidation in LBE only, and both.

The results of the weight change after the corrosion tests for T91 and SS316L are shown in Fig. 3. The weight loss of T91 was larger than that of SS316L. Steam oxidation and oxidation in LBE reduced the weight loss of both SS316L and T91, and the combination of these oxidation treatments further reduced the weight loss.

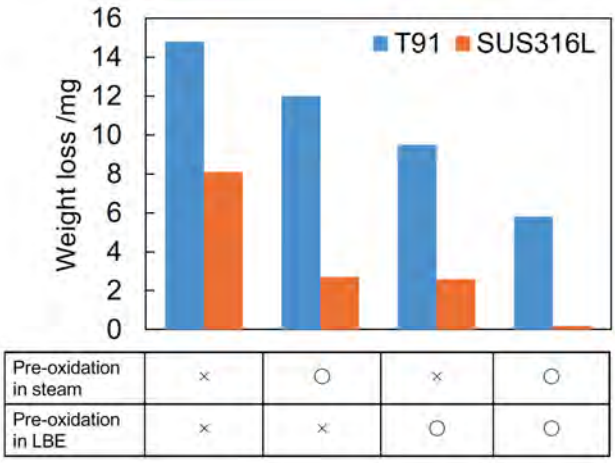

Fig. 3. The results of weight change after the corrosion test.

2. IMMORTAL

IMMORTAL is a mockup loop of the LBE spallation target in TEF-T. LBE, a low Prantl number fluid, shows different heat transfer behavior in comparison with common fluids, such as water. Experimental data to evaluate its heat transfer is are scarce due to the difficulty of experimental measurement. Therefore, we have been measuring the turbulent heat transfer of LBE in a circular flow channel with pressurized water as the secondary coolant using a heat exchanger of IMMORTAL. Continuing from the last fiscal year, we have been expanded the heat transfer data by using IMMORTAL. Figure 4 represents the updated relationship between the Nusselt number and Peclet number, which are commonly used to evaluate heat transfer phenomena. Two recommended correlations for LBE given in the literature [1] are presented in the figure. Then, we obtained a new correlation equation "$Nu=5+0.023Pe^{0.8}$". As a further challenge, we will start experiments in FY2024 to acquire experimental data on unsteady events, such as loss of flow accidents.

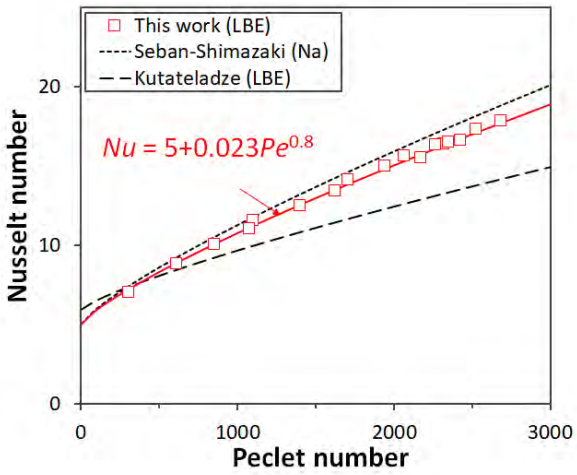

Fig. 4. Updated relationship between the Nusselt number and Peclet number.

References

[1] Handbook on Lead-bismuth Eutectic Alloy and Lead Properties, Materials Compatibility, Thermal-hydraulics and Technologies – 2015 Edition, (2015), 950p. NEA. No. 7268.

Super-conducting linac development for ADS

1. Low-energy beam transport line

The low-energy beam transport (LEBT) delivers and matches the 25-mA proton beam with an energy of 35 keV from the ion source to the Radio Frequency Quadrupole (RFQ). At this operation range, the main challenge is the control of the coulomb repulsion among the beam particles (space-charge) that degrades the beam quality.

To this end, we adopted a magnetostatic design composed of two solenoids, an electrostatic chopper, and a conical collimator, as shown in Fig. 5 (a). The principal advantage of the magnetostatic design is the space-charge compensation (SCC) phenomenon, also known as neutralization. SCC occurs when the main beam ionizes the residual gas and the ionized particles with opposite charge to the main beam are trapped on the beam potential until reaching a steady state, reducing the coulomb repulsion inside the beam. The time it takes for a particle of the beam to produce a neutralizing particle in the residual gas is called SCC transient time (τ_{scc}), this time depends on the beam properties, residual gas, and pressure level. Normally, it takes between two to three τ_{scc} to reach a steady state.

We developed the LEBT design using the particle-in-cell (PIC) code WARP to take into account the SCC of the beam by ionization of the residual gas to ensure a

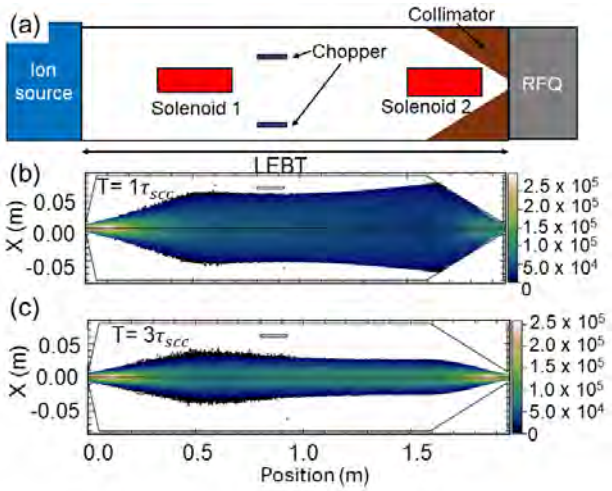

Fig. 5. (a) Schematic design of the LEBT and the horizontal beam distribution for a time equal to one τ_{scc} (b) and three τ_{scc} (c).

more realistic simulation of the beam transportation. Figures 5 (b) and (c) present the horizontal distribution at two different times. The SCC effectively reduces the increase in beam size caused by space charge, allowing us to deliver the beam to the RFQ according to the requirements.

2. Progress of the spoke cavity prototyping for the JAEA-ADS linac

As a first step toward the practical design of the JAEA-ADS linac, we have decided to prototype a low-beta single-spoke cavity and then conduct high-field performance tests of the prototype spoke cavity at liquid helium temperature. The spoke cavity prototyping will provide us with various insights into the development of superconducting cavities with transverse electromagnetic half-wave mode resonance.

We have started welding the cavity parts together in 2021. All the shaped cavity parts are joined together by electron beam welding (EBW). Before welding the actual cavity parts, EBW beam parameters for each welding condition were carefully investigated using mock-up test pieces. Furthermore, prior to each EBW, all welding joints were acid cleaned (chemically polished) to remove impurities. In the fiscal year 2023, we have successfully fabricated the body and two lid sections, as shown in Fig. 6. So far, any obvious welding defects, such as unpenetrated welds and welding holes, have not been found.

We have temporarily assembled the prototype spoke cavity and measured its resonant frequency. The measured frequency of 334.29 MHz is not far from that obtained by simulation (333.49 MHz), and the difference (0.80 MHz) is well within the range of frequency adjustment by shortening the body section longitudinally. It was confirmed that there were no significant problems with the cavity fabrication. We are now going to proceed to the final EBW assembly of the prototype spoke cavity.

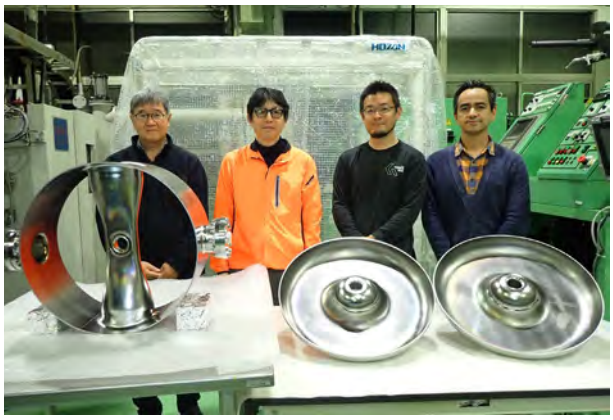

Fig. 6. Fabricated main parts of the prototype spoke cavity.

Nuclear technology

1. Measurement of nuclide-production cross sections

We have been measuring the production cross sections of radionuclides induced by proton bombardment at various energies at J-PARC. These data are essential for the design of ADS using high-energy proton accelerators. In this fiscal year, we compiled experimental data on Mg, Si, Fe, Zn, Cu, Ti, and Nb. The obtained data were used to validate various physics models [1,2]. Figure 7 compares the goodness-of-fit between different physics models for Fe, Zn, and Cu. These validations confirmed weaknesses in the predictive ability of each of the physical models.

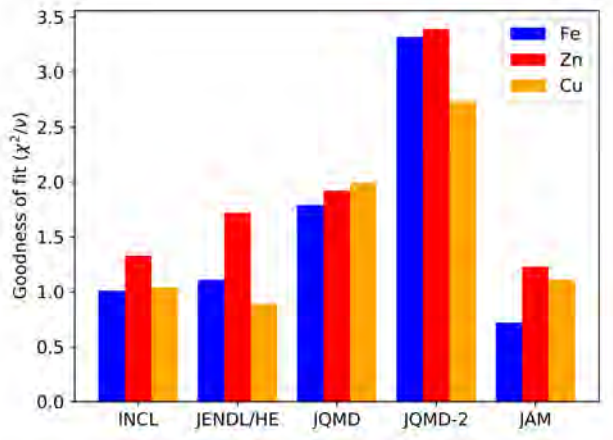

Fig. 7. Comparison of goodness-of-fit between different physics models for Fe, Zn, and Cu; the smaller these values are, the better the physics model reproduces the experimental values.

2. Development of a machine learning method to estimate nuclide-production cross sections

To build a database that integrates numerous experimental data on proton-induced nuclide production cross sections, we have developed a cross-section evaluation model based on machine learning (ML) using a Gaussian process regression method [3]. Traditional physics models based on nuclear theories cannot reproduce nuclide production cross sections with high accuracy. In contrast, our cross-section evaluation model estimates cross sections by learning from experimental data, achieving higher accuracy than physical models. Additionally, by assuming similarity among cross sections for different targets, we have successfully used transfer learning to estimate cross sections for a wide range of targets and energy regions.

Figure 8 shows the results of the ^{7}Be production cross sections for the Mo target as estimated by our developed model. The black dots represent the experimental data recently obtained at J-PARC, while the gray dots indicate experimental data from a previous study. Although there was only one experimental data point for Mo previously, we added three new experimental values. The red line shows the results of learning and estimation without including these experimental data in the training set. As illustrated in this figure, our ML model can accurately predict the experimental data for the Mo target. This demonstrates the model's effectiveness in regions where no experimental data exist.

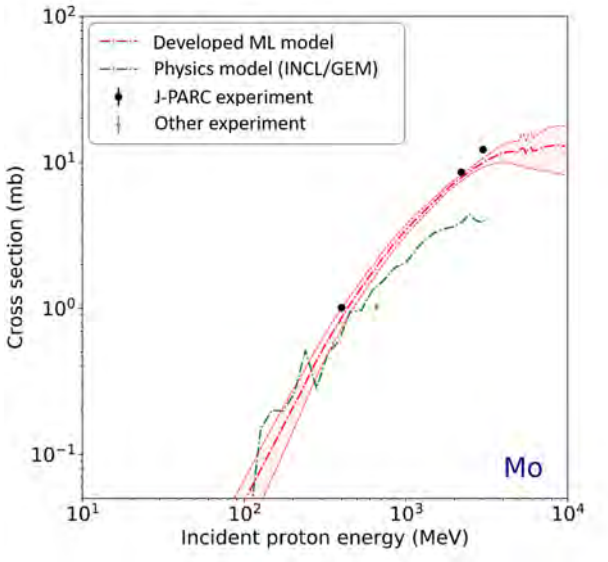

Fig. 8. Proton-induced ^{7}Be production cross section of Mo.

References

[1] K. Sugihara, *et al*., Measurement of nuclide production cross sections for GeV-region proton-induced reactions on ^{nat}Mg, ^{nat}Si, ^{nat}Fe, ^{nat}Cu, and ^{nat}Zn, Nucl. Instrum. Methods Phys. Res. B **549** 165299 (2023).

[3] K. Sugihara, *et al*., Measurement of nuclide production cross sections for proton-induced reactions on ^{nat}Ti and ^{93}Nb at 0.8 and 3.0 GeV, Nucl. Instrum. Methods Phys. Res. B **545** 165153 (2023).

[3] H. Iwamoto, *et al*., Comprehensive estimation of nuclide production cross sections using a phenom-enological approach, Phys. Rev. C **109** 054610 (2024).

International and Domestic Cooperation

We are collaborating with the Belgian Nuclear Research Centre (SCK CEN) for the ADS development under the collaboration arrangement between SCK CEN and JAEA. SCK CEN is promoting the MYRRHA (Multi-purpose hYbrid Research Reactor for High-tech Application) project, which is the world's first large scale ADS project at power levels scalable to industrial systems. We frequently held discussed discussions with the MYRRHA accelerator team for regarding the super-conducting linac development.

Under the SAKURA Mobility Programme funded by Swedish agencies, Dr. Bruce Yee-Rendon visited the European Spallation Source, and exchanged information about the super-conducting linac development.

We continued the collaboration with the Karlsruhe Institute of Technology in Germany on the LBE technology. We exchanged information about the LBE loop operation.

We are also collaborating with domestic universities and institutes. One of the collaborations is with the University of Fukui on the behavior of spallation and corrosion products in LBE. We are developing the Transport of RAdionuclides In Liquid metal systems (TRAIL) code. We continued the experimental study on the evaporation behavior of volatile elements from LBE.

Another collaboration is with the Tokyo Institute of Technology (TIT). Several steel specimens were provided by TIT, and these specimens were served for the materials corrosion test using the OLLOCHI loop.

Safety

Safety

1. Major events on safety culture and safety activities in the J-PARC

Through our experiences of the various accidents and incidents, J-PARC has reaffirmed that "The safety of the facility is achieved by the efforts of every person involved", and we actively implement safety culture development activities to upgrade the safety awareness and skills of each person. Our efforts to enforce the safety culture in J-PARC include sharing safety information, enhancement of safety awareness, education and training, etc. For these purposes, new approaches are being introduced sequentially. In addition, these activities are being reviewed internally and by external experts to ensure continuous improvement.

As we experienced two electrical fire incidents in the first quarter of FY2023, our safety activities were enhanced to respond adequately to similar incidents in the future. Table 1 lists the major events on safety in the J-PARC.

In order not to forget the radioactive material leak incident that occurred on May 23, 2013, the J-PARC exchanges safety information between each section and holds a workshop for fostering safety culture around May 23 every year. The Safety Day in FY2023 was held on May 23. Safety initiatives at each facility were introduced, and some good practices were awarded by the director. Following that, the main talk entitled "Psychological safety as the basis for teamwork" was given by Mika Aoshima, Laboratory for Developing Team Competence. Further, a discussion session was held to look back at the situation at the time of the 2013 incident.

At the Accelerator Facility Safety Symposium held on June 9th, safety personnel at the domestic accelerator facilities gathered to introduce and discuss the responses to the mandatory requirement to ensure the reliability of radiation measurements and efforts to prevent electrical fires.

An emergency drill was conducted on October 10 at the Neutrino Experimental Facility. This drill was conducted jointly with the Nuclear Science Research Institute and the Tsukuba campus of the High Energy Accelerator Research Organization and involved confirming the transmission of information and cooperation between each organization, under the assumption that a fire had broken out in the electrical equipment in the electrical room.

The fiscal 2023 J-PARC safety audit was conducted by two auditors on December 8 (remotely) and 18 (on site). They reviewed the following points: 1) response to the fire incidents that occurred in FY2023, 2) organizational structure for safety management, 3) safety management in works, 4) emergency response, 5) safety education and fostering safety culture. The auditors reported that the measures taken following the fire incidents were progressing steadily. However, it was believed that the cause of these incidents was due to issues pointed out in previous audits, such as the need to deal with aging facilities and develop personnel capable of design (especially electrical personnel). These measures were difficult to implement in the short term, so it was necessary to develop long-term plans and proceed step by step.

2. Radiological license update and facility inspection

No application to update the radiological license was submitted to the Nuclear Regulation Authority during FY2023.

The facility inspection for the power upgrade of the Neutrino Experimental Facility, which had been permitted in FY2022, was conducted by Radiation Management Research Institute, Inc., registered inspection agency, on December 4, 2023.

3. Meeting of the committee on the radiation safety matter

The J-PARC Radiation Safety Committee is organized as an advisory committee to both JAEA and KEK to discuss policy on radiation safety in J-PARC. Meanwhile, the Radiation Safety Review Committee has been established to discuss specific subjects of radiation safety in the J-PARC.

In FY2023, the J-PARC Radiation Safety Committee met twice, and the Radiation Safety Review Committee also met twice. Table 2 lists the major issues discussed by the committees.

4. Radiation exposure of radiation workers

The number of persons subject to annual measurement of external exposure in FY2023 was 3103.

Table 3 lists the distribution of annual exposed doses for each category of workers. There was no exposure exceeding the dose limit specified in the local radiation protection rule for J-PARC and the administrative dose limits (7 mSv/year) specified in the detailed rule of local radiation protection rule for J-PARC. The total annual effective dose was 10.4 person·mSv, and the maximum effective dose was 0.5 mSv.

Table 1. List of major events on safety in FY2023.

Day	Events
April 25, 2023	Electrical fire incident at the Main Ring
May 23, 2023	Safety Day (Meeting to exchange safety information between each section, Workshop for fostering safety culture)
June 9, 2023	9th Symposium on Safety in Accelerator Facilities
June 22, 2023	Electrical fire incident at the Hadron Experimental Facility
August 3, 2023	Liaison committee on safety and health for contractors
October-December	Refresher course on radiation safety for in-house staff (e-learning)
October 10, 2023	Emergency drill assuming an electrical fire accident at the Neutrino Experimental Facility
December 8&18, 2023	FY2023 J-PARC Safety Audit

Table 2. Radiation Safety Committee (RSC) and Radiation Safety Review Committee (RSRC) in FY2023

No.	Date	Major Issues
The Radiation Safety Committee		
41st	July 25, 2023	• Report on the progress status of change permission application, personal exposure situation, amount of radioactive waste released in FY2022
42th	March 19, 2024	• Report on the status of deliberations by the Radiation Safety Review Committee
The Radiation Safety Review Committee		
37th	June 26, 2023	• Revision of the detailed rule of local radiation protection
38th	March 8, 2024	• Procedure for revision of the local radiation protection rule, etc., due to a change in the internal name of the organization

Table 3. Annual exposure doses in FY2023

	# of workers	Dose range x (mSv)				Collective dose (person · mSv)	Maximum dose (mSv)
		ND	$0.1 \leq x \leq 1.0$	$1.0 < x \leq 5.0$	$5.0 < x$		
In-house staff	711	693	18	0	0	3.1	0.3
Users	1221	1221	0	0	0	0.0	0.0
Contractors	1177	1135	42	0	0	7.3	0.5
Total	3103	3043	60	0	0	10.4	0.5

*If the same worker changed the worker classification during the fiscal year, the worker was counted as one worker per the classification. Therefore, the total number does not match the sum of the respective classification.

User Service

Users Office (UO)

Outline

The J-PARC Users Office (UO) was established in 2007. It opened an office on the first floor of the IBARAKI Quantum Beam Research Center in Tokai-mura, in December 2008. UO maintains the Tokai Dormitory for the J-PARC users. UO provides on-site and WEB support with one-stop service for the utilization of the J-PARC. As of March 31, 2024, UO had 11 staffs and 5 WEB Support SE staffs in the Users Affairs Section. The J-PARC Users, after the approval of their experiment, follow the administrative procedures outlined on the Users Office (UO) WEB Portal Site, related to the registration as a J-PARC User, radiation worker registration, safety education, accommodation, invitation letter for visa and other requirements. Then the UO staffs provide them with support by e-mail. After their arrival at the J-PARC, UO gives on-site assistance to the J-PARC Users, like receiving the J-PARC ID, glass badge, and safety education. Since 2015, UO had been doing its part to improve the J-PARC on-line experiment system and make it more user-friendly

After the experiments UO may return the experiment samples at User's cost after cooling the radioactive activities.

Map to J-PARC Users Office

Activities of UO

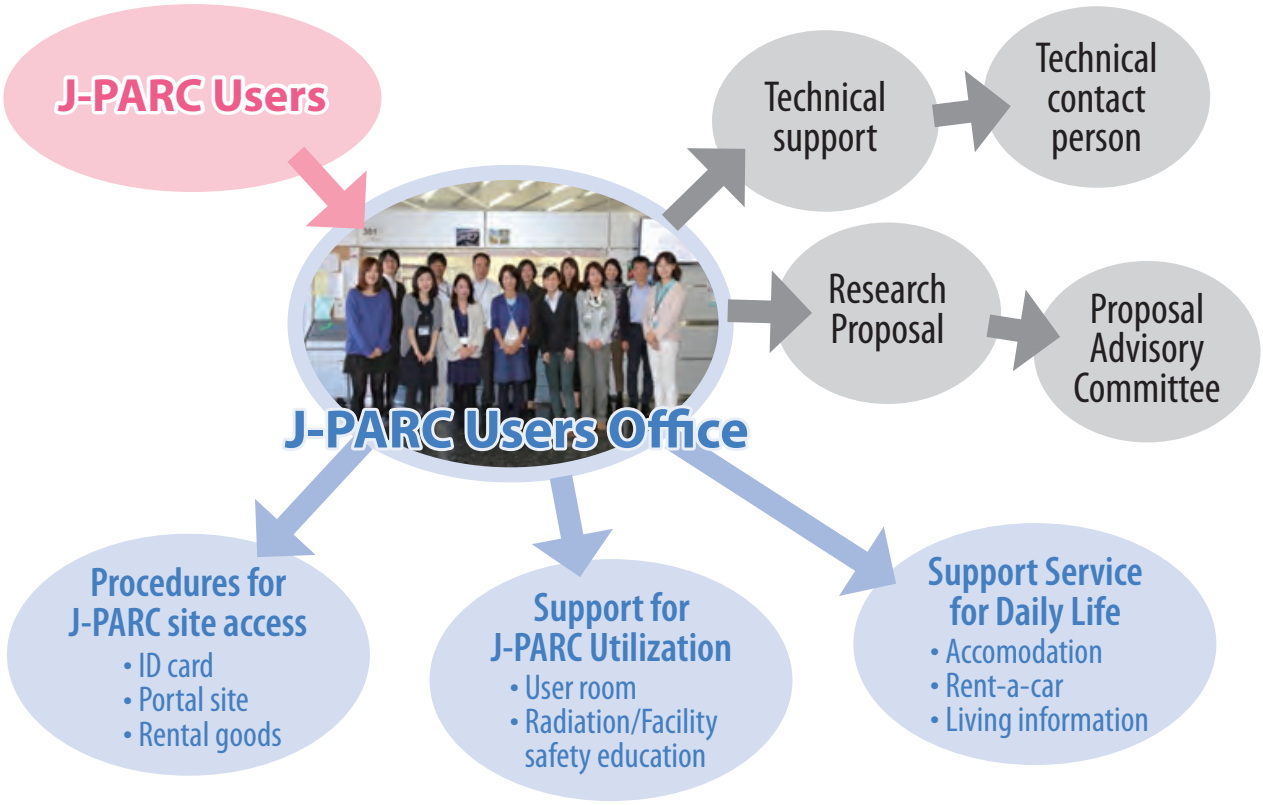

One stop service for J-PARC users

on the web

Step 1 User registration

New user: Getting user ID

Registered user: Annual registration, specifying of the visit

Approval of UO

Step 2-1 Obligatory application

Application form to visit J-PARC
Visit proposal (foreign nationality)
Reservation of safety training
On-line education video

Step 2-2 Optional application

J-PARC Card for facility access
Network registration
Radiation worker registration
Reservation of Dormitory
Invitation letter for Visa

on-site support

Step 3

Procedures upon arrival at the first day

Recieve J-Parc User ID card

Vehicle Permission pass

Safety education and dosimeter

Rental goods
Bicyle
PHS
Cafeteria card
Locker key
Office key

Step 4 J-PARC Experiment and meeting

Step 5 Leaving procedures

Retern all cards, keys, rental goods UO (office hours) or return box!

Users Office at AQBRC
Office hours(9:00-17:00, Mon.-Fri.)

Rental bicycle

Return box at AQBRC

User Statistics

Users in 2023 (Japanese/Foreigners, person-days)

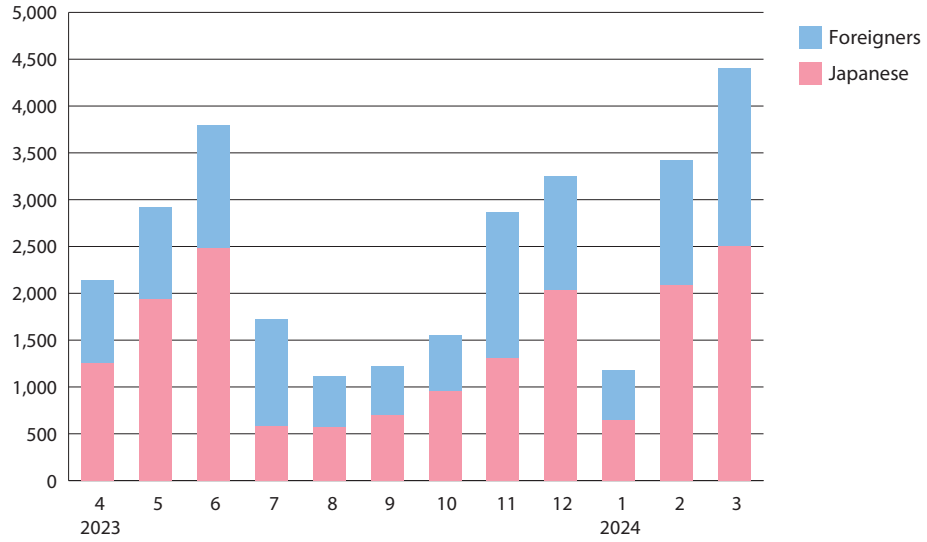

Users in 2023 (according to facilities, person-days)

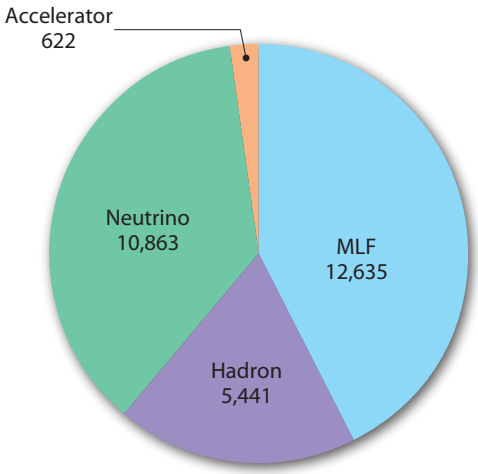

Users in 2023 (according to organizations, person-days)

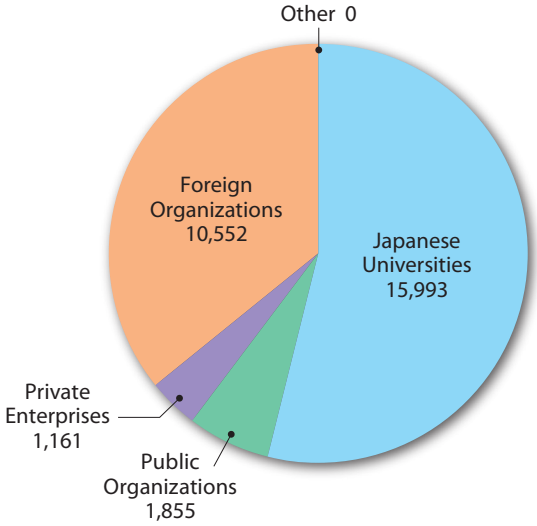

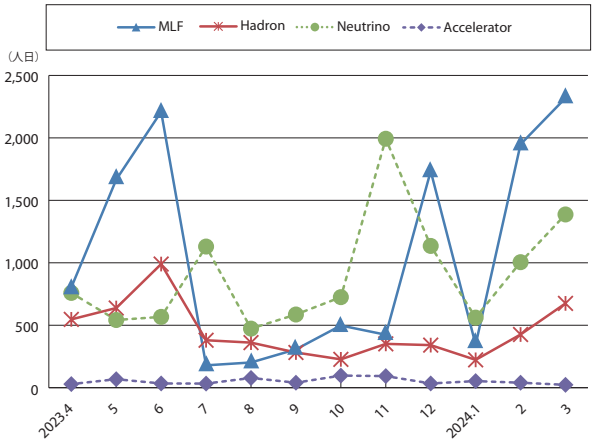

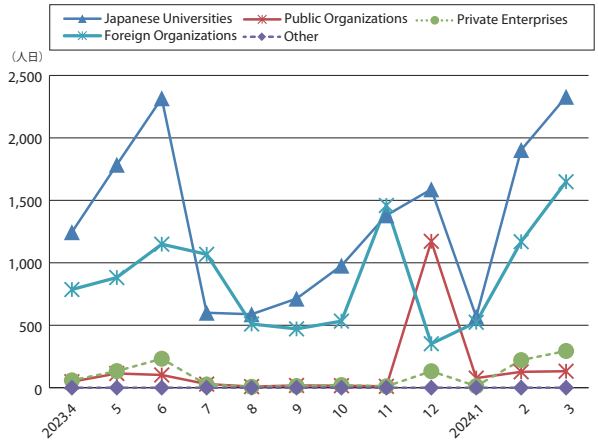

MLF Proposals Summary - FY2023

Table 1. Number of Proposals by Beamline

Beam-line	Instrument		2023A		2023B		Full Year			
			Submitted	Approved	Submitted	Approved	Submitted		Approved	
			GU	GU	GU	GU	PU/S	IU	PU/S	IU
BL01	4D-Space Access Neutron Spectrometer - ***4SEASONS***		22(1)	8(1)	29(0)	15(0)	0	1	0	1
BL02	Biomolecular Dynamics Spectrometer - ***DNA***		22(1)	7(1)	18(1)	16(1)	2	1	2	2
BL03	IBARAKI Biological Crystal Diffractometer - ***iBIX***	(100-β)‡	1	1	0	0	0	0	0	0
		(β)†	2	2	1	1	17※	0	16※	0
BL04	Accurate Neutron-Nucleus Reaction Measurement Instrument - ***ANNRI***		5	3	5	3	2	1	2	1
BL05	Neutron Optics and Physics - ***NOP***		4	4	10	7	1	0	1	0
BL06	Village of Neutron Resonance Spin Echo Spectrometers - ***VIN ROSE***		5	2	2	1	2	0	2	0
BL08	Super High Resolution Powder Diffractometer - ***SuperHRPD***		9	6	7	6	1	0	1	0
BL09	Special Environment Neutron Powder Diffractometer - ***SPICA***		3	3	4	4	1	0	1	0
BL10	Neutron Beam-line for Observation and Research Use - ***NOBORU***		10	8	11	10	2	1	2	1
BL11	High-Pressure Neutron Diffractometer - ***PLANET***		13(0)	8(0)	9(0)	8(0)	0	2	0	2
BL12	High Resolution Chopper Spectrometer - ***HRC***		5	3	13	8	1	0	1	0
BL14	Cold-Neutron Disk-Chopper Spectrometer - ***AMATERAS***		34	6	44	12	1	1	1	1
BL15	Small and Wide Angle Neutron Scattering Instrument - ***TAIKAN***		28(1)	8(1)	23(1)	17(1)	2	4	2	4
BL16	Soft Interface Analyzer - ***SOFIA***		17	10	18	8	1	1	1	1
BL17	Polarized Neutron Reflectometer - ***SHARAKU***		13(1)	11(1)	16(1)	16(1)	3	3	3	3
BL18	Extreme Environment Single Crystal Neutron Diffractometer - ***SENJU***		23(0)	8(0)	17(0)	10(0)	1	1	1	1
BL19	Engineering Materials Diffractometer - ***TAKUMI***		31	7	26	10	2	1	2	1
BL20	IBARAKI Materials Design Diffractometer - ***iMATERIA***	(100-β)‡	3	3	5	5	0	0	0	0
		(β)†	28	28	24	24	12	0	12	0
BL21	High Intensity Total Diffractometer - ***NOVA***		15	12	26	13	1	0	1	0
BL22	Energy Resolved Neutron Imaging System - ***RADEN***		17(0)	8(0)	18(2)	18(2)	0	1	0	1
BL23	Polarization Analysis Neutron Spectrometer - ***POLANO***		3	2	3	2	1	0	1	0
D1	Muon Spectrometer for Materials and Life Science Experiments - ***D1***		11(0)	5(0)	16(3)	6(1)	0	1	0	1
D2	Muon Spectrometer for Basic Science Experiments - ***D2***		5(1)	2(0)	8(2)	5(2)	3	1	3	1
S1	General purpose μSR spectrometer - ***ARTEMIS***		25(0)	15(0)	38(0)	21(0)	1	1	1	1
S2	Muonium Laser Physics Apparatus - ***S2***		0(0)	0(0)	0(0)	0(0)	0	1	0	1
U1A	Ultra Slow Muon Microscope - ***U1A***		0	0	0	0	0	1	0	1
U1B	Transmission Muon Microscope - ***U1B***		0	0	0	0	0	0	0	0
H1	High-intensity Muon Beam for General Use - ***H1***		0	0	0	0	0	1	0	1
Total			***354***	***180***	***391***	***247***	***49***	***23***	***48***	***23***

GU : General Use **PU** : Project Use or Ibaraki Pref. Project Use **S** : S-type Proposals
IU : Instrument Group Use
† : Ibaraki Pref. Exclusive Use Beamtime (β = 80% in FY2022)
‡ : J-PARC Center General Use Beamtime (100-β = 20% in FY2022)
( ) : Number of proposals under the New User Promotion (BL01, BL02, BL11, BL15, BL17, BL18, BL22) or P-type proposals (D1,D2, S1) in GU

※ : Operations period is held twice per year (for each of the A and B periods), with only the yearly total shown above.
The actual total number of proposals in each beamline named in the table does not match the number shown in the "Total" cell, because some proposals are submitted or approved across multiple beamlines.

Table 2. Number of Long-Term Proposals by Fiscal Year

Application FY	Submitted	Approved
2021	0	0
2022	5	4
2023	0	0

No Long-Term Proposals were called for FY2021 and FY2023.

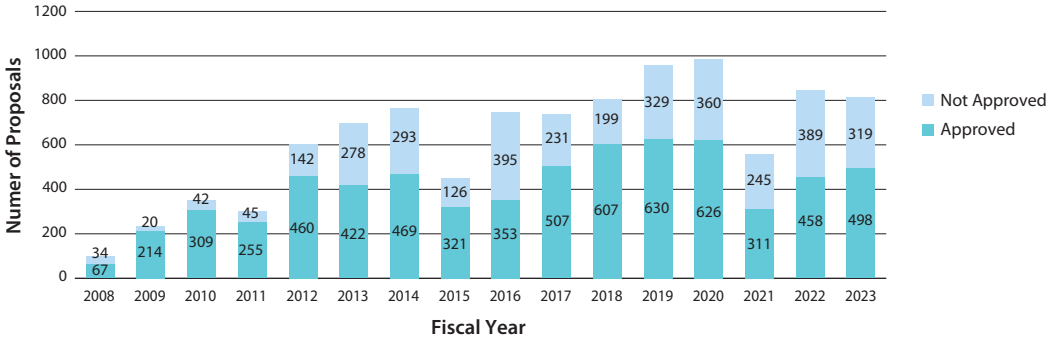

Fig. 1. Number of MLF Proposals over Time

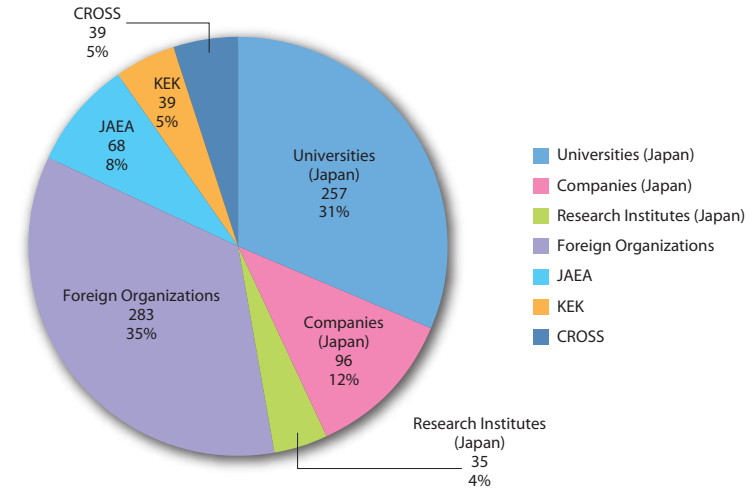

Fig. 2. Origin of Submitted Proposals by Affiliation - FY2023

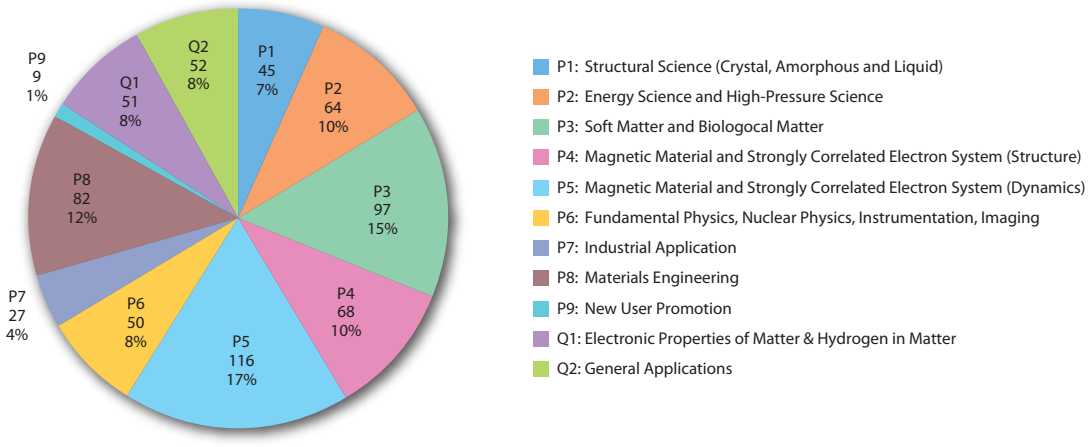

Fig. 3. Submitted Proposals by Sub-committee/Expert Panel – FY2023

J-PARC PAC Approval Summary for the 2023 Rounds

	(Co-) Spokespersons	Affiliation	Title of the experiment	Approval status (PAC recommendation)	Beamline	Status
E03	K.Tanida	JAEA	Measurement of X rays from X^- Atom	Stage 2	K1.8	Data taking
P04	J.C.Peng, S.Sawada	U of Illinois at Urbana-Champaign; KEK	Measurement of High-Mass Dimuon Production at the 50-GeV Proton Synchrotron	Deferred	Primary	
E05	T.Nagae	Kyoto U	Spectroscopic Study of X-Hypernucleus, $^{12}_{X}$Be, via the ^{12}C(K^-, K^+) Reaction	Stage 2 New experiment E70 based on the S-2S spectrometer	K1.8	Finished
E06	J.Imazato	KEK	Measurement of T-violating Transverse Muon Polarization in $K^+ \to p^0 m^+ n$ Decays	E36 as the first step	K1.1BR	
E07	K.Imai, K.Nakazawa, H.Tamura	JAEA, Gifu U, Tohoku U	Systematic Study of Double Strangeness System with an Emulsion-counter Hybrid Method	Stage 2	K1.8	Finished Data analysis
E08	A.Krutenkova	ITEP	Pion double charge exchange on oxygen at J-PARC	Stage 1	K1.8	
E10	A.Sakaguchi, T.Fukuda	Osaka U, Osaka EC U	Production of Neutron-Rich Lambda-Hypernuclei with the Double Charge-Exchange Reaction (Revised from Initial P10)	Stage 2	K1.8	Li run finished, Be target run with S-2S
E11	A.K.Ichikawa, F.Sanchez	Tohoku U, Geneva	Tokai-to-Kamioka (T2K) Long Baseline Neutrino Oscillation Experimental Proposal	Stage 2	neutrino	Data taking
E13	H.Tamura	Tohoku U	Gamma-ray spectroscopy of light hypernuclei	Stage 2	K1.8	Finished
E14	T.Nomura	KEK	Proposal for $K_L \to p^0$ n n-bar Experiment at J-PARC	Stage 2	KL	Data taking
E15	M.Iwasaki, T.Nagae	RIKEN, Kyoto U	A Search for deeply-bound kaonic nuclear states by in-flight 3He(K-, n) reaction	Stage 2	K1.8BR	Finished
E16	S.Yokkaichi	RIKEN	Measurements of spectral change of vector mesons in nuclei (previously "Electron pair spectrometer at the J-PARC 50-GeV PS to explore the chiral symmetry in QCD")	Stage 2 for Run 0 Deferred for Run 1. PAC recommended 101h+100h beam time for beam study & trigger study.	High p	Data taking
E17	R.Hayano, H.Outa	U Tokyo, RIKEN	Precision spectroscopy of Kaonic ^{3}He 3d->2p X-rays	Registered as E62 with an updated proposal	K1.8BR	
E18	H.Bhang, H.Outa, H.Park	SNU, RIKEN, KRISS	Coincidence Measurement of the Weak Decay of $^{12}_{L}$C and the three-body weak interaction process	Stage 2	K1.8	
E19	M.Naruki	KEK	High-resolution Search for Q^+ Pentaquark in $p^-p \to K^-X$ Reactions	Stage 2	K1.8	Finished
E21	Y.Kuno	Osaka U	An Experimental Search for μ – e Conversion at a Sensitivity of 10^{-16} with a Slow-Extracted Bunched Beam	Stage 2	COMET	
E22	S.Ajimura, A.Sakaguchi	Osaka U	Exclusive Study on the Lambda-N Weak Interaction in A=4 Lambda-Hypernuclei	Stage 1	K1.8	
T25	S.Mihara	KEK	Extinction Measurement of J-PARC Proton Beam at K1.8BR	Test Experiment	K1.8BR	Finished
E26	K.Ozawa	KEK	Search for w-meson nuclear bound states in the $p-+^AZ \to n+^{(A-1)}_{w}(Z-1)$ reaction, and for w mass modification in the in-medium $w \to p^0g$ decay	Stage 1	K1.8	
E27	T.Nagae	Kyoto U	Search for a nuclear Kbar bound state K^-pp in the d(p^+, K^+) reaction	Stage 2	K1.8	Fisnished
E29	H.Ohnishi	RIKEN	Search for f-meson nuclear bound states in the pbar + $^AZ \to f + ^{(A-1)}_{f}(Z-1)$ reaction	Stage 1	K1.1	
E31	H.Noumi	Osaka U	Spectroscopic study of hyperon resonances below KN threshold via the (K^-,n) reaction on Deuteron	Stage 2	K1.8BR	Finished Data analysis
T32	A.Rubbia	ETH, Zurich	Towards a Long Baseline Neutrino and Nucleon Decay Experiment with a next-generation 100 kton Liquid Argon TPC detector at Okinoshima and an intensity upgraded J-PARC Neutrino beam	Test Experiment	K1.1BR	Finished
P33	H.M.Shimizu	Nagoya U	Measurement of Neutron Electric Dipole Moment	Deferred	Linac	
E34	T. Mibe	KEK, RIKEN	An Experimental Proposal on a New Measurement of the Muon Anomalous Magnetic Moment g-2 and Electric Dipole Moment at J-PARC	Stage 2	MLF	

	(Co-) Spokespersons	Affiliation	Title of the experiment	Approval status (PAC recommendation)	Beamline	Status
E36	M.Kohl, S.Shimizu	Hampton U, Osaka U	Measurement of $G(K^+ \to e^+ n)/G(K^+ \to m^+ n)$ and Search for heavy sterile neutrinos using the TREK detector system	Stage 2	K1.1BR	Finished Data analysis
E40	K.Miwa	Tohoku U	Measurement of the cross sections of Σp scatterings	Stage 2	K1.8	Finished Data analysis
P41	M.Aoki	Osaka U	An Experimental Search for μ – e Conversion in Nuclear Field at a Sensitivity of 10^{-14} with Pulsed Proton Beam from RCS	Deferred	MLF	Reviewed in MLF/ IMSS
E42	J.K.Ahn	Pusan National U	Search for H-Dibaryon with a Large Acceptance Hyperon Spectrometer	Stage 2	K1.8	Finished
E45	K.H.Hicks, H.Sako	Ohio U, JAEA	3-Body Hadronic Reactions for New Aspects of Baryon Spectroscopy	Stage 2 PAC requests that the group further examine ways to reduce the total beam time requested and to find an efficient running scheme, including quick but careful beam tuning.	K1.8	
T46	K.Ozawa	KEK	EDIT2013 beam test program	Test Experiment	K1.1BR	Abandonded
T49	T.Maruyama	KEK	Test for 250L Liquid Argon TPC	Test Experiment	K1.1BR	Withdrawn
E50	H.Noumi	Osaka U	Charmed Baryon Spectroscopy via the (π, D^{*-}) reaction	Stage 1 The FIFC, IPNS, and E50 should investigate the beam-line feasibility	High p	
T51	S.Mihara	KEK	Research Proposal for COMET(E21) Calorimeter Prototype Beam Test	Test Experiment	K1.1BR	had to be stopped
T52	Y.Sugimoto	KEK	Test of fine pixel CCDs for ILC vertex detector	Test Experiment	K1.1BR	not performed yet
T53	D.Kawama	RIKEN	Test of GEM Tracker, Hadron Blind Detector and Lead-glass EMC for the J-PARC E16 experiment	Test Experiment	K1.1BR	not performed yet
T54	K.Miwa	Tohoku U	Test experiment for a performance evaluation of a scattered proton detector system for the Σp scattering experiment E40	Test Experiment	K1.1BR	not performed yet
T55	A.Toyoda	KEK	Second Test of Aerogel Cherenkov counter for the J-PARC E36 experiment	Test Experiment	K1.1BR	had to be stopped
E56	T.Maruyama	KEK	A Search for Sterile Neutrino at J-PARC Materials and Life Science Experimental Facility	Stage 2	MLF	Data taking
E57	J. Zmeskal	Stefan Meyer Institute for Subatomic Physics	Measurement of the strong interaction induced shift and width of the 1s state of kaonic deuterium at J-PARC	Stage 1	K1.8BR	in preparation
P58	M. Yokoyama	U. Tokyo	A Long Baseline Neutrino Oscillation Experiment Using J-PARC Neutrino Beam and Hyper-Kamiokande	Deferred	neutrino	
T59	A. Minamino	Kyoto U	A test experiment to measure neutrino cross sections using a 3D grid-like neutrino detector with a water target at the near detector hall of J-PARC neutrino beam-line	To be arranged by IPNS and KEK-T2K	neutrino monitor bld	Finished
T60	T. Fukuda	Toho U	Proposal of an emulsion-based test experiment at J-PARC	Arranged by IPNS and KEK-T2K	neutrino monitor bld	Finished
E61	M. Wilking	Stony Brook U	NuPRISM/TITUS	Superseded. E61 has been adopted in Hyper-K as IWCD. IWCD is reviewed by HK-PAC.	neutrino	
E62	R. Hayano, S. Okada, H. Outa	U. Tokyo, RIKEN	Precision Spectroscopy of kaonic atom X-rays with TES	Stage 2	K1.8BR	Finished
E63	H. Tamura	Tohoku U	Gamma-ray spectroscopy of light hypernuclei II	Stage 2	K1.1	BL not ready yet. Exp. in preparation
T64	Y. Koshio	Okayama U	Measurement of the gamma-ray and neutron background from the T2k neutrino/anti-neutrino at J-PARC B2 Hall	Arranged by IPNS and KEK-T2K	neutrino	
E65	A.K.Ichikawa, F.Sanchez	Tohoku U, Geneva	Proposal for T2K Extended Run	Stage-2	neutrino	
T66	T. Fukuda	Nagoya U	Proposal of an emulsion-based test experiment at J-PARC	Test Experiment	neutrino	

	(Co-) Spokespersons	Affiliation	Title of the experiment	Approval status (PAC recommendation)	Beamline	Status
P67	I. Meigo	JAEA	Measurement of displacement cross section of proton in energy region between 3 and 30 GeV for high-intensity proton accelerator facility	Carry out the experiment within the framework of facility development	MR	
T68	T. Fukuda	Nagoya U	Extension of T60/T66 Experiment: Proposal for the Run from 2017 Autumn	Test Experiment	neutrino	
E69	A. Minamino	Yokohama National U	Study of neutrino-nucleus ineraction at around 1GeV using cuboid lattice neutrino detector, WAGASHI, muon range detectors and magnetized spectrometer, Baby MIND, at J-PARC neutrino monitor hall	Superseded. Merged with T2K.	neutrino	
E70	T. Nagae	Kyoto U	Proposal for the next E05 run with the S-2S spectrometer	Stage-2	K1.8	
E71	T. Fukuda	Nagoya U	Proposal for precise measurement of neutrinop-water cross-section in NINJA physics run	Stage-2	neutrino	Data taking
E72	K. Tanida	JAEA	Search for a Narrow Λ* Resonance using the p(K-, Λ)η Reaction with the hypTPC Detector	Stage-2	K1.8BR	
E73	Yue Ma	RIKEN	$^{3}_{\Lambda}$H and $^{4}_{\Lambda}$H mesonic weak decay lifetime measurement with ^{3,4}He(K$^-$,π^0)$^{3,4}_{\Lambda}$H reaction	Stage-2	K1.8BR	
P74	A.Feliciello	INFN, Torino	Direct measurement of the 3ΛH and 4ΛH lifetimes using the 3,4He(π-,K0)3,4ΛH reactions	Rejected	K1.1	
E75	H.Fujioka	Tokyo Inst. Tech,	Decay Pion Spectroscopy of 5ΛΛH Produced by Ξ-hypernuclear Decay	Stage 2	K1.8	
P76	H.M.Shimizu	Nagoya U	Searches for the Breaking of the Time Reversal Invariance in Polarized Epithermal Neutron Optics	Deferred	MLF	
T77	Yue Ma	RIKEN	Feasibility study for 3ΛH mesonic weak decay lifetime measurement with 3,4He(K-,π0)3,4ΛH reaction	PAC supoorts the ontinuation of T77 by an explorative run with the 3He target.	K1.8BR	Finished Data analysis
T78	H.Nishiguchi	KEK	8GeV Operation Test and Extinction Measurement	Test Experiment	K1.8BR	Finished
E79	T.Ishikawa	Tohoku U	Search for an I=3 dibaryon resonance	Stage-1	High p	
E80	F.Sakuma	RIKEN	Systematic investgatin of the light kaonic nuclei	Stage-1 Deffered for Stage-2. TDR update based on FIFC comments is necessary.	K1.8BR	
T81	T.Fukuda	Nagoya U	Proposal of test experiment for technical improvements of neutrino measurements with nuclear emulsion detector	Test Experiment	neutrino	
E82	T.Maruyama	KEK	JSNS2-II	Stage-2	MLF	
E83	J. H. Yoo	Korea U	Search for sub-millicharged particles at J-PARC	Conditional to the satisfactory update of the TDR, PAC suggests Stage-2	neutrino	
P84	S. Nakamura	Tohoku U	High precision spectroscopy of Lambda hypernuclei with the (π^+, K$^+$) reaction at the High Intensity High Resolution beamline	Deferred This proposal is a part of the hadron extension discussion and PAC awaits the outcome of the special committee to convene in August for more information.	HIHR	
P85	K. Shirotori	Osaka U (RCNP)	Spectroscopy of Omega Baryons	Deferred This proposal is a part of the hadron extension discussion and PAC awaits the outcome of the special committee to convene in August for more information.	K10, T2 target	
E86	K. Miwa	Tohoku U	Measurement of the differential cross section and spin observables of the Λp scattering with a polarized Λ beam	Stage-1 status	K1.1	
P87	T. Gunji, K. Ozawa, H. Sako	Tokyo, KEK, JAEA	Proposal for dielectron measurements in heavy-ion collisions at J-PARC with E16 upgrades	Deferred PAC encourages the proponents to think about more versatile detector enabling (for example) concurrent measurement of leptonic and hadronic measurements.	HI, high-p	
E88	H. Sako	JAEA	Study of in-medium modification of phi mesons inside the nucleus with phi->K$^+$K$^-$ measurement with the E16 spectrometer	Stage-1	high-p	

	(Co-) Spokespersons	Affiliation	Title of the experiment	Approval status (PAC recommendation)	Beamline	Status
P89	T. Yamaga	RIKEN	Investigation of fundamental properties of the KNN state	Deferred. PAC would like to see the detailed feasibility of P89 after E80's TDR.	K1.8BR	
E90	Y.Ichikawa, K.Tanida	JAEA	High resolution spectroscopy of the "ΣN cusp" by using the d(K^-, π^-) reaction	Stage-1	K1.8	
P91	Y.Morino	KEK	Proposal for study of charm component in the nucleon via J/ψ measurement with the J-PARC E16 spectrometer	Deferred.	high-p	
P92	F.Sakuma	RIKEN	Proposal for the E80 Phase-I Experiment:Investigation of the KNNN $^-$ Bound State Focusing on the Λd Decay	Deferred.	K1.8BR	
P93	K.Shirotori	Osaka U (RCNP)	Proposal of test experiment to evaluate performances of secondary beam mode at the high-momentum beam line	Deferred. PAC requests the proponent to continue discussion with the Lab/ Facility management	high-p	
E94	T.Gogami	Kyoto U	New generation Λ hypernuclear spectroscopy with the (π+, K+) reaction by S-2S	Stage-1	K1.8	
P95	T.Ishikawa	Tohoku U	Pion-induced phi-meson production on the proton	deferred	high-p	
E96	T.O.Yamamoto	JAEA	Measurement of X rays from Ξ- C atom with an active fiber target system	PAC suggests Stage-2	K1.8	
E97	M. Naruki	Kyoto U	Cascade baryon spectroscopy at J-PARC high momentum beamline	PAC suggests Stage-1 status	high-p	
T98	K. Yorita	Waseda U	Measurement of Anti-Matter Reaction in Liquid Argon Time Projection Chamber (LArTPC)	Test Experiment	K1.8BR	
P99	H.Shimizu	Nagoya U	Study of Discrete Symmetries in Polarized Epithermal Neutron Optics	deffered	–	
P100	K.Mishima	KEK	Fundamental Physics with Pulsed Cold Neutrons	deffered	MLF BL05	
T101	H.Ito	Tokyo U of Science	Measurement of neutrino-induced neutron and γ-ray background for BGO-based detectors at J-PARC	Test Experiment	neutrino	
P102	H. Kohri	Osaka U (RCNP)	Study of the peculiar bump structure at 1680 MeV by the $\pi^- p \rightarrow \eta n$ reaction with momenta of $p\pi = 0.85$-1.2 GeV/c	deffered	K1.8	

Organization and Committees

Organization Structure

J-PARC Center Management System Chart

as of April 1, 2023

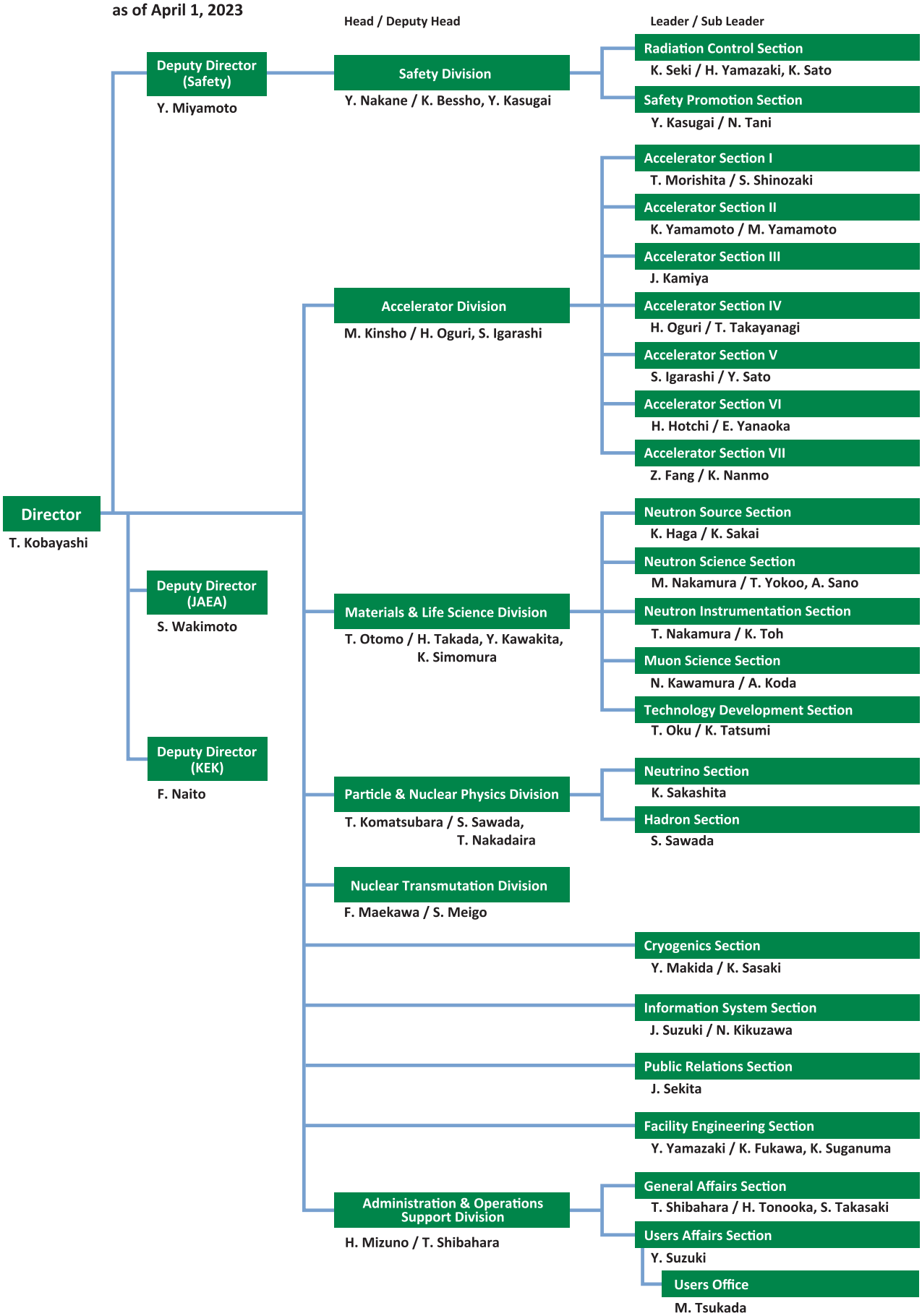

Members of the Committees Organized for J-PARC

(as of March, 2024)

1) Steering Committee (*) Chair

Junji Haba (*)	High Energy Accelerator Research Organization (KEK), Japan
Koki Uchimaru	High Energy Accelerator Research Organization (KEK), Japan
Naohito Saito	High Energy Accelerator Research Organization (KEK), Japan
Nobuhiro Kosugi	High Energy Accelerator Research Organization (KEK), Japan
Tadashi Koseki	High Energy Accelerator Research Organization (KEK), Japan
Hiroyuki Oigawa (*)	Japan Atomic Energy Agency (JAEA), Japan
Yoshinori Horiuchi	Japan Atomic Energy Agency (JAEA), Japan
Kenji Nakajima	Japan Atomic Energy Agency (JAEA), Japan
Toshiyuki Momma	Japan Atomic Energy Agency (JAEA), Japan
Teruhiko Kugo	Japan Atomic Energy Agency (JAEA), Japan
Takashi Kobayashi	J-PARC Center, Japan

2) International Advisory Committee (*) Chair

Thomas Prokscha	Paul Scherrer Institute (PSI), Switzerland
Yoko Sugawara	Kitasato University, Japan
Ken Andersen	Institut Laue-Langevin, France
Takeshi Egami	University of Tennessee, USA
Dan Alan Neumann	National Institute of Standards and Technology, USA
Robert McGreevy (*)	Science & Technology Facilities Council (STFC), UK
Jie Wei	Michigan State University, USA
John Thomason	Science & Technology Facilities Council (STFC), UK
Joachim Mnich	The European Organization for Nuclear Research(CERN), Switzerland
Dmitri Denisov	Brookhaven National Laboratory, USA
Angela Bracco	Unviversità degli studi di Milano and INFN, Istituto Nazionale di Fisica Nucleare, Italy
Reiner Kruecken	Lawrence Berkeley National Laboratory (LBNL), USA
Hamid Aït Abderrahim	Belgian Nuclear Research Centre (SCK CEN), Belgium
Akira Hasegawa	Tohoku University, Japan
Shinichi Kamei	Mitsubishi Research Institute, Japan
Hiromi Yokoyama	The University of Tokyo, Japan

3) User Consultative Committee for J-PARC (*) Chair

Masaki Ishitsuka	Tokyo University of Science, Japan
Hajime Nanjo	Osaka University, Japan
Shoji Asai	The University of Tokyo, Japan
Takeshi Komatsubara	High Energy Accelerator Research Organization (KEK), Japan
Satoshi Nakanura	The University of Tokyo, Japan
Tomofumi Nagae	Kyoto University, Japan
Fuminori Sakuma	RIKEN, Japan
Shinya Sawada	High Energy Accelerator Research Organization (KEK), Japan
Kouji Miwa	Tohoku University, Japan
Toshio Yamaguchi (*)	Fukuoka University, Japan
Taku Sato	Tohoku University, Japan
Takashi Kamiyama	Hokkaido University, Japan
Takatsugu Masuda	The University of Tokyo, Japan
Yoshie Otake	RIKEN, Japan
Toshiya Otomo	High Energy Accelerator Research Organization (KEK), Japan
Kenya Kubo	International Christian University, Japan
Tadashi Adachi	Sophia University, Japan
Koichiro Shimomura	High Energy Accelerator Research Organization (KEK), Japan
Yuko Kojima	Mitsubishi Chemical Corporation, Japan
Hiroyuki Kishimoto	Sumitomo Rubber Industries, Ltd. Japan
Hideto Imai	FC-Cubic, Japan
Kenji Ohoyama	Ibaraki Prefecture, Japan
Mitsuhiro Fukuda	Osaka University, Japan
Cheol-Ho Pyeon	Kyoto University, Japan
Kazufumi Tsujimoto	Japan Atomic Energy Agency (JAEA), Japan

4) Accelerator Technical Advisory Committee (*) Chair

Wolfram Fischer	Brookhaven National Laboratory (BNL), USA
Mats Lindroos	European Spallation Source, ERIC, Sweden
John Thomason	Science and Technology Facilities Council (STFC), UK
Sheng Wang	Institute of High Energy Physics, CAS, China
Toshiyuki Shirai	National Institutes for Quantum and Radiological Science and Technology, Japan
Alexander Aleksandrov	Oak Ridge National Laboratory, USA
Jie Wei (*)	Michigan State University., USA
Alexander A Valishev	Fermi National Accelerator Laboratory (FNAL), USA
Simone Gilardoni	European Organization for Nuclear Research (CERN), Switzerland

5) Neutron Advisory Committee (*) Chair

Phillip King	Rutherford Appleton Laboratory, UK
Bertrand Blau	Paul Scherrer Institut (PSI), Switzerland
Michael J Dayton	Oak Ridge National Laboratory (ORNL), USA
Guenter Muhrer	European Spallation Source(ESS), Sweden
Christiane Alba-Simionesco	Laboratoire Leon Brilloin (LLB) Sacley, France
Jamie Schulz (*)	Australian Nuclear Science and Technology Organization(ANSTO), Australia
Jon Taylor	Spallation Neutron Source(SNS), USA
Sungil Park	Korea Atomic Energy Research Institute(KAERI), Korea
Yoshie Ohtake	RIKEN, Japan
Takahisa Arima	RIKEN, Japan / The University of Tokyo, Japan
Toyohiko Kinoshita	Japan Synchrotron Radiation Research Institute(JASRI), Japan

6) Muon Advisory Committee (*) Chair

Martin Månsson	KTH Royal Institute of Technology, Sweden
Thomas Prokscha (*)	Paul Scherrer Institut (PSI), Switzerland
Andrew MacFarlane	The University of British Columbia, Canada
Klaus Kirch	ETH Zurich and Paul Scherrer Institute (PSI), Switzerland
Kenya Kubo	International Chiristian University, Japan
Nori Aoi	Osaka University, Japan
Hiroshi Amitsuka	Hokkaido University, Japan
Koji Yoshimura	Okayama University, Japan
Kenji Kojima	TRIUMF, Canada

7) Radiation Safety Committee (*) Chair

Hiroshi Watabe (*)	Tohoku University, Japan
Kanenobu Tanaka	Institute of Physical and Chemical Research (RIKEN), Japan
Takeshi Iimoto	The University of Tokyo, Japan
Michihiro Shibata	Nagoya University, Japan
Sumi Yokoyama	Nagasaki University, Japan
Toshiya Sanami	High Energy Accelerator Research Organization (KEK), Japan
Yoshihito Namito	High Energy Accelerator Research Organization (KEK), Japan
Makoto Tobiyama	High Energy Accelerator Research Organization (KEK), Japan
Teruhiko Kugo	Japan Atomic Energy Agency (JAEA), Japan
Kazuhiko Ogawa	Japan Atomic Energy Agency (JAEA), Japan
Hideki Hangai	Japan Atomic Energy Agency (JAEA), Japan

8) Radiation Safety Review Committee (*) Chair

Yukihiro Miyamoto (*)	Japan Atomic Energy Agency (JAEA), Japan
Yoshihiro Nakane	Japan Atomic Energy Agency (JAEA), Japan
Hirohito Yamazaki	High Energy Accelerator Researchi Organization (KEK), Japan
Hidetoshi Kikunaga	Tohoku University, Japan
Hiroshi Yashima	Kyoto Univaersity, Japan
Nobuyuki Chiga	National Institute for Quantum and Radiological Science and Technoloty (QST), Japan
Toshiro Itoga	Japan Synchrotron Radiation Research Institute (JASRI), Japan
Koji Kiriyama	Comprehensive Reserch Organization for Science and Society (CROSS), Japan
Masayuki Hagiwara	National Institute for Quantum and Radiological Science and Technoloty (QST), Japan
Makoto Kobayashi	Japan Atomic Energy Agency (JAEA), Japan
Hiroyuki Takahashi	Japan Atomic Energy Agency (JAEA), Japan
Hiroshi Miyauchi	High Energy Accelerator Researchi Organization (KEK), Japan
Hiroshi Iwase	High Energy Accelerator Researchi Organization (KEK), Japan
Michikazu Kinsho	Japan Atomic Energy Agency (JAEA), Japan
Takeshi Nakadaira	High Energy Accelerator Researchi Organization (KEK), Japan
Takeshi Komatsubara	High Energy Accelerator Researchi Organization (KEK), Japan
Hiroshi Takada	Japan Atomic Energy Agency (JAEA), Japan

9) MLF Advisory Board (*) Chair

Takahisa Arima (*)	The University of Tokyo, Japan / RIKEN, Japan
Osamu Yamamuro	The University of Tokyo, Japan
Hiroyuki Kagi	The University of Tokyo, Japan
Takashi Kamiyama	Hokkaido University, Japan
Shigeru Kimura	Japan Synchrotron Radiation Research Institute(JASRI), Japan
Isao Watanabe	RIKEN, Japan
Yoko Sugawara	Kitasato University, Japan
Tadashi Adachi	Sophia University, Japan
Hiroyuki Kishimoto	Sumitomo Rubber Industries, Japan
Yoshie Otake	RIKEN, Japan
Mikihito Takenaka	Kyoto University, Japan
Kenji Ohoyama	Ibaraki University, Japan
Masahiro Hino	Kyoto University, Japan
Kohzo Ito	The University of Tokyo, Japan
Toshiya Otomo	High Energy Accelerator Research Organization (KEK), Japan
Yukinobu Kawakita	Japan Atomic Energy Agency (JAEA), Japan
Hiroshi Takada	Japan Atomic Energy Agency (JAEA), Japan
Koichiro Shimomura	High Energy Accelerator Research Organization (KEK), Japan
Mitsutaka Nakamura	Japan Atomic Energy Agency (JAEA), Japan
Naritoshi Kawamura	High Energy Accelerator Research Organization (KEK), Japan
Shinichi Itoh	High Energy Accelerator Research Organization (KEK), Japan
Kenji Nakajima	Japan Atomic Energy Agency (JAEA), Japan
Masato Matsuura	Comprehensive Research Organization for Science and Society (CROSS), Japan

10) Program Advisory Committee (PAC) for Nuclear and Particle Physics Experiments at the J-PARC 50Gev Proton Synchrotron

(*) Chair

Kenkichi Miyabayashi	Nara Womens' University, Japan
Motoi Endo	High Energy Accelerator Research Organization (KEK), Japan
Hirokazu Ishino	Okayama University, Japan
Takahiro Kawabata	Osaka University, Japan
Hiroaki Ohnishi	Tohoku University, Japan
Makoto Oka	Japan Atomic Energy Agency (JAEA) / Tokyo Institute of Technology, Japan
Kohei Yorita	Waseda University, Japan
Patrick Achenbach	Thomas Jefferson National Accelerator Facility, USA
Vincenzo Cirigliano	University of Washington, USA
Laura Fields	University of Notre Dame, USA
David Jaffe	Brookhaven National Laboratory (BNL), USA
Cristina Lazzeroni	University of Birmingham, UK
Kam-Biu Luk	University of California at Berkley, USA
Horst Lenske	University of Giessen, Germany
Kyungseon Joo	University of Connecticut, USA
Rikutaro Yoshida (* –2023.10.31)	Argonne National Laboratory, USA
Taku Yamanaka (* 2023.11.1–)	Osaka University, Japan

11) TEF Technical Advisory Committee

(*) Chair

Marc Schyns (*)	Belgian Nuclear Research Center(SCK • CEN), Belgium
Michael Butzek	Forschungszentrum Jülich, Germany
Thierry Stora	European Organization for Nuclear Research (CERN), Switzerland
Yukinobu Watanabe	Kyushu University, Japan
Kazuo Hasegawa	National Institutes for Quantum and Radiological Science and Technology (QST), Japan
Georg Müller	Karlsruhe Institute of Technology, Germany
Kei Ito	Kyoto University, Japan

Main Parameters

Present main parameters of Accelerator

Linac	
Accelerated Particles	Negative hydrogen
Energy	400 MeV
Peak Current	50 mA
Pulse Width	0.50 ms for MLF 0.40 ms for MR-FX 0.20 ms for MR-SX
Repetition Rate	25 Hz
Freq. of RFQ, DTL, and SDTL	324 MHz
Freq. of ACS	972 MHz
RCS	
Circumference	348.333 m
Injection Energy	400 MeV
Extraction Energy	3 GeV
Repetition Rate	25 Hz
RF Frequency	1.23 MHz → 1.67 MHz
Harmonic Number	2
Number of RF cavities	12
Number of Bending Magnet	24
Main Ring	
Circumference	1567.5 m
Injection Energy	3 GeV
Extraction Energy	30 GeV
Repetition Rate	~0.4 Hz
RF Frequency	1.67 MHz → 1.72 MHz
Harmonic Number	9
Number of RF cavities	11
Number of Bending Magnet	96

Key parameters of Materials and Life Science Experimental Facility

Injection energy	3 GeV
Repetition rate	25 Hz
Neutron Source	
Target material	Mercury
Reflector material	Beryllium and Iron
Number of moderators	3
Moderator material	Liquid hydrogen
Moderator temperature/pressure	20 K/1.5 MPa
Number of neutron beam extraction ports	23
Muon Source	
Target material	Graphite
Number of muon beam extraction ports	4
Neutron Instruments	
Open for user program (general use)	21
Under commissioning/construction	0
Muon Instruments	
Open for user program (general use)	3
Under commissioning/construction	1/0

Events

Events

J-PARC Safety Day (May 23)

"J-PARC Safety Day" is held every year around May 23, the day when a radioactive material leak incident occurred in 2013, to build a safe J-PARC and keep the memory of the lessons learned from the incident. With a total of 358 attendees, this year's event was held in a hybrid format. A safety information exchange session was held in the morning, where various efforts to maintain radiation safety at each facility were presented. In the afternoon, the workshop for fostering a safety culture was held. AOSHIMA Mika, Director of the Laboratory for Developing Team Competence, gave a lecture entitled "Psychological Safety for a Foundation for Teamwork". Finally, a documentary film and a panel discussion were held under the title "Ten Years After the Radioactive Material Leak Incident."

Muography Project to See through Burial Mounds Held (June 18)

In April of this year, the Tokai Village Board of Education and the J-PARC Center jointly started a project to nondestructively see through the interior of an ancient burial mound in Tokai Village using muons, a type of cosmic ray. Project activities are held once a month. A hands-on class on observing cosmic rays was held in April, and a lecture on the ancient burial mounds of Tokai Village was held in May.

This month's lecture, the third in the series, was given by the J-PARC Director Takashi Kobayashi and Deputy Director Koichiro Shimomura of the Materials and Life Science Division on the topic of "What Descends from Space" and was attended by 43 people, including elementary school students. Muons cannot be seen or

felt, even though they constantly fly out of space. However, using a spark chamber device, the muon's path appears as a streak of light. The presence of muons in the visualization surprised and excited the participants.

Ibaraki Prefectural Namiki Secondary School SSH* Event Held (June 23)

This event was held under the theme of "Discussion with J-PARC researchers ~From general topics to cutting-edge science," and 15 students, ranging from the first grade of junior high school through the second grade of high school participated in the event.

The lecturer was Akihiko Miura of the Administration and Operations Support Division (concurrently in charge of Accelerator Section III), who introduced the characteristics of X-rays, neutrons, and muons, as well as J-PARC facilities, research, and roles in society. After that, the lecturer and students engaged in a lively discussion about the significance of learning science in group sessions.

This project was the brainchild of the Namiki Secondary School Student Council.

J-PARC Special Lecture 2023 Nobel Prize Laureate in Physics, Dr. Takaaki KAJITA, And Other Scientists Give Science Talks (on July 1, at Tokai Cultural Center and live-streamed on YouTube)

A special lecture entitled "The Hyper-Kamiokande Project Finally Begins" was held.

A total of 348 people came to the Tokai Cultural Center, and many others also watched the event via live streaming.

The lecture was moderated by Ms. Arisa Kuroda, a personality who had majored in physics, and began with opening remarks by Dr. Takashi Kobayashi, Director of J-PARC, and Mr. Osamu Yamada, Mayor of Tokai village.

At the beginning of the lecture, Dr. Takaaki KAJITA who received the Nobel Prize in Physics in 2015, President of the Science Council of Japan, Distinguished Professor and a Special University Professor Emeritus of the University of Tokyo, and Professor of the Institute for Cosmic Ray Research, explained the discovery of neutrinos, the existence of mass of the neutrino, and the mechanism of neutrino oscillation, along with the historical background, in a talk entitled "The Mystery of Neutrinos". Next, Dr. Ken Sakashita, Neutrino Section Leader, gave a talk entitled "Neutrinos Made at J-PARC," introducing neutrino research at J-PARC and explaining plans for upgrading the experimental facilities in the Hyper-Kamiokande project and the expected results. Subsequently, Dr. Atsuko Ichikawa, Professor of the Graduate School of Science and Faculty of Science, Tohoku University, gave a talk entitled "Secrets of the Universe Explored by the Hyper-Kamiokande," introducing the progress of the construction of the Hyper-Kamiokande and how the completion of upgrading the facility will accelerate the research on CP violation and other topics.

Dr. Takaaki KAJITA

2023 Neutron Industrial Application Report Meeting Held on July 13 and 14 (at Akihabara Convention Hall and partly online)

This report meeting focuses on matching the industry's requests and the industrial applications of neutrons and muons provided at the Materials and Life Science Experimental Facility (MLF) of J-PARC and the research reactor JRR-3.

The 6th annual event was held at the Akihabara Convention Hall, and 225 people attended over the two days at the venue.

This year marks the 15th anniversary of establishing the Industrial Users Society for Neutron Application. In addition to reviewing the progress to date, there were reports on achievements in a wide range of industries, from space science to polymers, biomaterials, metallic materials, and carbon neutrality, as well as efforts to address various issues, which were followed by a lively question-and-answer session.

The Director Delivered a Lecture at the Junior High School He Graduated from (July 14)

The J-PARC Director, KOBAYASHI Takashi, gave a lecture at his alma mater, Ochiai Junior High School in Maniwa City, Okayama Prefecture with a total of about 300 students. Almost all the students gathered in the

auditorium to listen to the lecture titled "Secrets of the Big Universe, Secrets of the Microscopic World, and Accelerators."

He then introduced J-PARC's features and role as the world's most powerful accelerator.

GSA Science Seminar (July 15, Hida City, Gifu Prefecture)

GSA (Geospace Adventure) is an underground exploration event that utilizes the actual tunnel of the Kamioka Mine and cutting-edge research facilities for astrophysics, such as Super-Kamiokande. This year, the event was held for the first time in four years, and 1,078 people applied for the 150-person limit. As part of the event, a KAGURA & J-PARC Science Seminar was held at the Kamioka-cho Community Center, with 43 people attending in the morning session and 32 in the afternoon. In the J-PARC seminar, which was entitled "Want to see? Want to know? J-PARC", Dr. Tatsuya Uzumaki of JAEA (formerly of the J-PARC Public Relations Section) explained that the neutrinos being launched into Super-Kamiokande are produced at J-PARC. Moreover, visitors were given an overview of J-PARC at the poster exhibition corner.

Eco Fes Hitachi 2023 (July 22, at Hitachi Civic Center)

J-PARC Center exhibited at "Eco Fes Hitachi 2023 - Let's find out what we can do to create a 'decarbonized city'" held by Hitachi City at the Hitachi Civic Center. Eco Fes Hitachi is an event where people can learn about environmental issues through experiments and hands-on experiences. About 250 people visited the J-PARC Center's booth despite the scorching weather. The superconducting coaster created by the Cryogenics Section of J-PARC Center was the most popular attraction this year, also. Superconductors cooled down to nearly -200°C glided along the rails like a roller coaster while levitating a few mm above the magnetic rails.

J-PARC staff explained about superconductivity.

Tokai Village Enjoy Summer School 2023 (July 25, August 1 and 9 at Tokai Library)

The Tokai Village Board of Education organized "Enjoy Summer School" for elementary school students in the village. The J-PARC Center held a series of experimental classes titled "Let's make a spinning top that spins while tilted!" Thirty-seven students joined them for three days in total.

Even when the magnets and coils were separated, the children observed how they interacted with each other due to the flowing current. On crafting spinning tops, children investigated how the motion of the spinning axis, precession, changed when the center of gravity was changed. Then, they were encouraged to find the center of gravity position where the precession did not occur.

Students worked on visualizing magnetic force.

Participation at the Magnet Power Exhibition (August 19 and 23, Hitachi Civic Center)

At the Magnet Power Exhibition at the Hitachi Civic Center, J-PARC demonstrated a superconducting coaster with the cooperation of the Cryogenics Section, attracting a total of 272 visitors. Two science shows were held in the science studio on both days, and a workshop

A boy astonished by the mysterious phenomena.

was held in the Orientation Room on August 19.

When a superconductor is cooled with liquid nitrogen, its electrical resistance becomes zero and a repulsive force called the Meissner effect is generated against a magnet. In this state, if a superconductor is forcibly pressed against a magnet, the superconductor will memorize the magnetic field lines of the magnet due to the pinning effect and an attractive force is also generated. In a superconducting coaster, the repulsive force and attractive force are balanced to allow a coaster made of a superconductor to float and glide on a track made of rubber magnets.

J-PARC Hello Science: "What is a 'Beam'?" (August 25)

At this month's Hello Science, Dr. Katsuhiro Moriya from the Accelerator Division gave a lecture on the definition of "beam," one of the most commonly used words at J-PARC, as well as the fun and challenges of handling beams.

In general, the word "beam" is often used in the construction industry and in science fiction anime. The beam that is accelerated at J-PARC is a collection of protons flying in the same direction. The laser beam that is familiar from stage performances is similar to the image of the beam that is handled at J-PARC. In an experiment during the lecture, the principle of beam convergence was introduced by using the light from an LED light source as a beam.

The three accelerators at J-PARC use the forces of electric fields and magnetic fields to accelerate and converge beams. However, it was introduced that in the J-PARC, the world's highest-performance accelerators, many challenges are being faced in controlling beams, as the electromagnetic fields created by high-intensity beams can have a negative impact on the beams themselves, and if the number of particles that make up the beams is too large it could destroy beam monitors.

Dr. Moriya, overflowing with love for a beam.

J-PARC Facility Open House Held On-Site for First Time in Four Years (October 1)

There were 1,163 visitors at the event. After a 4-year absence from public view, each of the J-PARC's facilities was very popular. The linear accelerator facility was especially popular, with all time slots fully booked in the morning. In the exhibition corner, special exhibits were displayed, including the experimental device that analyzed the rocks from the asteroid Ryugu brought back by the planetary probe Hayabusa2, and a cutaway model of a fuel cell car. Many visitors were interested in the exhibits and viewed them with great interest.

As part of J-PARC Hello Science, five lectures were given by the director of the J-PARC Center and researchers, introducing the status of J-PARC, the latest research, and results, etc.

Gauss Accelerator

Kaleidoscope of Light

Scientific Activities for Kids at Ozora Marche (October 7, Tokai Village)

The Ozora Marche, one of the four major festivals of the Tokai Village, was held in October. The J-PARC Center held a demonstration of an original toy coaster using superconducting materials and a workshop on making kaleidoscopes using polarizing sheets.

The J-PARC booth attracted 373 visitors.

The girls enjoyed making beautiful kaleidoscopes with polarized film and scotch tape.

KIPP Nakameguro Children's Class Held at Nakameguro Elementary School (October 11)

A lecture entitled "Let's Make the World's Smallest Mysterious Top and Touch the World of Elementary Particles!" was held at Nakameguro Elementary School in Meguro Ward. Dr. Masashi Otani of the Accelerator Division was the lecturer, and 14 students from grades one to four learned about the universe and elementary particles clearly and concisely. In the gyroscope experiment, the children were engaged in trying to spin the top as long and as beautifully as possible. They also realized that precession occurs due to differences in how the top is spun. In the handmade tops experiment, they enjoyed experimenting with their own ideas, such as connecting large and small tops together.

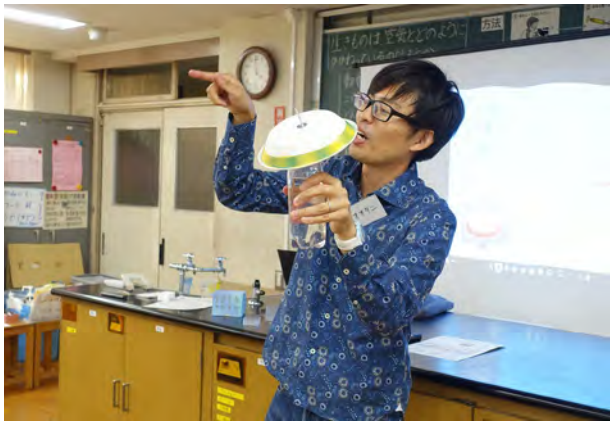

Dr. Otani explained in a simple way for kids.

J-PARC Photo Contest 2023 Held

The 10th J-PARC Photo Contest was held and received 43 entries this year. After careful selection by a panel of judges, including an invited expert, a photo by Mr. HARADA Takeshi from the Nuclear Hadron Physics Laboratory of Kyoto University Graduate School was awarded the grand prize.

The work was a photography of the active fiber target used for precision spectroscopy of hypernuclei.

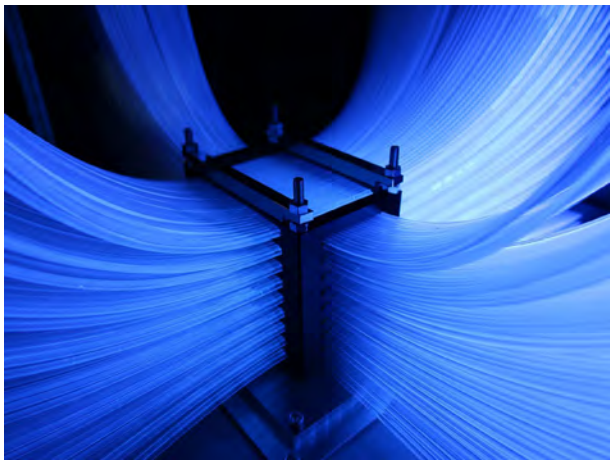

Grand Prize "Active fiber target" HARADA Takeshi

Youngsters' Science Festival in Hitachi (October 29)

There were over 3,000 people who attended the "Youngsters' Science Festival". The venue was packed with workshops with fascinating science experiments.

The J-PARC booth featured a crafts workshop to build a unipolar motor, whose copper wire coil was spun by the force of a magnetic field. The children immersed themselves in the experiment, forming copper wires into unique shapes.

Frustration Stick specially made by Dr. Takayanagi

8th Fusion of Humanities and Sciences Symposium (November 2-3, National Museum of Nature, and Science)

The world's highest-intensity negative muon beam generated at J-PARC's MLF is also used to study cultural artifacts and other humanities materials. To explore the potential of humanities research using such quantum beams, the KEK Institute of Materials Structure Science

has held an annual "Fusion of Humanities and Sciences Symposium" since 2019.

This time, the symposium was held at the National Museum of Nature and Science, Ueno Main Building, with the theme "Exploring History with Quantum Beams - The Horizon of Fusion of Humanities and Sciences Weaved by Accelerators." About 70 people attended, and there were 12 oral presentations on various topics, including coins, metals, asteroids and meteorites, ancient tombs, and tsunamis. A public lecture with three presentations was held on the second day's afternoon. The public lecture attracted a lot of interest, with questions coming from both the audience and about 110 Zoom attendees.

Group photo of Day 2

J-PARC Public Lecture 2023 "THE MUONS FOR THE FUTURE - Seeing the Invisible!" (November 25)

A lecture organized by the J-PARC Center, Tokai Village, and the Tokai Village Board of Education was held at the Tokai Cultural Center.

After opening remarks by the Director of the J-PARC Center and the Mayor of Tokai Village, Dr. Izumi Umegaki of the Muon Section explained the basic properties of muons and reported the research results on muon-based analysis of batteries at J-PARC. Next, Mr. Nakaizumi and Ms. Hayashi, curators of the Tokai Village Museum, introduced a project using cosmic ray muons, in which local students from elementary to high school collaborate to observe the ancient mounds of Tokai Village.

In the final presentation, Professor Tomoki Nakamura of the Graduate School of Tohoku University talked about the results of analyses of the asteroid samples using J-PARC's muon beam. The samples were recovered from the asteroid Ryugu by the Hayabusa2 spacecraft. The event was attended by 168 on-site participants and 72 online participants, who engaged in lively discussions during the Q&A sessions following each presentation.

Hyper-Kamiokande Project Promotion Council Held (February 14)

The 4th Hyper-Kamiokande Project Promotion Council was held at J-PARC on February 14. The Hyper-Kamiokande Project is an international collaborative scientific initiative hosted by Japan.

During the council, reports were provided on the progress of the Hyper-Kamiokande project, budget planning, and the status of agreements with international research organizations. The on-site council, held for the first time in four years, facilitated a lively exchange of opinions, confirming further collaboration between KEK and the University of Tokyo.

Following the conclusion of the council, participants had the opportunity to tour the facility and observe the upgraded Near Neutrino Detector for the T2K experiment.

Group photo

Tokai Forum (February 21, Tokai Culture Center)

JAEA has been holding this forum as an opportunity to report the results of research and development and the progress of JAEA's projects to the local community. This year, the 18th forum was held under the theme of "Making Nuclear Power Closer".

Dr. Takenao Shinohara from the Neutron Science Section and Dr. Hiroshi Nozaki, an adjunct researcher at J-PARC Center, reported on their studies to improve the performance of fuel cells and Li ion batteries for automobile application.

This technique is employed to improve the performance of electric vehicles and to evaluate the safety of used lithium-ion batteries for their reuse and recycle, so as to contribute to the mitigation of global warming

and the carbon neutrality.

International Advisory Committee 2024 (IAC 2024) Held (March 4, 5)

International Advisory Committee, operating under the "Fundamental Collaboration Agreement Regarding the Management of High-Intensity Proton Accelerator Facilities," serves as the superior committee overseeing four specialized subcommittees in the fields of accelerators, nuclear transmutation, neutrons, and muons. It convenes external members to deliberate on matters crucial to the operation, utilization, and facility development of J-PARC. Of the 16 committee members,12 from overseas and 4 from Japan, 14 attended the meeting, including Chairperson Robert McGreevy, to discuss research and development activities at J-PARC for the fiscal year 2023 and to deliberate on recommendations for the years ahead.

During the parallel session, young researchers presented their recent research and development activities.

Group photo

■FY2023 Quantum Beam Science Festa Held (March 5-7, Mito City Hall) The 15th MLF Symposium and the 41st PF* Symposium

The Quantum Beam Science Festa is organized annually by the Institute of Materials Structure Science (KEK), J-PARC Center, Comprehensive Research Organization for Science and Society (CROSS), PF Users Association, and J-PARC MLF Users Society. At this year's event held from March 5 to 7 at the Mito Civic Hall, the on-site participants totaling approximately 470 exceeded the number of attendees from the previous year.

Following the PF symposium on the first day, two keynote lectures were given on the 6th. In addition, parallel sessions in six fields and around 260 poster presentations were demonstrated. The 15th MLF Symposium on the 7th consisted of two parts.

*Photon Factory, Institute of Materials Structure, KEK

Photo by Institute of Material Structure Science, KEK

Visitors

TSUZUKU Jun-ya, Mayor, Hida-City (April 13)

HIBINO Katsuhiko, President, Tokyo University of the Arts (June 19)

Singtong Lapisatepun, Ambassador, the Kingdom of Thailand to Tokyo (July 24)

MORIYAMA Masahito, Minister, Ministry of Education, Culture, Sports, Science and Technology (December 18)

There were 2,675 visitors to J-PARC for the period from April 2023 to the end of March 2024.

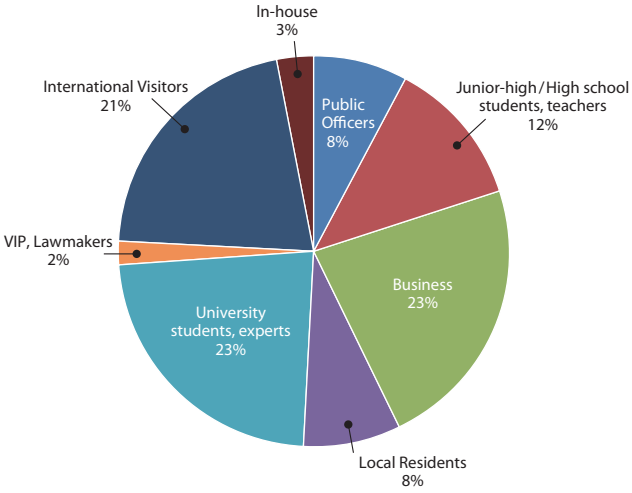

Publications

Publications in Periodical Journals

A-001
K. Ohishi, *et al*.
Ion Dynamics in P2-Na_xCoO_2 Detected with Operando Muon Spin Rotation and Relaxation
ACS Appl. Energy Mater., 6 8111–8119 (2023).

A-002
Y. Idemoto, *et al*.
Rate Dependence of the Average Crystal Structure and Electronic Structure of $0.5Li_2MnO_3$ –$0.5LiMn_{10/24}Ni_{7/24}Co_{7/24}O_2$ for a Lithium-Ion Battery Positive Electrode Material in Steady State
ACS Appl. Energy Mater., 6 8327–8335 (2023).

A-003
M. Harada, *et al*.
Equation Elucidating the Catalyst-Layer Proton Conductivity in a Polymer Electrolyte Fuel Cell Based on the Ionomer Distribution Determined Using Small-Angle Neutron Scattering
ACS Appl. Mater. Interfaces, 15 42594–42602 (2023).

A-004
T. Kämäräinen, *et al*.
Tailoring the Self-Assembly of Steviol Glycoside Nanocarriers with Steroidal Amphiphiles
ACS Biomater. Sci. Eng., 9 5747–5760 (2023).

A-005
S. Misaki, *et al*.
Pd Nanoparticles on the Outer Surface of Microporous Aluminosilicates for the Direct Alkylation of Benzenes Using Alkanes
ACS Catal., 13 12281–12287 (2023).

A-006
T. Murakawa, *et al*.
Neutron Crystallography of a Semiquinone Radical Intermediate of Copper Amine Oxidase Reveals a Substrate-Assisted Conformational Change of the Peptidyl Quinone Cofactor
ACS Catal., 13 12403–12413 (2023).

A-007
T. Osawa, *et al*.
Development of Nondestructive Elemental Analysis System for Hayabusa2 Samples Using Muonic X-Rays
ACS Earth Space Chem., 7 699–711 (2023).

A-008
W. Yoshimune, *et al*.
3D Water Management in Polymer Electrolyte Fuel Cells toward Fuel Cell Electric Vehicles
ACS Energy Lett., 8 3485–3487 (2023).

A-009
K. Yamashita, *et al*.
The Hydrogen-Bond Network in Sodium Chloride Tridecahydrate: Analogy with Ice VI
Acta Crystallogr. Sect. B Struct. Sci. Cryst. Eng. Mater., 79 414–426 (2023).

A-010
T.-N. Lam, *et al*.
Tensile Overload-Induced Texture Effects on the Fatigue Resistance of a CoCrFeMnNi High-Entropy Alloy
Acta Mater., 245 118585 (2023).

A-011
W. Woo, *et al*.
Competitive Strengthening between Dislocation Slip and Twinning in Cast-Wrought and Additively Manufactured CrCoNi Medium Entropy Alloys
Acta Mater., 246 118699 (2023).

A-012
H. Kwon, *et al*.
High-Density Nanoprecipitates and Phase Reversion via Maraging Enable Ultrastrong yet Strain-Hardenable Medium-Entropy Alloy
Acta Mater., 248 118810 (2023).

A-013
W. Gong, *et al*.
Lattice Parameters of Austenite and Martensite during Transformation for Fe–18Ni Alloy Investigated through In-Situ Neutron Diffraction
Acta Mater., 250 118860 (2023).

A-014
S. Harjo, *et al*.
Strengthening of αMg and Long-Period Stacking Ordered Phases in a Mg-Zn-Y Alloy by Hot-Extrusion with Low Extrusion Ratio
Acta Mater., 255 119029 (2023).

A-015
W. Mao, *et al*.
Quantitatively Evaluating Respective Contribution of Austenite and Deformation-Induced Martensite to Flow Stress, Plastic Strain, and Strain Hardening Rate in Tensile Deformed TRIP Steel
Acta Mater., 256 119139 (2023).

A-016
Y. Izumi, *et al*.
Electropositive Metal Doping into Lanthanum Hydride for H^- Conducting Solid Electrolyte Use at Room Temperature
Adv. Energy Mater., 13 2301993 (2023).

A-017
H. Zhou, *et al*.
Fast Lithium Intercalation Mechanism on Surface-Modified Cathodes for Lithium-Ion Batteries
Adv. Energy Mater., 13 2302402 (2023).

A-018
X. Liu, *et al*.
In Situ Neutron Diffraction Investigating Microstructure and Texture Evolution upon Heating of Nanostructured CoCrFeNi High-Entropy Alloy
Adv. Eng. Mater., 25 2201256 (2023).

A-019
H. Yaguchi, *et al*.
High Oxide-Ion Conductivity through the Interstitial Oxygen Site in Sillén Oxychlorides
Adv. Funct. Mater., 33 2214082 (2023).

A-020
J. Nakayama, *et al*.
Electrical Double Layer Formation at Intercalation Cathode–Organic Electrolyte Interfaces During Initial Lithium-Ion Battery Reactions
Adv. Mater. Interfaces, 11 2300780 (2023).

A-021
K. Kubota, *et al*.
Impact of Ti and Zn Dual-Substitution in P2 Type $Na_{2/3}Ni_{1/3}Mn_{2/3}O_2$ on Ni–Mn and Na-Vacancy Ordering and Electrochemical Properties
Adv. Mater., 35 2300714 (2023).

A-022
H. Asai, *et al*.
Micelle-crosslinked Hydrogels with Stretchable, Self-healing, and Selectively Adhesive Properties: Random Copolymers Work as Dynamic yet Self-sorting Domains
Aggregate, 4 e316 (2023).

A-023
C. Shito, *et al*.
Hydrogen Occupation and Hydrogen-Induced Volume Expansion in $Fe_{0.9}Ni_{0.1}D_x$ at High *P-T* Conditions
Am. Mineral., 108 659–666 (2023).

A-024
Y. Miyagi, *et al*.
Presence of a Chiral Soliton Lattice in the Chiral Helimagnet $MnTa_3S_6$
APL Mater., 11 101105 (2023).

A-025
Y. Wang, *et al*.
In Situ Neutron Diffraction Study on the Deformation Behavior of the Plastic Inorganic Semiconductor Ag_2S
Appl. Phys. Lett., 123 011903 (2023).

A-026
J. Shimada, *et al*.
Quasi-Elastic Neutron Scattering Studies on

Fast Dynamics of Water Molecules in Tetra-*n*-Butylammonium Bromide Semiclathrate Hydrate
Appl. Phys. Lett., 123 044104 (2023).

A-027
H. Yamamoto, *et al*.
Magnetic Field-Induced Phase Transition in Ilmenite-Type $CoVO_3$
Appl. Phys. Lett., 123 132404 (2023).

A-028
Y. Hirota, *et al*.
Differences in Water Dynamics between the Hydrated Chitin and Hydrated Chitosan Determined by Quasi-Elastic Neutron Scattering
Bioengineering, 10 622 (2023).

A-029
E. Saiki, *et al*.
Structure and Conformation of Hydroxypropylmethyl Cellulose with a Wide Range of Molar Masses in Aqueous Solution–Effects of Hydroxypropyl Group Addition
Biomacromolecules, 24 4199–4207 (2023).

A-030
Y. Hanazono, *et al*.
Description of Peptide Bond Planarity from High-Resolution Neutron Crystallography
Biophys. Physicobiology, 20 e200035 (2023).

A-031
S. Ito, *et al*.
Muon Spin Rotation (μSR) for Characterizing Radical Addition to C=S in Xanthene-9-Thione and Thioxanthene-9-Thione
Bull. Chem. Soc. Jpn., 96 461–464 (2023).

A-032
S. Takagi, *et al*.
Operando Structural Analysis of Phase Transition of Graphite Electrode during Li De-Intercalation Process Using Neutron and Synchrotron Radiation X-Ray Diffraction
Carbon, 215 118414 (2023).

A-033
M. Akamatsu, *et al*.
Dynamic Control of Interfacial Properties and Self-Assembly with Photoirradiation
Chem. Lett., 52 573–581 (2023).

A-034
Y. Cao, *et al*.
Pressure-Modulated Magnetism and Negative Thermal Expansion in the Ho_2Fe_{17} Intermetallic Compound
Chem. Mater., 35 3249–3255 (2023).

A-035
Y. Cao, *et al*.
Quantified Zero Thermal Expansion in Magnetic R_2Fe_{17}-Based Intermetallic Compounds (R = Rare Earth)
Chem. Mater., 35 4549–4555 (2023).

A-036
K. Ogawa, *et al*.
Orbital Engineering in Sillén–Aurivillius Phase Bismuth Oxyiodide Photocatalysts through Interlayer Interactions
Chem. Mater., 35 5532–5540 (2023).

A-037
S. Yamagishi, *et al*.
Ferroaxial Transitions in Glaserite-Type Compounds: Database Screening, Phonon Calculations, and Experimental Verification
Chem. Mater., 35 747–754 (2023).

A-038
Y. Sakuda, *et al*.
Dimer-Mediated Cooperative Mechanism of Ultrafast-Ion Conduction in Hexagonal Perovskite-Related Oxides
Chem. Mater., 35 9774–9788 (2023).

A-039
T. Xia, *et al*.
Chemistry of Zipping Reactions in Mesoporous Carbon Consisting of Minimally Stacked Graphene Layers
Chem. Sci., 14 8448–8457 (2023).

A-040
T. Hiromoto, *et al*.
New Insights into the Oxidation Process from Neutron and X-Ray Crystal Structures of an O_2-Sensitive [NiFe]-Hydrogenase
Chem. Sci., 14 9306–9315 (2023).

A-041
A. Zhang, *et al*.
Chiral Dirac Fermion in a Collinear Antiferromagnet
Chin. Phys. Lett., 40 126101 (2023).

A-042
H. Nakao, *et al*.
Impact of Transmembrane Peptides on Individual Lipid Motions and Collective Dynamics of Lipid Bilayers
Colloids Surf. B Biointerfaces, 228 113396 (2023).

A-043
M. Harada, *et al*.
Scattering Investigations into the Structures of Polymer-Electrolyte-Fuel-Cell Catalyst Layers Exhibiting Robust Performance against Varying Water Fractions of Catalyst Ink Solvents
Colloids Surf. Physicochem. Eng. Asp., 665 131183 (2023).

A-044
N. Terada, *et al*.
Crystal Electric Field Level Scheme Leading to Giant Magnetocaloric Effect for Hydrogen Liquefaction
Commun. Mater., 4 13 (2023).

A-045
R. Morikawa, *et al*.
High Proton Conduction in Ba_2LuAlO_5 with Highly Oxygen-Deficient Layers
Commun. Mater., 4 42 (2023).

A-046
E. Nocerino, *et al*.
Competition between Magnetic Interactions and Structural Instabilities Leading to Itinerant Frustration in the Triangular Lattice Antiferromagnet $LiCrSe_2$
Commun. Mater., 4 81 (2023).

A-047
G. Sala, *et al*.
Field-Tuned Quantum Renormalization of Spin Dynamics in the Honeycomb Lattice Heisenberg Antiferromagnet $YbCl_3$
Commun. Phys., 6 234 (2023).

A-048
S. Shamoto, *et al*.
Spiral Spin Cluster in the Hyperkagome Antiferromagnet Mn_3RhSi
Commun. Phys., 6 248 (2023).

A-049
I. E. Golub, *et al*.
Structural Insight into the Magnesium Borohydride – Ethylenediamine Solid-State Mg-Ion Electrolyte System
Dalton Trans., 52 2404–2411 (2023).

A-050
J. Kamiya, *et al*.
Evaluation of vacuum firing effect on stainless steel from vacuum and surface point of view
e-Journal of Surface Science and Nanotechnology (Internet), 21(3), p.144 - 153, 2023/06

A-051
J. Kamiya, *et al*.
Investigation of niobium surface roughness and hydrogen content with different polishing conditions for performance recovery of superconducting QWRs in JAEA Tokai-Tandem Accelerator
e-Journal of Surface Science and Nanotechnology (Internet), 21(4), p.344 - 349, 2023/05

A-052
E. M. Germany, *et al*.
Dual Recognition of Multiple Signals in Bacterial Outer Membrane Proteins Enhances Assembly and Maintains Membrane Integrity
eLife, 12 RP90274 (2023).

A-053
E. M. Germany, *et al*.
Simultaneous Recognition of Multiple Signals in Bacterial Outer Membrane Proteins Enhance Assembly and Maintain Membrane Integrity
eLife, 12 RP90274 (2023).

A-054
H. Yamada, *et al*.
Lithium Ion Transport Environment by Molecular Vibrations in Ion-Conducting Glasses
ENERGY Environ. Mater., 7 e12612 (2024).

A-055
T. Saito, *et al*.
Heterogeneous Aggregation of Humic Acids Studied by Small-Angle Neutron and X-Ray Scattering
Environ. Sci. Technol., 57 9802–9810 (2023).

A-056
S. Endo, *et al*.
Measurements of Neutron Total and Capture Cross Sections of ^{139}La and Evaluation of Resonance Parameters
Eur. Phys. J. A, 59 288 (2023).

A-057
A. Abed Abud, *et al*.
Reconstruction of interactions in the ProtoDUNE-SP detector with Pandora
Eur. Phys. J. C 83, 618 (2023)

A-058
K. Abe, *et al*.
Measurements of neutrino oscillation parameters from the T2K experiment using 3.6×10^{21} protons on target
Eur. Phys. J. C 83, 782 (2023)

A-059
K. Aoki, R. Muto, *et al*.
Experimental Study of In-medium Spectral Change of Vector Mesons at J-PARC
Few-Body Systems 64, 63 (2023)

A-060
H. Mamiya, *et al*.
Polarized Neutron Transmission Spectroscopy on Carbon Steel
IEEE Trans. Magn., 59 1–5 (2023).

A-061
H. Iwashita, *et al*.
Energy-Resolved SEU Cross Section From 10-meV to 800-MeV Neutrons by Time-of-Flight Measurement
IEEE Trans. Nucl. Sci., 70 216–221 (2023).

A-062
R. Honda
New Clock Distribution System Based on Clock-Duty-Cycle-Modulation for Distributed Data-Aquisition System
IEEE Trans. Nucl. Sci., 70, 1102 (2023)

A-063
T. Kishishita, *et al*.
Hybrid SiC Pixel Detector for Charged-Particle Beam Monitor
IEEE Trans. Nucl. Sci., 70, 1210 (2023)

A-064
T. Takahashi, *et al*.
Streaming DAQ Software Prototype at the J-PARC Hadron Experimental Facility
IEEE Trans. Nucl. Sci., 70, 922 (2023)

A-065
S. Oyama, *et al*.
Evaluation of the Magnetic Field Error Due to Manufacturing Tolerance of Superconducting Magnet for the J-PARC Muon *g*-2/EDM Experiment
IEEE Transactions on Applied Superconductivity, Vol 33, 4001005 (2023)

A-066
K. Sasaki, *et al*.
Study of Vibration Effect on Magnetic Field Homogeneity in the Magnet System for the *g*-2/EDM Experiment at the J-PARC
IEEE Transactions on Applied Superconductivity, Vol 33, 4002305 (2023)

A-067
M. Dhakarwal
Design Optimization of Combined Function Accelerator Magnet Using Truncated Singular Value Decomposition
IEEE Transactions on Applied Superconductivity, Vol 33, 4003305 (2023)

A-068
N. Sumi, *et al*.
Construction and Commissioning Status of the Superconducting Magnets for COMET Phase-I Experiment at J-PARC
IEEE Transactions on Applied Superconductivity, Vol 33, 4500205 (2023)

A-069
K. Sasaki, *et al*.
Design of the Superconducting Magnet System for the New *g*-2/EDM Experiment in the J-PARC
IEEE Transactions on Applied Superconductivity, Vol 33, 4500305 (2023)

A-070
T. Onji, *et al*.
Demonstration of 10 KJ-Capacity Energy Storage Coil Made of MgB_2 With Liquid Hydrogen Indirect Cooling
IEEE Transactions on Applied Superconductivity, Vol 33, 5700105 (2023)

A-071
C. Reis, *et al*.
Investigating Irradiated Superconducting Magnet Insulation Materials for Particle Accelerators and Other High-Dose Environments
IEEE Transactions on Applied Superconductivity, Vol 33, 7700307 (2023)

A-072
M. Nakamoto, *et al*.
Influence of Axial Strain and Transverse Compressive Load on Critical Current of Nb_3Sn Wires for the FCC
IEEE Transactions on Applied Superconductivity, Vol 33, 8400505 (2023)

A-073
H. Ubukata, *et al*.
Structural Transformation in LnHS (Ln = La, Nd, Gd, and Er) with Coordination Change between an S-Centered Octahedron and a Trigonal Prism
Inorg. Chem., 62 6696–6703 (2023).

A-074
M. Minohara, *et al*.
Control of Hole Density in Russellite Bi_2WO_6 via Intentional Chemical Doping
Inorg. Chem., 62 8940–8947 (2023).

A-075
Y. Su, *et al*.
Residual Stress Relaxation by Bending Fatigue in Induction-Hardened Gear Studied by Neutron Bragg Edge Transmission Imaging and X-Ray Diffraction
Int. J. Fatigue, 174 107729 (2023).

A-076
T. Yamashita, *et al*.
Martensitic Transformation Behavior of Fe–Ni–C Alloys Monitored by *In-Situ* Neutron Diffraction during Cryogenic Cooling
ISIJ Int., 64 192–201 (2024).

A-077
A. Yasue, *et al*.
Evaluation of Bond Repair Effect for Ultra-High-Strength Concrete Specimens by Neutron Diffraction Method
J. Adv. Concr. Technol., 21 337–350 (2023).

A-078
P. Thirathipviwat, *et al*.
Microstructure, Dislocation Density and Microhardness of 1 %C-Doped CoCrFeNi Complex Concentrated Alloys during Isochronal Annealing
J. Alloys Compd., 930 167504 (2023).

A-079
M. R. Joo, *et al*.
High-Ductility Aluminium Alloys Including Small Sub-Grains with Wide Low Angle Boundary
J. Alloys Compd., 934 167868 (2023).

A-080
K. Chu, *et al*.
Grain Size Effect on the Temperature-Dependence of Elastic Modulus of Nanocrystalline NiTi
J. Alloys Compd., 934 167907 (2023).

A-081
T. Kurumaji, *et al*.
Single Crystal Growths and Magnetic Properties of Hexagonal Polar Semimetals

*R*AuGe (*R*=Y, Gd–Tm, and Lu)
J. Alloys Compd., 947 169475 (2023).

A-082
Y. Onuki, *et al*.
Ductile Behavior Assisted by Continuous Dynamic Recrystallization during High-Temperature Deformation of Calcium-Added Magnesium Alloy AZX612
J. Alloys Compd., 962 171147 (2023).

A-083
A. Morimura, *et al*.
High-Pressure Syntheses, Crystal Structures, and Magnetic Properties of Novel Quadruple Perovskite Oxides $LaMn_3Ru_2Mn_2O_{12}$ and $LaMn_3Ru_2Fe_2O_{12}$
J. Alloys Compd., 968 172263 (2023).

A-084
M. Kaneko, *et al*.
Enhanced Li-ion Conductivity of Strontium Doped Li-excess Garnet-type $Li_{7+x}La_{3-x}Sr_xZr_2O_{12}$
J. Am. Ceram. Soc., 106 4480–4487 (2023).

A-085
T. Nakanishi, *et al*.
Development of an Iron(II) Complex Exhibiting Thermal- and Photoinduced Double Proton-Transfer-Coupled Spin Transition in a Short Hydrogen Bond
J. Am. Chem. Soc., 145 19177–19181 (2023).

A-086
Y. Noda, *et al*.
Water Distribution in Human Hair Microstructure Elucidated by Spin Contrast Variation Small-Angle Neutron Scattering
J. Appl. Crystallogr., 56 1015–1031 (2023).

A-087
H. Iwase, *et al*.
New Measurement System Based on Small-Angle Neutron Scattering for Structural Analysis of Light-Responsive Materials
J. Appl. Crystallogr., 56 110–115 (2023).

A-088
H. Shishido, *et al*.
Orientation Mapping of $YbSn_3$ Single Crystals Based on Bragg-Dip Analysis Using a Delay-Line Superconducting Sensor
J. Appl. Crystallogr., 56 1108–1113 (2023).

A-089
F. Malamud, *et al*.
An Optimized Single-Crystal to Polycrystal Model of the Neutron Transmission of Textured Polycrystalline Materials
J. Appl. Crystallogr., 56 143–154 (2023).

A-090
H. Arima-Osonoi, *et al*.
Development of a D_2O/H_2O Vapor Generator for Contrast-Variation Neutron Scattering
J. Appl. Crystallogr., 56 1802–1812 (2023).

A-091
M.-M. Schiavone, *et al*.
Extended *Q* -Range Small-Angle Neutron Scattering to Understand the Morphology of Proton-Exchange Membranes: The Case of the Functionalized Syndiotactic-Polystyrene Model System
J. Appl. Crystallogr., 56 947–960 (2023).

A-092
A. Muneem, *et al*.
Investigation of Neutron Imaging Applications Using Fine-Grained Nuclear Emulsion
J. Appl. Phys., 133 054902 (2023).

A-093
K. Cho, *et al*.
Weak Trimer Distortion and Planar Spin Configuration in Hexagonal $Lu_{0.6}In_{0.4}FeO_3$
J. Appl. Phys., 133 194103 (2023).

A-094
M. Hiraishi, *et al*.
Photo-Excited Charge Carrier Lifetime Enhanced by Slow Cation Molecular Dynamics in Lead Iodide Perovskite $FAPbI_3$
J. Appl. Phys., 134 055106 (2023).

A-095
Y. Oba, H. Sasaki
Neutron Imaging Technology and Diverse Applications: Observation of Microstructures in Cu Using Bragg Edge Imaging
J. At. Energy Soc. Jpn., 65 499–502 (2023).

A-096
T. Joutsuka, *et al*.
Neutron Crystallography and Quantum Chemical Analysis of Bilin Reductase PcyA Mutants Reveal Substrate and Catalytic Residue Protonation States
J. Biol. Chem., 299 102763 (2023).

A-097
T. Okuyama, *et al*.
Comparison of Phase Separation Structures between Undercooled Cu–Fe and Cu–Co Alloys Solidified Under a Static Magnetic Field
J. Chem. Eng. Jpn., 56 2211117 (2023).

A-098
S. Hashimoto, *et al*.
Anomalous Behavior of Liquid Molecules near Solid Nanoparticles: Novel Interpretation on Thermal Conductivity Enhancement in Nanofluids
J. Colloid Interface Sci., 638 475–486 (2023).

A-099
S. Abeykoon, *et al*.
Deuterium Content and Site Occupancy in Iron Sulfide at High Pressure and Temperature Determined Using In Situ Neutron Diffraction Measurements
J. Geophys. Res. Solid Earth, 128 e2023JB026710 (2023).

A-100
K. Kanno, *et al*.
Commissioning of a hadron blind detector for dielectron measurement in *p*A reactions at J-PARC
J. Instrum., 18, C06021 (2023)

A-101
I. Alekseev, *et al*.
SuperFGD prototype time resolution studies
J. Instrum., 18, P01012 (2023)

A-102
A. Abed Abud, *et al*.
Highly-parallelized simulation of a pixelated LArTPC on a GPU
J. Instrum., 18, P04034 (2023)

A-103
C. Shin, *et al*.
The acrylic vessel for $JSNS^2$-II neutrino target
J. Instrum., 18, T12001 (2023)

A-104
S. Kobayashi, *et al*.
Polarized Neutron Scattering Study of Hollow Fe_3O_4 Submicron Spherical Particles
J. Magn. Magn. Mater., 569 170410 (2023).

A-105
A. Matsushita, *et al*.
Effects of Loading Direction on the Anisotropic Tensile Properties of Duplex Stainless Steels Based on Phase Strains Obtained by In Situ Neutron Diffraction Experiments
J. Mater. Eng. Perform., 33 6352–6361 (2024).

A-106
T. Yokoyama, *et al*.
Resveratrol Derivatives Inhibit Transthyretin Fibrillization: Structural Insights into the Interactions between Resveratrol Derivatives and Transthyretin
J. Med. Chem., 66 15511–15523 (2023).

A-107
Y. Kameda, *et al*.
Direct Determination of Intramolecular Structure of D_2O in the First Hydration Shell of Ni^{2+}
J. Mol. Liq., 382 121927 (2023).

A-108
T. Kikuchi, *et al*.
Overall Picture and Details of Diffusion Dynamics for Liquid Benzene by Quasielastic Neutron Scattering and Mode Distribution Analysis
J. Mol. Liq., 385 121868 (2023).

A-109
H. Abe, *et al*.
Nanoconfined Water in Ionic Liquid and Lyotropic Ionic Liquid Crystals by Small- and Wide-Angle X-Ray and Neutron Scattering: 1-Decyl-3-Methylimidazolium Nitrate
J. Mol. Liq., 386 122551 (2023).

A-110
G. Wang, *et al*.
Atomic Insights into the Heterogeneity and the Interface Interactions of Nanoconfined Aqueous Electrolyte Solution
J. Mol. Liq., 388 122746 (2023).

A-111
R. Toyoda, *et al*.
Atomic Structure of ZrO_2-Doped Li_2O–SiO_2-Based Multi-Component Glasses Revealed by Molecular Dynamics–Reverse Monte Carlo Modeling
J. Non-Cryst. Solids, 616 122472 (2023).

A-112
G. Rovira, *et al*.
^{241}Am Neutron Capture Cross Section Measurement Using the NaI(Tl) Spectrometer of the ANNRI Beamline of J-PARC
J. Nucl. Sci. Technol., 61 459–477 (2024).

A-113
H. Takei
Investigating Random Beam Trips in a Linear Accelerator of the Japan Proton Accelerator Research Complex for the Development of an Accelerator-Driven Nuclear Transmutation System
J. Nucl. Sci. Technol., 61, 1075–1088 (2023).

A-114
M. Akamatsu
Inner and Interfacial Environmental Nanoarchitectonics of Supramolecular Assemblies Formed by Amphiphiles: From Emergence to Application
J. Oleo Sci., 72 105–116 (2023).

A-115
M. Nakada
Low-Temperature Behaviors, Cold Crystallization, and Glass Transition in Poly(vinylpyrrolidone) Aqueous Solution
J. Phys. Chem. B, 127 10556–10563 (2023).

A-116
Y. Kameda, *et al*.
Direct Determination of the Relationship between the Intramolecular Oxygen–Hydrogen Bond Length and Its Stretching Vibrational Frequency of the Methanol Molecule in the Liquid State
J. Phys. Chem. B, 127 7758–7763 (2023).

A-117
Y. Fujita, *et al*.
Structural Investigation of Li_2O–LiI Amorphous Solid Electrolytes
J. Phys. Chem. C, 127 14687–14693 (2023).

A-118
A. Kitajou, *et al*.
Cathode Properties of *x* LiF–$LiCrO_2$ Composites (*x* = 0–1.5) Prepared by Dry Ball-Milling Method for Lithium Ion Batteries
J. Phys. Chem. C, 127 2866–2874 (2023).

A-119
K. Mori, *et al*.
Effects of Mixed Phases on Electrical Conductivities for $(CeF_3)_{1-m}(CaF_2)_m$ Fast-Fluoride-Ion-Conducting Solid Electrolytes
J. Phys. Chem. C, 127 59–68 (2023).

A-120
K. Ikeda, *et al*.
Vacancies Introduced during the Crystallization Process of the Glass-Ceramics Superionic Conductor, Na_3PS_4, Investigated by Neutron Total Scattering and Reverse Monte Carlo Method
J. Phys. Chem. C, 127 6199–6206 (2023).

A-121
H. Kobayashi, *et al*.
Slightly Hydrogen-Ordered State of Ice IV Evidenced by *In Situ* Neutron Diffraction
J. Phys. Chem. Lett., 14 10664–10669 (2023).

A-122
Z. Jing, *et al*.
Hydration of Alkali Metal and Halide Ions from Static and Dynamic Viewpoints
J. Phys. Chem. Lett., 14 6270–6277 (2023).

A-123
T. Kumada, *et al*.
Polarized Neutrons Observed Nanometer-Thick Crystalline Ice Plates in Frozen Glucose Solution
J. Phys. Chem. Lett., 14 7638–7643 (2023).

A-124
J. G. Nakamura, *et al*.
Short-Range Spin Order in Paramagnetic $AgCrSe_2$
J. Phys. Chem. Solids, 175 111199 (2023).

A-125
R. Kadono, *et al*.
Local Electronic Structure of Interstitial Hydrogen in MgH_2 Inferred from Muon Study
J. Phys. Condens. Matter, 35 285503 (2023).

A-126
Y. Sakaguchi, *et al*.
Direct Observation of Concentration Fluctuations in Au–Si Eutectic Liquid by Small-Angle Neutron Scattering
J. Phys. Condens. Matter, 35 415403 (2023).

A-127
E. Nocerino, *et al*.
Unusually Large Magnetic Moment and Tricritical Behavior of the CMR Compound $NaCr_2O_4$ Revealed with High Resolution Neutron Diffraction and μ^+ SR
J. Phys. Mater., 6 035009 (2023).

A-128
T. Taniguchi, *et al*.
Magnetic Instability of $Pr_3Ru_4Sn_{13}$
J. Phys. Soc. Jpn., 92 124703 (2023).

A-129
M. Maeda, *et al*.
Development of Correction Method for Sample Density Effect on PGA
J. Radioanal. Nucl. Chem., 332 2995–2999 (2023).

A-130
E. Nocerino, *et al*.
Q-Dependent Electron-Phonon Coupling Induced Phonon Softening and Non-Conventional Critical Behavior in the CDW Superconductor $LaPt_2Si_2$
J. Sci. Adv. Mater. Devices, 8 100621 (2023).

A-131
K. Yoshida, *et al*.
In Situ Observation of the Decomposition Process of Woodchips in Subcritical- and Supercritical Water by Neutron Imaging
J. Solut. Chem., 53 680–688 (2023).

A-132
M. Mentink, *et al*.
Superconducting detector magnets for high energy physics
Journal of Instrumentation, Vol 18, T06013 (2023)

A-133
Y. Liu, *et al*.
Neutron Reflectometry Analysis of Condensed Water Layer Formation at a Solid Interface of Epoxy Resins Under High Humidity
Langmuir, 39 10154–10162 (2023).

A-134
H. Iwase, *et al*.
Time-Resolved Structural Analysis of Fast-Photoresponsive Surfactant Micelles by Stroboscopic Small-Angle Neutron Scattering
Langmuir, 39 12357–12364 (2023).

A-135
S. Yada, *et al*.
Stability and Structural Analysis Using Small-Angle Neutron Scattering for Foam of Homogeneous Polyoxyethylene-Type Nonionic Surfactants with Multibranched Chains
Langmuir, 39 15355–15361 (2023).

A-136
K. J. Bichler, *et al*.
Side Chain Dynamics of Poly(norbornene)-*g*-Poly(propylene oxide) Bottlebrush Polymers
Macromol. Rapid Commun., 44 2200902 (2023).

A-137
Y. Song, *et al*.
Effects of Polarity of Polymers on Conformation and Lubricating Film

Formation of Adsorbed Films
Macromolecules, 56 1954–1964 (2023).

A-138
Y. Shiraki, *et al*.
Adhesion to Untreated Polyethylene and Polypropylene by Needle-like Polyolefin Crystals
Macromolecules, 56 2429–2436 (2023).

A-139
M. Hibino, *et al*.
Dynamic Exchange of Amphiphilic Random Copolymers between Micelles in Water: Kinetics and Mechanism Analyzed by TR-SANS
Macromolecules, 56 2955–2964 (2023).

A-140
M. Saito, *et al*.
Mechanical Properties and Swelling Behaviors of Ultrathin Chemically Cross-Linked Polybutadiene Films
Macromolecules, 56 4000–4011 (2023).

A-141
R. Sujita, *et al*.
Microphase Separation of Cationic Homopolymers Bearing Alkyl Ammonium Salts into Sub-4 Nm Lamellar Materials with Water Intercalation Channels
Macromolecules, 56 9738–9749 (2023).

A-142
Z. Zhang, *et al*.
A Colossal Barocaloric Effect Induced by the Creation of a High-Pressure Phase
Mater. Horiz., 10 977–982 (2023).

A-143
P. Thirathipviwat, *et al*.
A Correlation between Texture Evolution and Dislocation Density in Al-Mg Alloys during Uniaxial Tensile Deformation
Mater. Lett., 349 134829 (2023).

A-144
N. Tsuchida, *et al*.
Role of Retained Austenite in Improving the Mechanical Properties of 1.5 GPa-Grade High-Strength Martensitic Steels
Mater. Sci. Eng. A, 873 144989 (2023).

A-145
Y. Wang, *et al*.
Cryogenic Impact Fracture Behavior of a High-Mn Austenitic Steel Using Electron Backscatter Diffraction and Neutron Bragg-Edge Transmission Imaging
Mater. Sci. Eng. A, 887 145768 (2023).

A-146
N. Tsuchida, *et al*.
Effects of Pre-Strain and Tempering on Mechanical Properties in High-Strength Martensitic Steels
Mater. Sci. Forum, 1105 129–133 (2023).

A-147
Y. Fang, *et al*.
Pressure Engineering of van Der Waals Compound RhI_3: Bandgap Narrowing, Metallization, and Remarkable Enhancement of Photoelectric Activity
Mater. Today Phys., 34 101083 (2023).

A-148
M. Kawasaki, *et al*.
Synchrotron High-Energy X-Ray & Neutron Diffraction, and Laser-Scanning Confocal Microscopy: *In-Situ* Characterization Techniques for Bulk Nanocrystalline Metals
Mater. Trans., 64 1683–1694 (2023).

A-149
S. Harjo, *et al*.
Effect of Extrusion Ratio in Hot-Extrusion on Kink Deformation during Compressive Deformation in an αMg/LPSO Dual-Phase Magnesium Alloy Monitored by I*n Situ* Neutron Diffraction
Mater. Trans., 64 766–773 (2023).

A-150
T. Wakui, *et al*.
Cavitation Damage Prediction in Mercury Target for Pulsed Spallation Neutron Source Using Monte Carlo Simulation
Materials, 16 5830 (2023).

A-151
T. Tsuru, *et al*.
Identification of Hydrogen Trapping in Aluminum Alloys Via Muon Spin Relaxation Method and First-Principles Calculations
Metall. Mater. Trans. A, 54 2374–2383 (2023).

A-152
I. Chiu, *et al*.
Non-destructive Elemental Analysis of Lunar Meteorites Using a Negative Muon Beam
Meteorit. Planet. Sci., 58 1333–1344 (2023).

A-153
M. Hirai, *et al*.
Fibrillization Process of Human Amyloid-Beta Protein (1–40) under a Molecular Crowding Environment Mimicking the Interior of Living Cells Using Cell Debris
Molecules, 28 6555 (2023).

A-154
M. Teshigawara, *et al*.
New Material Exploration to Enhance Neutron Intensity below Cold Neutrons: Nanosized Graphene Flower Aggregation
Nanomaterials, 13 76 (2023).

A-155
Y. Yasui, *et al*.
Hidden Chemical Order in Disordered $Ba_7Nb_4MoO_{20}$ Revealed by Resonant X-Ray Diffraction and Solid-State NMR
Nat. Commun., 14 2337 (2023).

A-156
S. Bao, *et al*.
Direct Observation of Topological Magnon Polarons in a Multiferroic Material
Nat. Commun., 14 6093 (2023).

A-157
K. Saito, M. Yashima
High Proton Conductivity within the 'Norby Gap' by Stabilizing a Perovskite with Disordered Intrinsic Oxygen Vacancies
Nat. Commun., 14 7466 (2023).

A-158
P. Park, *et al*.
Tetrahedral Triple-Q Magnetic Ordering and Large Spontaneous Hall Conductivity in the Metallic Triangular Antiferromagnet $Co_{1/3}TaS_2$
Nat. Commun., 14 8346 (2023).

A-159
S. Procureur, *et al*.
Precise characterization of a corridor-shaped structure in Khufu's Pyramid by observation of cosmic-ray muons
Nat. Commun., 14, 1144 (2023)

A-160
I. Konuma, *et al*.
A near Dimensionally Invariable High-Capacity Positive Electrode Material
Nat. Mater., 22 225–234 (2023).

A-161
Q. Ren, *et al*.
Extreme Phonon Anharmonicity Underpins Superionic Diffusion and Ultralow Thermal Conductivity in Argyrodite Ag_8SnSe_6
Nat. Mater., 22 999–1006 (2023).

A-162
C. Kim, *et al*.
Bond-Dependent Anisotropy and Magnon Decay in Cobalt-Based Kitaev Triangular Antiferromagnet
Nat. Phys., 19 1624–1629 (2023).

A-163
S. Han, *et al*.
Strong Phonon Softening and Avoided Crossing in Aliovalence-Doped Heavy-Band Thermoelectrics
Nat. Phys., 19 1649–1657 (2023).

A-164
F. Wu, *et al*.
Fluctuation-Enhanced Phonon Magnetic Moments in a Polar Antiferromagnet
Nat. Phys., 19 1868–1875 (2023).

A-165
Y. Shangguan, *et al*.
A One-Third Magnetization Plateau Phase as Evidence for the Kitaev Interaction in a Honeycomb-Lattice Antiferromagnet
Nat. Phys., 19 1883–1889 (2023).

A-166
H. Takagi, *et al*.
Spontaneous Topological Hall Effect Induced by Non-Coplanar Antiferromagnetic Order in Intercalated van Der Waals Materials
Nat. Phys., 19 961–968 (2023).

A-167
P. Wu, *et al*.
Experimental Evidence for the Significance of Optical Phonons in Thermal Transport of Tin Monosulfide
New J. Phys., 25 013032 (2023).

A-168
K. Yadav, *et al*.
Existence of Complex Magnetic Ground State and Topological Hall Effect in Centrosymmetric Silicide DyScSi
New J. Phys., 25 123030 (2023).

A-169
K. Futatsukawa, *et al*.
Demonstration of beam loading compensation system for discrete beam with comb-like structure in proton linear accelerator
NIM-A 1047, 167778 (2023)

A-170
J. Tamura, *et al*.
Measurement of H^0 particles generated by residual gas stripping in the Japan Proton Accelerator
NIM-A 1049, 168033 (2023)

A-171
K. Sugihara, S. Meigo, *et al*.
Measurement of nuclide production cross sections for proton-induced reactions on ^{nat}Ti and ^{93}Nb at 0.8 and 3.0 GeV
NIM-B 545, 165153 (2023)

A-172
S. Miyahara, *et al*.
Development and Validation of Analysis Code for Spallation Products Behavior in LBE Coolant System of ADS Comparing with the Distribution Data in MEGAPIE Spallation Target
Nucl. Eng. Des., ***403****, 112147 (2023).*

A-173
J. Kim, *et al*.
Simulation of angular resolution of a new electromagnetic sampling calorimeter
Nucl. Instrum. Methods Phys. Res. A1052, 168261 (2023)

A-174
N. Tomida, *et al*.
Development of an 1-m long prototype TOF-RPC for the J-PARC π20 beam line
Nucl. Instrum. Methods Phys. Res. A1056, 168581 (2023)

A-175
H. Iwamoto, *et al*.
Neutron-Production Double-Differential Cross Sections of ^{nat}Pb and ^{209}Bi in Proton-Induced Reactions near 100 MeV
Nucl. Instrum. Methods Phys. Res. ***B544****, 165107 (2023).*

A-176
H. Akatsuka, *et al*.
Characterization of Electroless Nickel-Phosphorus Plating for Ultracold-Neutron Storage
Nucl. Instrum. Methods Phys. Res. Sect. Accel. Spectrometers Detect. Assoc. Equip., 1049 168106 (2023).

A-177
M. Sato, *et al*.
Non-Destructive Measurement of the Beryllium Thickness of the iBNCT Neutron-Generation Target Using Negative Muons
Nucl. Instrum. Methods Phys. Res. Sect. Accel. Spectrometers Detect. Assoc. Equip., 1052 168291 (2023).

A-178
M. Tsunoda, *et al*.
Radial Collimator Performance and Future Collimator Updates for the High-Intensity Total Scattering Diffractometer NOVA at J-PARC
Nucl. Instrum. Methods Phys. Res. Sect. Accel. Spectrometers Detect. Assoc. Equip., 1055 168484 (2023).

A-179
S. Nishimura, *et al*.
Development of Transient μSR Method for High-Flux Pulsed Muons
Nucl. Instrum. Methods Phys. Res. Sect. Accel. Spectrometers Detect. Assoc. Equip., 1056 168669 (2023).

A-180
S. Itoh, *et al*.
Demonstration of Simultaneous Measurement of the Spin Rotation of Dynamically-Diffracted Neutrons from Multiple Crystal Planes Using Pulsed Neutrons
Nucl. Instrum. Methods Phys. Res. Sect. Accel. Spectrometers Detect. Assoc. Equip., 1057 168734 (2023).

A-181
S. Saito, *et al*.
Mechanical Properties of Pure Tungsten and Tantalum Irradiated by Protons and Neutrons at the Swiss Spallation-Neutron Source
Nucl. Mater. Energy, ***34****, 101338 (2023).*

A-182
S. Endo, *et al*.
Measurements of the Neutron Total and Capture Cross Sections and Derivation of the Resonance Parameters of ^{181}Ta
Nucl. Sci. Eng., 198 786–803 (2023).

A-183
J. Tamura, *et al*.
Measurement of H^0 particles generated by residual gas stripping in the Japan Proton Accelerator Research Complex linac
Nuclear Inst. and Methods in Physics Research, A 1049 (2023) 168033

A-184
N. Sumi, *et al*.
The LiNA experiment: Development of multi-layered time projection chamber
Nuclear Instruments & Methods in Physics Research Section A, Vol 1045, 167586 (2023)

A-185
J. K. Ahn, *et al*.
Superconducting dipole magnet for Hyperon spectrometer
Nuclear Instruments & Methods in Physics Research Section A, Vol 1047, 167775 (2023)

A-186
T. Nakanishi, *et al*.
Observation of Proton-Transfer-Coupled Spin Transition by Single-Crystal Neutron-Diffraction Measurement
Phys. Chem. Chem. Phys., 25 12394–12400 (2023).

A-187
R. Kitamura, *et al*.
Measurement of the longitudinal bunch-shape distribution for a high-intensity negative hydrogen ion beam in the low-energy region
Phys. Rev. Accel. Beams, 26, 032802 (2023)

A-188
S. K. Dey, *et al*.
Local Spin Dynamics in the Geometrically Frustrated Mo Pyrochlore Antiferromagnet $Lu_2Mo_2O_{5-y}N_2$
Phys. Rev. B, 107 024407 (2023).

A-189
M. Fujihala, *et al*.
Spin Gap in the Weakly Interacting Quantum Spin Chain Antiferromagnet $KCuPO_4{\cdot}H_2O$
Phys. Rev. B, 107 054435 (2023).

A-190
Z. Liu, *et al*.
Spin Excitation in the Coupled Honeycomb Lattice Compound Ni_2InSbO_6
Phys. Rev. B, 107 064428 (2023).

A-191
M. Pardo-Sainz, *et al*.
New (αβγ)-Incommensurate Magnetic Phase Discovered in the $MnCr_2O_4$ Spinel at Low Temperatures
Phys. Rev. B, 107 144401 (2023).

A-192
H. Tamatsukuri, *et al*.
Quasielastic Neutron Scattering Probing H^- Dynamics in the H^- Conductors $LaH_{3-2x}O_x$
Phys. Rev. B, 107 184114 (2023).

A-193
H. Kikuchi, *et al*.
Inelastic Neutron Scattering in the Weakly Coupled Triangular Spin Tube Candidate $CsCrF_4$
Phys. Rev. B, 107 184405 (2023).

A-194
S. Yano, *et al*.
Weak Trimerization in the Frustrated Two-Dimensional Triangular Heisenberg Antiferromagnet $Lu_yY_{1-y}MnO_3$
Phys. Rev. B, 107 214407 (2023).

A-195
S. Aji, *et al*.
Direct Observations of Spin Fluctuations in Hedgehog–Anti-Hedgehog Spin Lattice States in $MnSi_{1-x}Ge_x$ (x = 0.6 and 0.8) at Zero Magnetic Field
Phys. Rev. B, 108 054445 (2023).

A-196
T. Kitazawa, *et al*.
Observation of Field-Induced Single-Ion Magnetic Anisotropy in a Multiorbital Kondo Alloy (Lu, Yb) Rh_2Zn_{20}
Phys. Rev. B, 108 085105 (2023).

A-197
H. Saito, *et al*.
In-Plane Anisotropy of Single-q and Multiple-q Ordered Phases in the Antiferromagnetic Metal CeRh2Si2
Phys. Rev. B, 108 094440 (2023).

A-198
T. U. Ito, *et al*.
Understanding Muon Diffusion in Perovskite Oxides below Room Temperature Based on Harmonic Transition State Theory
Phys. Rev. B, 108 224301 (2023).

A-199
T. Okudaira, *et al*.
Angular Distribution of γ Rays from a Neutron-Induced *p*-Wave Resonance of ^{132}Xe
Phys. Rev. C, 107 054602 (2023).

A-200
T. Harada, *et al*.
Production spectra with a Σ^- hyperon in (π^-, K^+) reactions on light to heavy nuclei
Phys. Rev. C, 107, 54611 (2023)

A-201
N. Muramatsu, *et al*.
First measurement of differential cross sections and photon beam asymmetries for photoproduction of the $f_0(980)$ meson decaying into $\pi^0\pi^0$ at $E_\gamma < 2.4$ GeV
Phys. Rev. C, 107, L042201 (2023)

A-202
S. Imajo, *et al*.
Diffuse Scattering Model of Ultracold Neutrons on Wavy Surfaces
Phys. Rev. C, 108 034605 (2023).

A-203
J. Dove, *et al*.
Measurement of flavor asymmetry of the light-quark sea in the proton with Drell-Yan dimuon production in $p+p$ and $p+d$ collisions at 120 GeV
Phys. Rev. C, 108, 35202 (2023)

A-204
A. Abed Abud, *et al*.
Impact of cross-section uncertainties on supernova neutrino spectral parameter fitting in the Deep Underground Neutrino Experiment
Phys. Rev. D, 107, 112012 (2023)

A-205
I.W. Park, *et al*.
Disentangling longitudinal and transverse modes of the ϕ meson through dilepton and kaon decays
Phys. Rev. D, 107, 74033 (2023)

A-206
M. Shinoki, *et al*.
Measurement of the cosmogenic neutron yield in Super-Kamiokande with gadolinium loaded water
Phys. Rev. D, 107, 92009 (2023)

A-207
A. Abed Abud, *et al*.
Identification and reconstruction of low-energy electrons in the ProtoDUNE-SP detector
Phys. Rev. D, 107, 92012 (2023)

A-208
K. Abe, *et al*.
First measurement of muon neutrino charged-current interactions on hydrocarbon without pions in the final state using multiple detectors with correlated energy spectra at T2K
Phys. Rev. D, 108, 112009 (2023)

A-209
K. Abe, *et al*.
Updated T2K measurements of muon neutrino and antineutrino disappearance using 3.6×10^{21} protons on target
Phys. Rev. D, 108, 72011 (2023)

A-210
K. Abe, *et al*.
Measurements of the νμ and νμ -induced coherent charged pion production cross sections on 12C by the T2K experiment
Phys. Rev. D, 108, 92009 (2023)

A-211
G.J. Wang, *et al*.
Quark confinement for multiquark systems: Application to fully charmed tetraquarks
Phys. Rev. D, 108, L071501 (2023)

A-212
W.A. Yamada, *et al*.
Survival probability of unstable states in coupled-channels: Nonexponential decay of threshold cusp
Phys. Rev. D, 108, L071502 (2023)

A-213
T. Okumura, *et al*.
Proof-of-Principle Experiment for Testing Strong-Field Quantum Electrodynamics with Exotic Atoms: High Precision X-Ray Spectroscopy of Muonic Neon
Phys. Rev. Lett., 130 173001 (2023).

A-214
C. Lin, *et al*.
Search for the Pair Production of Dark Particles X with $K_L^0 \to XX$, $X \to \gamma\gamma$
Phys. Rev. Lett., 130, 111801 (2023)

A-215
K. Abe, *et al*.
Search for Cosmic-Ray Boosted Sub-GeV Dark Matter Using Recoil Protons at Super-Kamiokande
Phys. Rev. Lett., 130, 31802 (2023)

A-216
W. G. F. Krüger, *et al*.
Triple-q Order in $Na_2Co_2TeO_6$ from Proximity to Hidden-SU(2)-Symmetric Point
Phys. Rev. Lett., 131 146702 (2023).

A-217
P. Strasser, *et al*.
Improved Measurements of Muonic Helium Ground-State Hyperfine Structure at a Near-Zero Magnetic Field
Phys. Rev. Lett., 131 253003 (2023).

A-218
Q. Li, *et al*.
Role of Thermal Expansion Anisotropy on the Elastocaloric Effect of Shape Memory Alloys with Slim-Hysteresis Superelasticity
Phys. Rev. Mater., 7 013606 (2023).

A-219
K. Iwasa, *et al*.
Weyl–Kondo Semimetal Behavior in the Chiral Structure Phase of $Ce_3Rh_4Sn_{13}$
Phys. Rev. Mater., 7 014201 (2023).

A-220
S. Tanaka, *et al*.
Incommensurate Helimagnetic Structure of $Ba(Fe_{1-x}Sc_x)_{12}O_{19}$ Determined by Single-Crystal Neutron Diffraction
Phys. Rev. Mater., 7 014403 (2023).

A-221
Y. Shobuda, *et al*.
Demonstration of a kicker impedance reduction scheme with diode stack and resistors by operating the 3-GeV rapid cycling synchrotron of the Japan Proton Accelerator Research Complex
Physical Review Accelerators and Beams (Internet), 26(5), p.053501_1 - 053501_45, 2023/05

A-222
A. Kobayashi, *et al*.
New determination of the branching ratio of the structure dependent radiative $K^+ \rightarrow e^+ \nu_e \gamma$
Physics Letters B, 843, 138020 (2023)

A-223
T. Akaishi, *et al*.
Precise lifetime measurement of ${}^{4}_{\Lambda}\mathrm{H}$ hypernucleus using in-flight ${}^{4}\mathrm{He}(K^-, \pi^0){}^{4}_{\Lambda}\mathrm{H}$ reaction
Physics Letters B, 845, 138128 (2023)

A-224
S. Aikawa, *et al*.
Pole position of Λ(1405) measured in $d(K^-, n)\pi\Sigma$ reactions
Physics Letters B, 847, 137637 (2023)

A-225
L. Meng, *et al*.
Chiral perturbation theory for heavy hadrons and chiral effective field theory for heavy hadronic molecules
Physics Report-Review Section of Physics Letters, 1019, 1 (2023)

A-226
D. Kawaguchi
Aggregation States, Thermal Molecular Motion and Carrier Properties in Functional Polymer Thin Films
Polym. J., 55 1237–1245 (2023).

A-227
T. Matsumoto, *et al*.
Selective Acetylation of Amorphous Region of Poly(Vinyl Alcohol) in Supercritical Carbon Dioxide
Polym. J., 55 1287–1293 (2023).

A-228
H. Yoshioka, *et al*.
Effect of Molecular Weight Distribution on the Thermal Adhesion of Polystyrene and PMMA Brushes
Polymer, 264 125561 (2023).

A-229
Z. Huang, *et al*.
Local Conformations and Heterogeneities in Structures and Dynamics of Isotactic Polypropylene Adsorbed onto Carbon Fiber
Polymer, 265 125584 (2023).

A-230
P. Goux, *et al*.
Angular Correlation of the Two Gamma Rays Produced in the Thermal Neutron Capture on Gadolinium-155 and Gadolinium-157
Prog. Theor. Exp. Phys., 2023 063H01 (2023).

A-231
M. Yamamoto, *et al*.
Development of a single-ended magnetic alloy loaded cavity in the Japan Proton Accelerator Research Complex rapid cycling synchrotron
Prog. Theor. Exp. Phys., 2023, 073G01(2023)

A-232
V.D. Burkert, *et al*.
Precision studies of QCD in the low energy domain of the EIC
Progress in Particle and Nuclear Physics, 131, 104032 (2023)

A-233
M. Watanabe, *et al*.
Automated Pulsed Magnet System for Neutron Diffraction Experiments at the Materials and Life Science Experimental Facility in J-PARC
Quantum Beam Sci., 7 1 (2023).

A-234
S. Harjo, *et al*.
Stress Evaluation Method by Neutron Diffraction for HCP-Structured Magnesium Alloy
Quantum Beam Sci., 7 32 (2023).

A-235
S. Machiya, *et al*.
Measurement of Mechanical Behavior of ${}^{11}\mathrm{B}$-Enriched MgB_2 Wire Using a Pulsed Neutron Source
Quantum Beam Sci., 7 34 (2023).

A-236
S. Koizumi, *et al*.
Microscopic Depictions of Vanishing Shampoo Foam Examined by Time-of-Flight Small-Angle Neutron Scattering
Quantum Beam Sci., 7 4 (2023).

A-237
J. Abe, *et al*.
A High-Temperature and High-Pressure Cell for *In Situ* Visualization of Reaction Processes by Neutron Imaging
Rev. Sci. Instrum., 94 083904 (2023).

A-238
Y. Goto, *et al*.
Facile Formation of Barium Titanium Oxyhydride on a Titanium Hydride Surface as an Ammonia Synthesis Catalyst
RSC Adv., 13 15410–15415 (2023).

A-239
E. Nakamura, *et al*.
Effect of Water Content on Stratum Corneum Penetration Mechanism of W/O Type Microemulsions
RSC Adv., 13 17742–17749 (2023).

A-240
Z. Jin, *et al*.
Magnetic Molecular Orbitals in MnSi
Sci. Adv., 9 eadd5239 (2023).

A-241
Y. Oba, *et al*.
Neutron Resonance Absorption Imaging of Simulated High-Level Radioactive Waste in Borosilicate Glass
Sci. Rep., 13 10071 (2023).

A-242
T. Kozawa, *et al*.
Atomic Reconstruction Induced by Uniaxial Stress in MnP
Sci. Rep., 13 13750 (2023).

A-243
N. Yamashita, *et al*.
Neutron Reflectometry under High Shear in Narrow Gap for Tribology Study
Sci. Rep., 13 18268 (2023).

A-244
H. Nozaki, *et al*.
In Situ Neutron Imaging of Lithium-Ion Batteries during Heating to Thermal Runaway
Sci. Rep., 13 22082 (2023).

A-245
H. Mamiya, *et al*.
Neutron Imaging for Magnetization inside an Operating Inductor
Sci. Rep., 13 9184 (2023).

A-246
Y. Li, *et al*.
A Lithium Superionic Conductor for Millimeter-Thick Battery Electrode
Science, 381 50–53 (2023).

A-247
X. Wen, *et al*.
Strong Work-Hardenable Body-Centered-Cubic High-Entropy Alloys at Cryogenic Temperature
Scr. Mater., 231 115434 (2023).

A-248
W. Mao, *et al*.
Quantitatively Evaluating the Huge Lüders Band Deformation in an Ultrafine Grain Stainless Steel by Combining *In Situ* Neutron Diffraction and Digital Image Correlation Analysis
Scr. Mater., 235 115642 (2023).

A-249
H. Dannoshita, *et al*.
Effects of Dislocation Arrangement and

Character on the Work Hardening of Lath Martensitic Steels
Scr. Mater., 236 115648 (2023).

A-250
K. Wu, *et al*.
Localizing Oxygen Lattice Evolutions Eliminates Oxygen Release and Voltage Decay in All-Mn-Based Li-Rich Cathodes
Small, 19 2300419 (2023).

A-251
K. Aomura, *et al*.
Quasi-Elastic Neutron Scattering Study on Dynamics of Polymer Gels with Controlled Inhomogeneity under Uniaxial Deformation
Soft Matter, 19 147–152 (2023).

A-252
K. Shimokita, *et al*.
Neutron Reflectivity Study on the Nanostructure of PMMA Chains near Substrate Interfaces Based on Contrast Variation Accompanied with Small Molecule Sorption
Soft Matter, 19 2082–2089 (2023).

A-253
T. Kimura, *et al*.
Synthesis and Ionic Conductivity of an Argyrodite-Type Li_6SbS_5I Electrolyte
Solid State Ion., 399 116287 (2023).

A-254
C. Micheau, *et al*.
Deuterated Malonamide Synthesis for Fundamental Research on Solvent Extraction Systems
Solvent Extr. Ion Exch., 41 221–240 (2023).

A-255
Md. K. Rahman, *et al*.
Quasi-Elastic Neutron Scattering Reveals the Relationship between the Dynamical Behavior of Phospholipid Headgroups and Hydration Water
Struct. Dyn., 10 044701 (2023).

A-256
M. Abe, *et al*.
Test Shimming Operations to Obtain Excellent Homogeneous Magnetic Field Using an MRI Whole-body Magnet and TSVD Shimming Calculation
TeionKogaku (低温工学), Vol 58, 132 (2023)

A-257
H. Gu, *et al*.
Tribological Performance of a Surfactant Derived from Its Structure of Molecular Aggregates in Water
Tribol. Int., 188 108881 (2023)

Conference Reports and Books

B-001
T. Sato, H. Takabayashi
Effect of Si/Al Addition on Magnetic Properties of Fe-Co Alloy
AIP Adv., 13 035306 (2023).

B-002
S. Endo, *et al*.
Covariance of Resonance Parameters Ascribed to Systematic Uncertainties in Experiments
EPJ Web Conf., 281 00012 (2023).

B-003
T. Katabuchi, *et al*.
Fast-Neutron Capture Cross Section Data Measurement of Minor Actinides for Development of Nuclear Transmutation Systems
EPJ Web Conf., 281 00014 (2023).

B-004
S. Kunieda, *et al*.
Updates to the AMUR Code for R-Matrix Analyses on Heavy Nuclei
EPJ Web Conf., 281 00017 (2023).

B-005
A. Kimura, *et al*.
Uncertainty Estimation in Neutron TOF Measurements with ANNRI
EPJ Web Conf., 281 00025 (2023).

B-006
T. Yamazaki, *et al*.
New Beamlines and Future Prospects of the J-PARC Muon Facility
EPJ Web Conf., 282 01016 (2023).

B-007
Y. Kodama, *et al*.
Measurements of the Neutron Capture Cross Section of Am-243 with the ANNRI Beamline, MLF/J-PARC
EPJ Web Conf., 284 01024 (2023).

B-008
H. Nakano, *et al*.
Neutron Capture Cross Section Measurement and Resonance Analysis of ^{107}Pd Using ANNRI at MLF/J-PARC
EPJ Web Conf., 284 01032 (2023).

B-009
G. Rovira, *et al*.
Neutron Filtering System for Neutron Capture Cross Section Measurement at the ANNRI Beamline of MLF/J-PARC
EPJ Web Conf., 284 06007 (2023).

B-010
H. Iwamoto, *et al*.
Nuclide Production Cross sections in Proton-Induced Reactions on Bi at GeV Energies
EPJ Web Conf., 284, 01022 (2023).

B-011
H. Iwamoto, *et al*.
Measurement of Double-Differential Neutron Yields for Iron, Lead, and Bismuth Induced by 107-MeV Protons for Research and Development of Accelerator Driven Systems
EPJ Web Conf., 284, 01023 (2023).

B-012
S. Meigo, *et al*.
Measurement of Displacement Cross-sections of Nb Irradiated by Protons with Kinetic Energy Range between 0.4 and 3 GeV
EPJ Web Conf., 284, 05001 (2023).

B-013
K. Akutsu-Suyama, *et al*.
Effective Synthesis of Deuterated N-Octylamine and Its Analogues
EPJ Web Conf., 286 01004 (2023).

B-014
T. Yamazaki, *et al*.
New beamlines and future prospects of the J-PARC muon facilit
EPJ Web of Conferences, Vol 282, 1016 (2023)

B-015
P.K. Saha, *et al*.
Recent results of beam loss mitigation and extremely low beam loss operation of J-PARC RCS
J. Phys. Conf. Ser., 2420, 012040 (2023)

B-016
H. Okita, *et al*.
Design studies on a high-power wide-band RF combiner for consolidation of the driver amplifier of the J-PARC RCS
J. Phys. Conf. Ser., 2420, 012092 (2023)

B-017
K. Horie, *et al*.
Measurement of Muon Spin Relaxation Time in Various Scintillating Materials
J. Phys. Conf. Ser., 2446 012040 (2023).

B-018
K. Shiomi
Search for the $K_L \to \pi^0\nu\bar{\nu}$ decay at the J-PARC KOTO experiment
J. Phys. Conf. Ser., 2446, 12003 (2023)

B-019
K. Sakashita
Neutrino Physics
J. Phys. Conf. Ser., 2446, 12026 (2023)

B-020
M. Tampo, *et al*.
Developments of Muonic X-Ray Measurement System for Historical-Cultural Heritage Samples in Japan Proton Accelerator Research Complex (J-PARC)
J. Phys. Conf. Ser., 2462 012002 (2023).

B-021
I.-H. Chiu, *et al*.
Non-Destructive Elemental Analysis of Lunar Materials with Negative Muon Beam at J-PARC
J. Phys. Conf. Ser., 2462 012004 (2023).

B-022
Y. Miyake, *et al*.
Integration of Arts and Sciences Using Negative Muon Non-Destructive Analysis at J-PARC MUSE
J. Phys. Conf. Ser., 2462 012005 (2023).

B-023
A. D. Pant, *et al*.
Search of Ultracold Muonium Generation Material: Muon Spin Rotation and Relaxation Study in SiC
J. Phys. Conf. Ser., 2462 012016 (2023).

B-024
I. Umegaki, *et al*.
Non-Destructive Operando Measurements of Muonic x-Rays on Li-Ion Battery
J. Phys. Conf. Ser., 2462 012018 (2023).

B-025
R. Iwai, *et al*.
Precise Measurement of the Hyperfine Splitting in Muonium with a High Intensity Pulsed Muon Beam at J-PARC
J. Phys. Conf. Ser., 2462 012019 (2023).

B-026
P. Strasser, *et al*.
Status of the New Muonic Helium Atom HFS Measurements at J-PARC MUSE
J. Phys. Conf. Ser., 2462 012023 (2023).

B-027
Y. Oishi, *et al*.
Intense Lyman-Alpha Light Source for Ultra-Slow Muon Generation
J. Phys. Conf. Ser., 2462 012026 (2023).

B-028
S. Kanda
In-Flight Muon Spin Resonance and Muonium Interferometry
J. Phys. Conf. Ser., 2462 012029 (2023).

B-029
S. Kanda, *et al*.
The Ultra-Slow Muon Beamline at J-PARC: Present Status and Future Prospects
J. Phys. Conf. Ser., 2462 012030 (2023).

B-030
S. Matoba, *et al*.
Development of Monitoring System for the Muon Rotating Target at J-PARC Using an Infrared Camera
J. Phys. Conf. Ser., 2462 012031 (2023).

B-031
K. Shimomura, *et al*.
Present Status of J-PARC MUSE
J. Phys. Conf. Ser., 2462 012033 (2023).

B-032
N. Teshima, *et al*.
A Simulation Study of Muon Transport in the Ultra-Slow Muon Beamline at J-PARC
J. Phys. Conf. Ser., 2462 012036 (2023).

B-033
J. Sugiyama, *et al*.
Negative Muon Spin Rotation and Relaxation on Li Metal
J. Phys. Conf. Ser., 2462 012045 (2023).

B-034
K. Ohishi, *et al*.
Sodium Diffusion in Hard Carbon Studied by Small- and Wide-Angle Neutron Scattering and Muon Spin Relaxation
J. Phys. Conf. Ser., 2462 012048 (2023).

B-035
D. P. Sari, *et al*.
Superconductivity Nearby Quantum Critical Region in Hole-Doped Organic Strange Metal κ-$(ET)_4Hg_{3-\delta}Br_8$, δ=11%
J. Phys. Conf. Ser., 2462 012061 (2023).

B-036
V.V.de Toro Sanchez, *et al*.
Development and test of a next-generation positron detector
J. Phys. Conf. Ser., 2462, 12014 (2023)

B-037
S. Takahashi, *et al*.
The First Polarized Neutron Diffraction Experiment at the Time-of-Flight Single Crystal Neutron Diffractometer SENJU at J-PARC
J. Phys. Conf. Ser., 2481 012005 (2023).

B-038
T. Dang Vu, *et al*.
Superconducting Neutron Transmission Imaging for Investigating a Sequential Change in Phase Separations of Low-Melting Wood's Metal
J. Phys. Conf. Ser., 2545 012019 (2023).

B-039
K. Oikawa, *et al*.
Update of Bragg Edge Analysis Software "GUI-RITS"
J. Phys. Conf. Ser., 2605 012013 (2023).

B-040
Y. Tsuchikawa, *et al*.
Development of an Areal Density Imaging for Boron and Other Elements
J. Phys. Conf. Ser., 2605 012022 (2023).

B-041
H. Okita, *et al*.
Improvement of the longitudinal phase space tomography at J-PARC synchrotrons
J. Phys. Conf. Ser., 2687, 072005 (2023)

B-042
I. Yamada, *et al*.
Observation of beam emittance reduction due to gas sheet injection for beam profile measurement
J. Phys. Conf. Ser., 2687, 072018 (2023)

B-043
A. Ueno, *et al*.
120 mA operation of J-PARC cesiated RF-driven H^- ion source
Journal of Instrumentation (Internet), 18(8), p.C08002_1 - C08002_8, 2023/08

B-044
A. Shimoda, *et al*.
Magnetic Ordering and Structural Phase Transitions of $Nd_3T_4Sn_{13}$ (*T* = Rh and Ir)
JPS Conf. Proc., 38 011091 (2023).

B-045
H. Okabe, *et al*.
Local Magnetism in the Spin-singlet State of VO_2
JPS Conf. Proc., 38 011117 (2023).

B-046
R. B. Figueiredo
In-Situ Heating Observations on Microstructure Relaxation of Ultrafine-grained High-Entropy Alloys Using Neutron Diffraction and Laser-scanning Confocal Microscopy
Materials Research Proceedings, 32 235–243 (2023).

B-047
N. Sumi, *et al*.
The LiNA Experiment: Development of Multi-Layered Time Projection Chamber
Nucl. Instrum. Methods Phys. Res. Sect. Accel. Spectrometers Detect. Assoc. Equip., 1045 167586 (2023).

B-048
Y. Nakazawa, *et al*.
Interdigital *H*-Mode Drift Tube Linear Accelerator for a Muon Linear Accelerator
Phys. Sci. Forum, 8 20

B-049
K. Sumi

Prototyping of a disk-loaded structure for muon acceleration
Proc. 14th Int. Particle Acc. Conf.(Internet), 933-936(2023)

B-050
Y. Ibaraki
Development of the diagnostic beamline for muon acceleration test with APF IH-DTL
Proc. 14th Int. Particle Acc. Conf.(Internet), 937-940(2023)

B-051
F. Tamura, *et al*.
Effects of the longitudinal impedances on non-adiabatic bunch manipulation at flattop of J-PARC MR
Proc. 19th Ann. Mtg. PASJ, 175-178(2023)

B-052
H. Okita, *et al*.
Evaluation of higher harmonics generated in acceleration gaps during the high power beam acceleration at J-PARC RCS
Proc. 19th Ann. Mtg. PASJ, 262-266(2023)

B-053
T. Nakanoya, *et al*.
Recent usage status of charge-exchange stripper foil for 3GeV synchrotron of J-PARC
Proc. 19th Ann. Mtg. PASJ, 629-633(2023)

B-054
T. Ito, *et al*.
Operating Status of the J-PARC DTL/SDTL
Proc. 20th Ann. Mtg. PASJ (internet), 1002-1006 (2023)

B-055
R. Kitamura, *et al*.
Studies of transient response for RF chopper in the J-PARC linac
Proc. 20th Ann. Mtg. PASJ (internet), 280-281 (2023)

B-056
K. Shinto, *et al*.
Design of a matching circuit for a high-intensity negative hydrogen ion source driving with 324 MHz RF power source
Proc. 20th Ann. Mtg. PASJ (internet), 392-395 (2023)

B-057
K.Hirano, *et al*.
STUDY OF BEAM TARGET MATERIALS FOR A 3-MeV LINAC AT J-PARC
Proc. 20th Ann. Mtg. PASJ (internet), 415-419 (2023)

B-058
S.Arai, *et al*.
INVESTIGATION OF AN RF WINDOW FOR THE J-PARC DTL
Proc. 20th Ann. Mtg. PASJ (internet), 455-458 (2023)

B-059
K. Shinto, *et al*.
Operation status of the J-PARC high-intensity RF-driven negative hydrogen ion source
Proc. 20th Ann. Mtg. PASJ (internet), 928-931 (2023)

B-060
Y. Kuriyama, *et al*.
Development of EPICS-based data acquisition system for beam loss monitor and sX-map
Proc. 20th Ann. Mtg. PASJ(Internet), 303-306(2023)

B-061
Y. Fuwa *et al*.
Design Study of MEBT1 magnets for J-PARC LINAC power upgrade
Proc. 20th Ann. Mtg. PASJ(Internet), 531-534(2023)

B-062
H. Nakano, *et al*.
Performance test of J-PARC Linac 972MHz semiconductor amplifier
Proc. 20th Ann. Mtg. PASJ(Internet), 577-578(2023)

B-063
F. Tamura, *et al*.
Consideration of high intensity single bunch acceleration in J-PARC RCS
Proc. 20th Ann. Mtg. PASJ, 64-68(2023)

B-064
M. Yoshimoto, *et al*.
Development of new data acquisition system for several beam monitors in J-PARC RCS
Proc. 20th Ann. Mtg. PASJ, 839-843(2023)

B-065
T. Nakanoya, *et al*.
Challenge to charge exhange with pure carbon foil in the J-PARC 3GeV synchrotron
Proc. 20th Ann. Mtg. PASJ, 937-941(2023)

B-066
A. Toyoda, *et al*.
NETWORK MONITORING SYSTEM FOR J-PARC HADRON BEAMLINE CONTROL
Proc. Ann. Mtg Part. Accel. Soc. Jpn, 2023, 822 (2023)

B-067
S. Ogawa, *et al*.
STORAGE BEAM MONITOR FOR PRESICE THREE-DIMENSIONAL BEAM INJECTION AT J-PARC MUON *g*-2/EDM EXPERIMENT
Proc. Ann. Mtg Part. Accel. Soc. Jpn, Vol 2023, 136 (2023)

B-068
S. Makimura, *et al*.
PAST ACTIVITIES AND PROSPECTS OF RaDIATE COLLABORATION AT J-PARC
Proc. Ann. Mtg Part. Accel. Soc. Jpn, Vol 2023, 160 (2023)

B-069
M. Abe, *et al*.
DESIGN OF WEAK FOCUS FIELD COIL TO STABILIZE MUON ORBITS AND FOR PRECISION MEASUREMENTS OF *g*-2/EDM IN THE SUPERCONDUCTING MUON STORAGE MAGNET
Proc. Ann. Mtg Part. Accel. Soc. Jpn, Vol 2023, 245 (2023)

B-070
H. Iwamoto, *et al*.
Measurements of Nuclear Data on Proton-Induced Reactions Using FFAG Accelerator
Proc. Ann. Mtg PASJ, 150 (2023).

B-071
S. Meigo, *et al*.
Advanced Secondary GeV Protons Utilization Using Scattering at Beam Window
Proc. Ann. Mtg PASJ, 230 (2023).

B-072
M. Sugita, *et al*.
Waveform pattern control of paint bump power supply for J-PARC RCS using machine learning
Proc. Ann. Mtg PASJ, 519-522 (2023)

B-073
B. Yee-Rendon, *et al*.
Design of the Low Energy Beam Transport Line for the JAEA-ADS Linac
Proc. Ann. Mtg PASJ, 545 (2023).

B-074
S. Meigo, *et al*.
SiC Sensor Wire Test by Heavy Ion Beam Irradiation
Proc. Ann. Mtg PASJ, 825 (2023).

B-075
T. Yasui
SPACE CHARGE INDUCED RESONANCES AND SUPPRESSION IN J-PARC MR
Proc. HB2023, 222 (2023)

B-076
F. Tamura, *et al*.
RF SYSTEMS OF J-PARC PROTON SYNCHROTRONS FOR HIGH-INTENSITY LONGITUDINAL BEAM OPTIMIZATION AND HANDLING
Proc. HB2023, 305 (2023)

B-077
C. Ohmori, M.Paoluzzi
MAGNETIC ALLOY LOADED CAVITIES IN J-PARC AND CERN
Proc. HB2023, 316 (2023)

B-078
A. Kobayashi
MAJOR LONGITUDINAL IMPEDANCE

SOURCES IN THE J-PARC MAIN RING
Proc. HB2023, 53 (2023)

B-079
R. Muto, *et al*.
DEVICES FOR HIGH-EFFICIENCY SLOW EXTRACTION AT J-PARC MAIN RING
Proc. HB2023, 656 (2023)

B-080
K. Satou, T. Toyama, S. Yamada
THE CONCEPTUAL DESIGN STUDY FOR NEW BPM SIGNAL PROCESSING SYSTEM OF J-PARC MAIN RING (MR)
Proc. IBIC2023, 78 (2023)

B-081
S. Yamada
15 YEARS OF THE J-PARC MAIN RING CONTROL SYSTEM OPERATION AND ITS FUTURE PLAN
Proc. ICALEPCS2023, 639 (2023)

B-082
R. Matsushita, at al.
DEMONSTRATION OF THREE-DIMENSIONAL SPIRAL INJECTION FOR THE J-PARC MUON *g*-2/EDM EXPERIMENT
Proc. IPAC, 2023, 327 (2023)

B-083
T. Yasui
J-PARC MR OPERATION WITH THE HIGH REPETITION RATE UPGRADE
Proc. IPAC2023, 1294 (2023)

B-084
R. Kitamura, *et al*.
Ionization ot fthe munoium using the electron
Proc. IPAC2023, 1433 (2023)

B-085
J. Tamura, *et al*.
Fabrication Progress of the Prototype Spoke Cavity for the JAEA-ADS Linac
Proc. IPAC2023, 1588 (2023).

B-086
B. Yee-Rendon, *et al*.
Design and Optimization of a Proton Source Extraction System for the JAEA-ADS Linac
Proc. IPAC2023, 1591 (2023).

B-087
H. Hotchi, *et al*.
NUMERICAL SIMULATION STUDY TOWARDS 1.3-MW BEAM OPERATION AT J-PARC MR
Proc. IPAC2023, 2316 (2023)

B-088
Y. Sugiyama, *et al*.
ESTIMATION OF THE ANODE POWER SUPPLY CURRENT OF THE J-PARC MR RF SYSTEM FOR 1.36 s CYCLE OPERATION
Proc. IPAC2023, 2320 (2023)

B-089
M. Yamamoto, *et al*.
VACUUM TUBE OPERATION ANALYSIS UNDER A POSITIVE GRID BIASING IN J-PARC RCS
Proc. IPAC2023, 2327 (2023)

B-090
P.K. Saha, *et al*.
HIGH INTENSITY BEAM OPERATION OF J-PARC RCS WITH MINIMUM BEAM LOSS
Proc. IPAC2023, 2331 (2023)

B-091
P.K. Saha, *et al*.
STATUS OF THE LASER MANIPULATIONS OF H^- BEAM AT J-PARC
Proc. IPAC2023, 2335 (2023)

B-092
T. Shibata, *et al*.
THE LEAKAGE FIELD OF THE NEW HIGH-FIELD SEPTUM MAGNETS FOR FAST EXTRACTION IN MAIN RING OF J-PARC
Proc. IPAC2023, 2459 (2023)

B-093
S. Iwata, *et al*.
DEVELOPMENT OF A PULSE CURRENT MONITORING DEVICE FOR THE EDDY SEPTUM MAGNETS IN J-PARC MAIN RING
Proc. IPAC2023, 2463 (2023)

B-094
M. Tomizawa, *et al*.
IMPACT OF SLOW-EXTRACTED BEAM BY MAIN POWER SUPPLY TRIP IN J-PARC MAIN RING
Proc. IPAC2023, 2467 (2023)

B-095
R. Muto, *et al*.
SIMULATION STUDY ON THE SLOW EXTRACTION FOR THE IMPROVEMENT OF THE BEAM SPILL STRUCTURE AT J-PARC MAIN RING
Proc. IPAC2023, 2470 (2023)

B-096
J. Takano, *et al*.
A NEW POWER SUPPLY FOR THE PULSED BENDING MAGNET IN J-PARC 3-50BT
Proc. IPAC2023, 2477 (2023)

B-097
C. Ohmori, *et al*.
IRRADIATION TESTS OF A CAVITY CORE MATERIAL AND GaN DEVICES IN J-PARC MAIN RING
Proc. IPAC2023, 2955 (2023)

B-098
T. Asamim, *et al*.
HIGH ACCURACY OPTICS MEASUREMENT IN J-PARC MR FOR 1.3 MW UPGRADE PLAN
Proc. IPAC2023, 3276 (2023)

B-099
Y. Morita, *et al*.
UPGRADING MAGNET POWER SUPPLY SYSTEM IN J-PARC MAIN RING
Proc. IPAC2023, 3762 (2023)

B-100
A. Plaçais, *et al*.
Development of a Tool for Cavity Failure Compensation in Superconducting Linacs: Progress and Comparative Study
Proc. IPAC2023, 4097 (2023).

B-101
K. Futatsukawa, *et al*.
DESIGN STUDY OF 972-MHZ RF AND CLOCK GENERATOR BOARD AT J-PARC LINAC
Proc. IPAC2023, 4198 (2023)

B-102
T. Toyama, K. Satou, S. Hatakeyama
RECOVERY AND CHECK OF THE SWITCHING RELAY IN THE BPMS IN THE J-PARC MR
Proc. IPAC2023, 4706 (2023)

B-103
H. Okita, *et al*.
IMPROVEMENT OF THE LONGITUDINAL PHASE SPACE TOMOGRAPHY AT THE J-PARC SYNCHROTRONS
Proc. IPAC2023, 4710 (2023)

B-104
T. Ito, *et al*.
OPERATING STATUS OF THE J-PARC DTL/SDTL
Proc. Journal of Physics: Conference Series 2023, 12040 (2023)

B-105
S. Ogawa, M. OTANI, *et al*.
STORAGE BEAM MONITOR FOR PRESICE THREE-DIMENSIONAL BEAM INJECTION AT J-PARC MUON *g*-2/EDM EXPERIMENT
Proc. Journal of Physics: Conference Series 2023, 136 (2023)

B-106
S. Makimura, S. Meigo, Y. Sato, *et al*.
PAST ACTIVITIES AND PROSPECTS OF RaDIATE COLLABORATION AT J-PARC
Proc. Journal of Physics: Conference Series 2023, 160 (2023)

B-107
S. Yamada
15 YEARS OF THE J-PARC MAIN RING CONTROL SYSTEM OPERATION AND ITS FUTURE PROSPECTS
Proc. Journal of Physics: Conference Series 2023, 172 (2023)

B-108
K. Futatsukawa, *et al*.
ADVANCEMENTS IN LLRF SYSTEM AT J-PARC LINAC
Proc. Journal of Physics: Conference Series 2023, 195 (2023)

B-109
N. Yoshimura, T. Toyama, *et al*.
STUDY ON SIMULATION CODE FOR TRANSVERSE INSTABILITIES FOR THE J-PARC MR
Proc. Journal of Physics: Conference Series 2023, 260 (2023)

B-110
T. Sasaki, *et al*.
DEVELOPMENT OF A WIDE DYNAMIC-RANGE BEAM PROFILE MONITOR USING OTR AND FLUORESCENCE FOR INJECTED BEAMS IN J-PARC MAIN RING (4)
Proc. Journal of Physics: Conference Series 2023, 282 (2023)

B-111
T. Shibata, *et al*.
THE LEAKAGE FIELD OF THE NEW SEPTUM MAGNETS FOR FAST EXTRACTION OF J-PARC MR
Proc. Journal of Physics: Conference Series 2023, 324 (2023)

B-112
T. Asamim, *et al*.
EVALUATION OF QUADRUPOLE ERROR FIELDS AROUND THE RING BY OPTICS MEASUREMENT FOR J-PARC MR 1.3 MW UPGRADE PLAN
Proc. Journal of Physics: Conference Series 2023, 339 (2023)

B-113
K. Moriya, *et al*.
BEAM MONITORS IN THE J-PARC LINAC AND ITS CURRENT ACTIVITIES
Proc. Journal of Physics: Conference Series 2023, 475 (2023)

B-114
M. Yoshii, *et al*.
FAST SEQUENTIAL INTERLOCK BETWEEN THE MAIN MAGNET POWER SUPPLIES TO PREVENT A SHORT PULSE BEAM DURING SLOW BEAM EXTRACTION AT J-PARC MR
Proc. Journal of Physics: Conference Series 2023, 535 (2023)

B-115
S. Iwata, *et al*.
SOLUTIONS FOR MANUFACTURING DEFECTS OF THE NEW SEPTUM MAGNETS USING FOR FAST EXTRACTION IN J-PARC MAIN RING
Proc. Journal of Physics: Conference Series 2023, 539 (2023)

B-116
H. Nakano, *et al*.
PERFORMANCE TEST OF J-PARC LINAC 972 MHz SEMICONDUCTOR AMPLIFIER
Proc. Journal of Physics: Conference Series 2023, 577 (2023)

B-117
P.K. Saha, *et al*.
STATUS OF THE LASER STRIPPING OF H^- BEAM AT J-PARC RCS
Proc. Journal of Physics: Conference Series 2023, 59 (2023)

B-118
F. Tamura, *et al*.
CONSIDERATION OF HIGH INTENSITY SINGLE BUNCH ACCELERATION IN J-PARC RCS
Proc. Journal of Physics: Conference Series 2023, 64 (2023)

B-119
A. Kobayashi, *et al*.
MODELING OF THE IMPEDANCE OF RF CAVITIES IN THE J-PARC MAIN RING
Proc. Journal of Physics: Conference Series 2023, 669 (2023)

B-120
H. Iinuma, M. Otani, *et al*.
SPECIFICATION AND DESIGN STUDY OF BEAM PHASE SPACE WITH STRONG X-Y COUPLED BEAM IN THE STORAGE MAGNET FOR J-PARC MUON *g*-2/EDM EXPERIMENT
Proc. Journal of Physics: Conference Series 2023, 674 (2023)

B-121
T. Toyama, *et al*.
RECOVERY AND CHECK OF THE RELAY SWITCH INTEGRITY IN THE BPM SIGNAL PROCESSING CIRCUITS IN THE J-PARC MR
Proc. Journal of Physics: Conference Series 2023, 683 (2023)

B-122
K. Miura, *et al*.
EFFECT OF MAGNETIC HYSTERESIS ON THE MAIN MAGNET WHEN OPERATED AT 8 GeV IN J-PARC MR
Proc. Journal of Physics: Conference Series 2023, 712 (2023)

B-123
S. Iwata, *et al*.
OPTIMIZATION OF EXTRACTED BEAM ORBIT DURING ACCELERATION AT J-PARC MAIN RING
Proc. Journal of Physics: Conference Series 2023, 724 (2023)

B-124
K. Numai, *et al*.
MEASUREMENT OF ELECTROSTATIC SEPTUM RIBBONS ALIGNMENT AT J-PARC MR
Proc. Journal of Physics: Conference Series 2023, 783 (2023)

B-125
K. Watanabe, K. Niki, *et al*.
UPGRADE OF ACQUISITION AND MONITORING SYSTEM FOR J-PARC ACCELERATOR PPS
Proc. Journal of Physics: Conference Series 2023, 844 (2023)

B-126
M. Uota
EVALUATION OF BAKE-OUT OPERATION WHEN NEW EQUIPMENT IS ADDED TO J-PARC MR
Proc. Journal of Physics: Conference Series 2023, 907 (2023)

B-127
S. Mizobata, *et al*.
OVERVIEW OF THE J-PARC KLYSTRON DISCHARGE MONITORING SYSTEM
Proc. Journal of Physics: Conference Series 2023, 912 (2023)

B-128
K. Shinto, *et al*.
OPERATION STATUS OF THE J-PARC HIGH-INTENSITY RF-DRIVEN NEGATIVE HYDROGEN ION SOURCE
Proc. Journal of Physics: Conference Series 2023, 928 (2023)

B-129
Y. Sato
The beam operation of J-PARC main ring after the first step of the high repetition upgrade
Proc. Journal of Physics: Conference Series 2023, WEOB4 (2023)

B-130
T. Shibata, *et al*.
The new eddy current type septum magnet for upgrading of fast extraction in main ring of J-PARC
Proc. Journal of Physics: Conference Series 2420, 12078 (2023)

B-131
T. Shibata, *et al*.
The reduction of the leakage field of the injection septum magnet in main ring of J-PARC
Proc. Journal of Physics: Conference Series 2420, 12081 (2023)

B-132
T. Shibata, *et al*.
The new high field septum magnet for upgrading of fast extraction in main ring of J-PARC
Proc. Journal of Physics: Conference Series 2420, 12082 (2023)

B-133
S. Kamioka
Muon cooling at J-PARC
Proc. Sci., Muon4Future2023, 8 (2023)

B-134
Y. Kondo, *et al*.
Development of Single-Spoke Cavities for ADS at JAEA
Proc. SRF2023, 947 (2023).

B-135
P. K. Saha, *et al*.
Achievement of low beam loss at high-intensity operation of J-PARC 3 GeV RCS
Proceedings of 19th Annual Meeting of Particle Accelerator Society of Japan, p.1 - 5, 2023/01

B-136
M. Chimura, *et al*.
Development of quadrupole-octupole combined magnet for emittance-growth mitigation in the J-PARC Linac
Proceedings of 19th Annual Meeting of Particle Accelerator Society of Japan, p.237 - 241, 2023/01

B-137
P. K. Saha, *et al*.
Status of POP demonstration of 400 MeV H^- laser stripping at J-PARC RCS
Proceedings of 19th Annual Meeting of Particle Accelerator Society of Japan, p.272 - 276, 2023/01

B-138
Y. Shobuda, *et al*.
Two-dimensional resistive-wall impedance with finite thickness; Its mathematical structures and their physical meanings
Proceedings of 19th Annual Meeting of Particle Accelerator Society of Japan, p.28 - 32, 2023/01

B-139
H. Takahashi, *et al*.
Development of beam window protection unit for J-PARC Linac
Proceedings of 19th Annual Meeting of Particle Accelerator Society of Japan, p.300 - 304, 2023/01

B-140
S. Nagayama, *et al*.
Study of non-destructive slow beam extraction method in particle accelerator
Proceedings of 19th Annual Meeting of Particle Accelerator Society of Japan, p.503 - 507, 2023/01

B-141
H. Fujiyama, *et al*.
Reducing the effect of noise generated from stepper motor for H0 collimator in J-PARC RCS
Proceedings of 19th Annual Meeting of Particle Accelerator Society of Japan, p.529 - 531, 2023/01

B-142
K. Nii, *et al*.
Reports of electro-polishing implementation for quarter-wave resonators, 2
Proceedings of 19th Annual Meeting of Particle Accelerator Society of Japan, p.601 - 604, 2023/01

B-143
K. Watanabe, *et al*.
Upgrade of acquisition and monitoring system for J-PARC accelerator PPS
Proceedings of 20th Annual Meeting of Particle Accelerator Society of Japan , p.844 - 847, 2023/11

B-144
K. Kojima, *et al*.
Identification and compensation of beam loss sources for further beam power ramp-up in J-PARC RCS
Proceedings of 20th Annual Meeting of Particle Accelerator Society of Japan, p.127 - 131, 2023/11

B-145
S. Nagayama, *et al*.
Beam separation experiment with prototype non-destructive electrostatic septum and study for device improvement
Proceedings of 20th Annual Meeting of Particle Accelerator Society of Japan, p.526 - 530, 2023/11

B-146
P. K. Saha, *et al*.
Status of the laser stripping of H^- beam at J-PARC RCS
Proceedings of 20th Annual Meeting of Particle Accelerator Society of Japan, p.59 - 63, 2023/11

B-147
P. K. Saha, *et al*.
1-MW beam operation at J-PARC RCS with minimum beam loss
Proceedings of 68th ICFA Advanced Beam Dynamics Workshop on High Intensity and High Brightness Hadron Beams (HB2023) (Internet), p.147 - 152, 2023/10

B-148
Y. Shobuda, *et al*.
A Kicker impedance reduction scheme with diode stack and resistor at the RCS in J-PARC
Proceedings of 68th ICFA Advanced Beam Dynamics Workshop on High Intensity and High Brightness Hadron Beams (HB2023) (Internet), p.162 - 169, 2023/10

B-149
S. Machida, *et al*.
Summary of the working group C on accelerator systems
Proceedings of 68th ICFA Advanced Beam Dynamics Workshop on High Intensity and High Brightness Hadron Beams (HB2023) (Internet), p.670 - 674, 2023/12

B-150
K. Sasaki, *et al*.
The upper limit on antideuteron flux with BESS-Polar II
Proceedings of Science, ICRC2023, 134 (2023)

B-151
R. Iwai, *et al*.
Precision muonium spectroscopy
Proceedings of Science, Muon4Future2023, 7 (2023)

KEK Reports

C-001
T. Shibata (as Editorial Board)
Development of long-life Radio Frequency negative hydrogen ion (H^-) source for J-PARC
2022 at KEK Annual Report, p70

C-002
Safety Division, J-PARC Center
Annual Report on the Activities of Safety in J-PARC, FY2022
KEK Internal 2023-006

C-003
C. Ohmori, *et al*.
Temperature Shift Measurements of Nano-crystalline Formation for $Fe_{81}Cu_1Nb_3$ and $Fe_{bal}Cu_1Nb_3Si_{15.5}B_7$ by high-temperature uSR
KEK-MSL REPORT 2021, p44

C-004
K. Miura
J-PARC MR 主電磁石システムの高繰り返し化対応
Proc of the Meetings on the Engineering Study and Engineering Seminar at KEK, 2022, p23

C-005
S. Iwata
J-PARC MR 速い取り出し用セプタム電磁石アップグレードの進捗状況
Proc of the Meetings on the Engineering Study and Engineering Seminar at KEK, 2022, p28

C-006
T. Sasaki
採用2年目の活躍報告
Proc of the Meetings on the Engineering Study and Engineering Seminar at KEK, 2022, p9

JAEA Reports

D-001
J. Tamura
Beam Loss Assessment of High-Intensity Negative Hydrogen Ion Beams
JAEA R&D Review 2023-24, p.45

D-002
Safety Division, J-PARC Center
Annual Report on the Activities of Safety in J-PARC, FY2022
JAEA-Review 2023-041(2023)

D-003
S. Saito, *et al*.
Development of Freezed Seal Valve by Using Test Stand for LBE Technology
JAEA-Technology 2022-032 (2023).

D-004
S. Kosaka, *et al*.
How to confirm the polarity of the DTQ in the J-PARC DTL
JAEA-Technology 2023-003(2023)

D-005
S. Arai, *et al*.
Cleaning of the inner surface for Separated-type Drift Tube Linac with Dilute Hydrochloric Acid
JAEA-Technology 2023-009 (2023)

D-006
S. Saito, *et al*.
Conceptual Study of Post Irradiation Examination (PIE) Facility at J-PARC
JAEA-Technology 2023-025 (2023).

Others

E-001
M. Chimura
Emittance Growth Due to the Strong Space-Charge Field and Its Mitigation Using a Combined Multipole Magnet
Doctoral thesis, Tohoku University, 2023/07

E-002
M. Chimura, *et al*.
Multi-pole electromagenet
Japanese Unexamined Patent Application Publication, 2024-22311, 2024/02

E-003
M. Chimura
Introduction of Ph.D
Kasokuki Vol. 20, No. 2, p. 139 - 140, 2023/08

J-PARC Annual Report 2023
Vol.1: Highlight

December 2024

J-PARC

JAPAN PROTON ACCELERATOR RESEARCH COMPLEX

High Energy Accelerator Research Organization (KEK)
Japan Atomic Energy Agency (JAEA)

2-4 Shirakata, Tokai-mura, Naka-gun, Ibaraki 319-1195, Japan

https://j-parc.jp/